UNIVERSITÀ DEGLI STUDI DI TORINO

DIPARTIMENTO DI PSICOLOGIA

DOTTORATO DI RICERCA IN NEUROSCIENZE

CICLO XXIX

TITOLO DELLA TESI:

PERSISTENCE OF FMRI BOLD SIGNAL AT REST AND ITS USE AS PHYSIOLOGICAL MARKER

TESI PRESENTATA DA: Ugo Vercelli

TUTOR: Prof. Franco Cauda

COORDINATORE DEL DOTTORATO: Prof. Marco Sassoè

ANNI ACCADEMICI:

1Gennaio 2014- 31 Dicembre 2017

Index

1 Thesis Introduction

My PhD main interest has focused on the functional magnetic resonance (fMRI) blood oxygen level dependent (BOLD) signal at rest, particularly on its persistence.

When we consider signals or data time courses, the aspect of persistence concern how the past dynamics of a system underline the signals. These concepts are also used in economic time series analysis. For instance, in economy and finance people are very interested in forecasting, which is based on the analysis of the past and its correlation to the future.

Preliminarily, my research aimed at validating a parameter capable of measuring the BOLD signal persistence. This was achieved by comparing the spatial distribution of this parameter with the well known spatial distribution of functional brain areas and networks.

1.1 Autocorrelation

The parameter I took into consideration to measure persistence is the autocorrelation (AC) of the fMRI BOLD signal at rest, which is described in detail in the first study introduction. To put it simply, AC is the correlation of a signal with itself shifted in time. In other words, compared to correlation where there are 2 different variables, in AC the second variable is substituted with the values of the same variable shifted in time.

This is the correlation formula between variables *x* and *y*:

$$r_{xy} = \frac{\sum_{i=1}^{n}(x_i - \bar{x})(y_i - \bar{y})}{\sqrt{\sum_{i=1}^{n}(x_i - \bar{x})^2 \sum_{i=1}^{n}(y_i - \bar{y})^2}} \quad (1)$$

And this is the AC formula at lag K:

$$r_k = \frac{\sum_{t=k+1}^{n}(y_t - \bar{y})(y_{t-k} - \bar{y})}{\sum_{t=1}^{n}(y_t - \bar{y})^2} \quad (2)$$

Where $y_t$is the value of the signal at time t, k is a time lag, y_{t-k} the value of the signal at time $t-k$, $\bar{y}$ the average of all *y* values. $(y_t - \bar{y})$ and $(y_{t-k} - \bar{y})$ are the absolute deviation of $y_t$and y_{t-k} from their avarege.

AC is calculated at different time lags and the results could be described in a correlogram graph (Fig. 1.1).

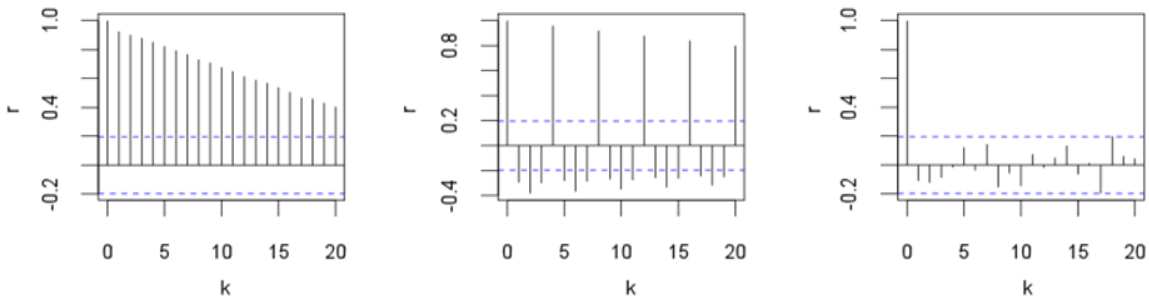

Figure 1.1. These are three different types of correlograms: the first describes a slow decade of the AC, the second illustrates a cyclic trend, the third refers to a random time series.

Different types of signal, such as trends, cycles or stochastic time series are described by different kinds of correlograms. When the autocorrelation exhibits a very long decay, we say that the signal is characterized by a “long memory” process.

As the expression “long memory” may cause a misunderstanding in a neuroscientific context, I propose to substitute it with “persistence”. This can be done if the trend of the AC is like the one described in the first correlogram of figure 1.1. We will see in my first study that this is the case of BOLD signal AC. BOLD persistence has been investigated previously by using the Hurst exponent as a parameter. BOLD persistence at rest was found to be higher in gray matter rather than in white matter areas (Wink et al., 2008). Moreover, studies have investigated how BOLD persistence changes under the influence of pharmacological treatment, aging and/or brain disorders (Maxim et al., 2005; Suckling et al., 2008; Wink et al., 2006). Although this parameter has been measured in a variety of cognitive tasks, results are arguable (Anderson et al., 2006; Ball et al., 2011).

The AC of BOLD signal is generally considered as a type of noise (Aguirre et al., 1997; Bullmore et al., 2001; Lenoski et al., 2008; Lund et al., 2006; Purdon and Weisskoff, 1998; Zarahn et al., 1997). However, this process could be neurophysiologically informative, especially during resting state.

1.2 Research workflow

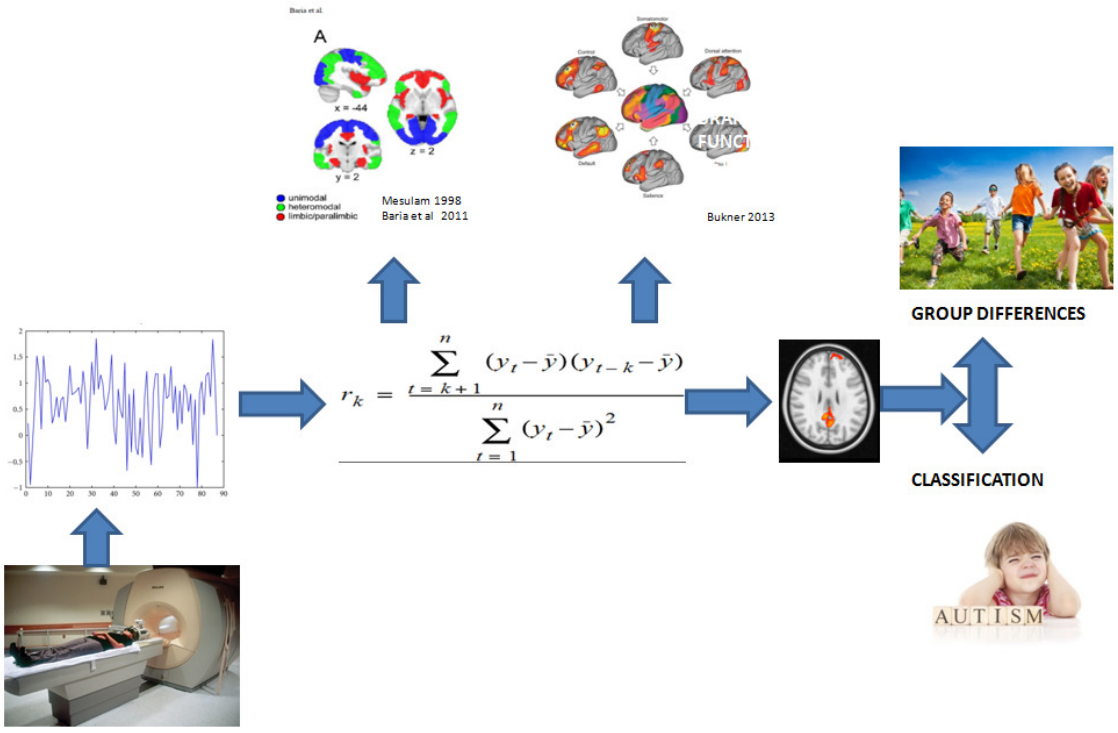

Figure 1.2. An illustration of the workflow of my research.

In order to verify the informativeness of AC I examined the spatial organization of the resting state BOLD signal of the human brain; in particular, I analyzed the voxel-wise AC spatial distribution of the resting state BOLD signal of 15 subjects, using time lag 1+ time lag 2 as parameter.

My analysis identified a spatial pattern that, from the anatomical point of view, was meaningfully distributed across the brain. In line with previous studies on the complexity and space distribution of BOLD signal persistence, I expected a higher AC in the brain areas supporting higher cognitive functions. And in fact I found out that most of the brain areas with higher AC values support associative or heteromodal functions, while most of the brain areas with lower AC values support

unimodal or limbic functions. These results demonstrate that the spatial distribution of the AC in the BOLD signal may contain not only noise but also important information about the structural and functional architecture of the brain. This was my first study.

Then in a second study I tested autocorrelation as a biomarker for brain disorders by analyzing differences at group level and providing classification at single subject level.

On the ground of the results of my first study I hypothesized that brain areas performing iterative tasks require a high level of in-line memory, which is revealed by an increased level of temporal autocorrelation (Ciuciu et al., 2012; He, 2011; Turner and Jones, 2003).

In order to better understand the meaning of this higher AC and to verify the possibility to apply this parameter to a clinical contest I turned my attention to a particular brain disease: autism spectrum disorder (ASD).

Despite a large number of neuroimaging studies investigating the brain structure of subjects with ASD, there is still disagreement on neuroanatomical evidence.

Some studies report atypical increases of gray matter (GM) (Watanabe, 2005) 2016) with several altered cortical and subcortical regions (Amaral et al., 2018), but also significantly thicker cortex in other brain areas (Haar et al., 2016).

The hypothesis of my study was that a structural modification might influence the BOLD signal at rest.

In light of this, I investigated the spatial distribution of AC in autistic subjects, compared to a control group, and verified whether or not AC could be a useful biomarker.

Before discussing my original research, as both my studies analyzed fMRI data, the following is an essential description about magnetic resonance principles, anatomical and functional techniques and data preprocessing. I will also dedicate a brief overview of ASD, as the spatial distribution of AC in people with ASD is the topic of my second study.

1.3 MRI

1.3.1 General physical principles of MRI.

Magnetic resonance imaging is based on some physical principles that need to be simply introduced. Matter is formed by atoms and atoms are composed of a nucleus made of protons and neutrons (except for hydrogenous that has just one proton) and of electrons spinning around it. The protons of the nucleus are like small planets that rotate on their axis; in virtue of this rotation they generate a magnetic field. If protons are placed in a strong magnetic field, they all align: most of them in one direction (parallel), while the others in a 180 degrees inverted direction (antiparallel).

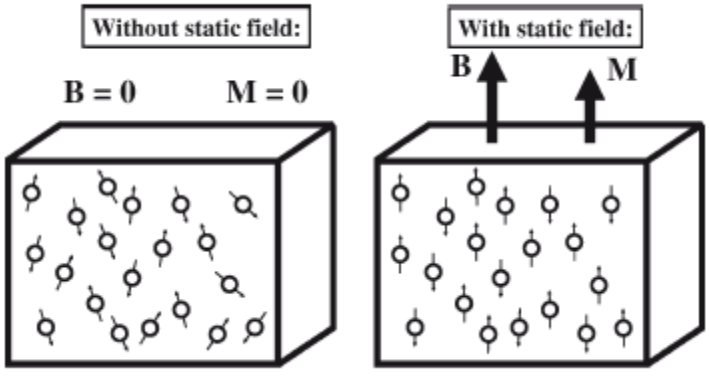

Figure 1.3 .The rotation axes of the protons are aligned in a strong magnetic field. (Filippi, 2009).

The rotation axis oscillates like a spinning top that is going to stop. This oscillation is called precession and has a frequency that can be calculated, as it is proportional to the strength of the external magnetic field and to a coefficient, different for each material (gyromagnetic ratio). These physical characteristics are linked by the Larmor equation:

$$\omega 0 = \gamma B0 \qquad (3)$$

where

ω0 is the precession frequency expressed in Hz or MHz,

γ è is the gyromagnetic ratio and

B0 is the strength of the external magnetic field expressed in Tesla.

Opposed strengths of parallel and antiparallel protons equals, but given that parallel oriented protons are slightly more, the result is a strength of the total body of the subject in the machine.

When a radio frequency impulse, with a certain precession frequency, is sent, protons with the same Larmor frequencies are excited and part of the impulse energy is captured by some of them.

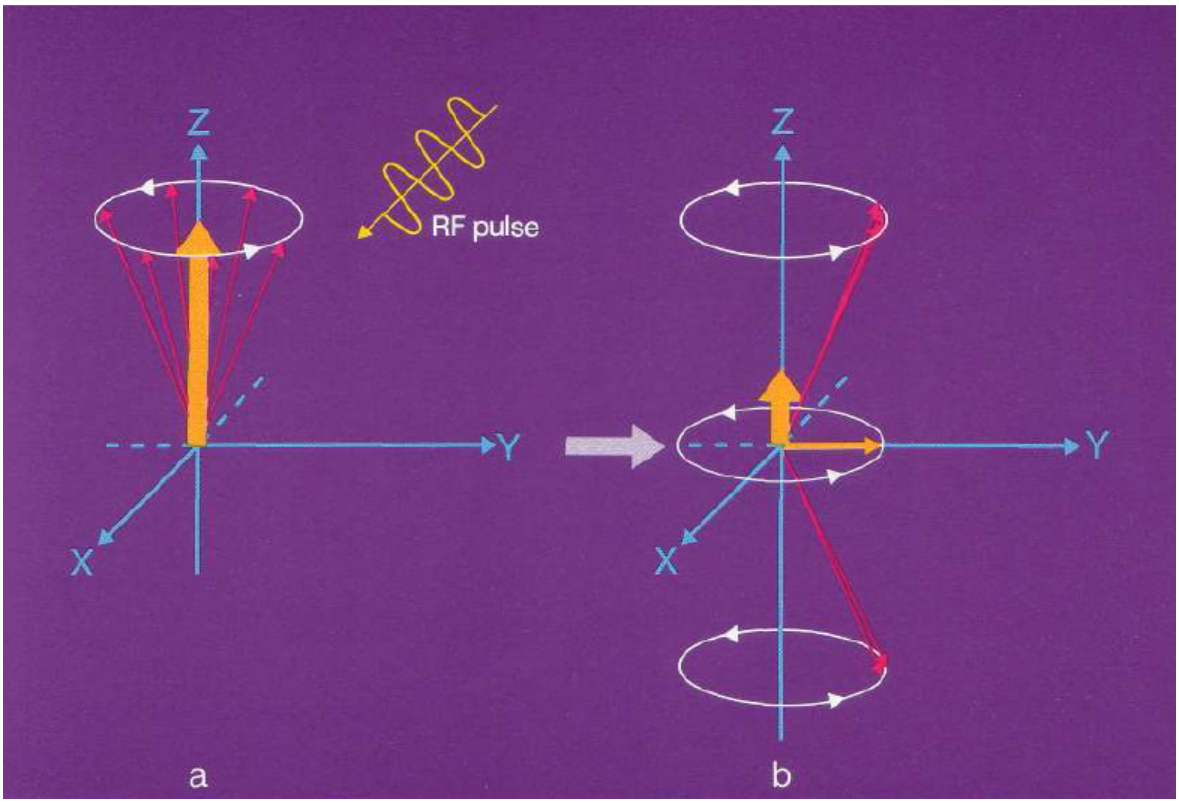

Figure 1.4. Effects of a radiofrequencies input synchronized with the precession frequence (Schild and Laboratories, 1992).

This phenomenon is called resonance and causes an inversion of the rotational axis that becomes antiparallel, thus reducing longitudinal magnetization. Another effect is the synchronization of the proton precession, which causes a transversal magnetization, so that a precession frequency can be detected. The increase of transversal magnetization decreases the longitudinal magnetization. The movement of a magnetic field creates electricity, for example in an antenna; this is the detected MRI signal, which has the same frequency of precession.

1.3.2 Localization of the signal

To construct images, the source of the signal needs to be localized. In order to do so, the magnetic field is not constant but changes with a spatial gradient like an inclined plane, so that in every place there is a different level. As the precession frequency of the protons is linked to the magnetic field strength of their position, protons in different positions have also different precession frequencies and different MRI signal frequency.

1.3.3 Signal modification

Synchronization and longitudinal magnetization reduction tend to decay by relaxation, specifically through a transversal magnetic field decrease (transversal relaxation) and a longitudinal magnetization increase (longitudinal relaxation or spin-lattice-relaxation).

In figure 1.5 the increasing curve describes the longitudinal relaxation (the temporal constant measuring the speed of this process is called T1), while the decreasing curve describes the transversal relaxation (which is measured by the T2 temporal constant).

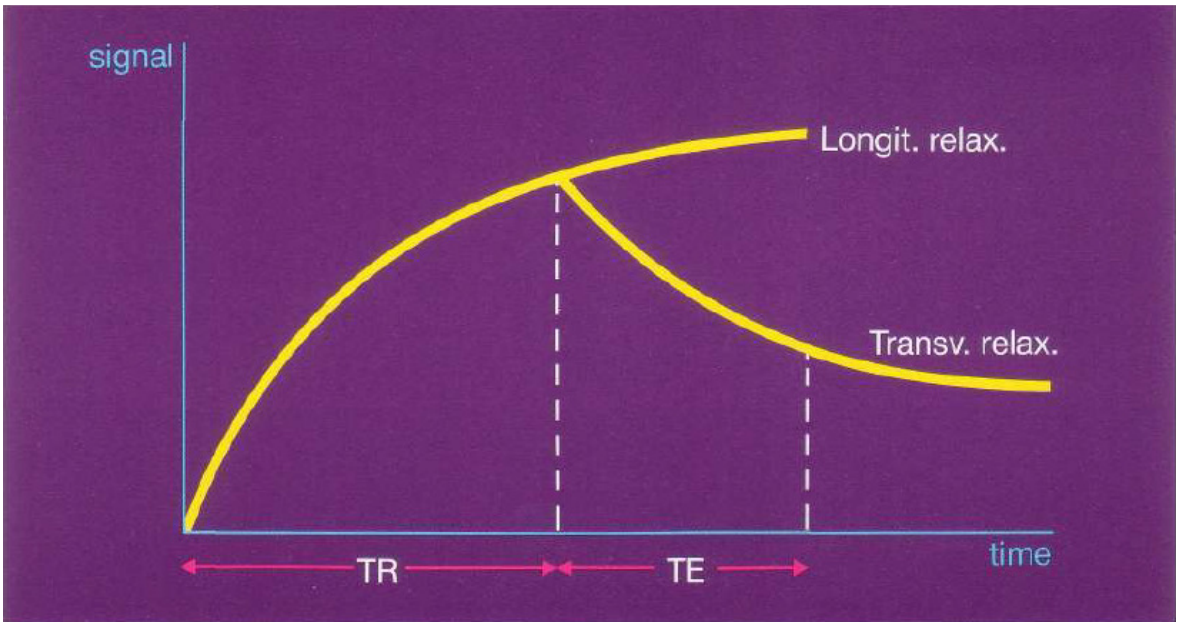

Figure 1.5. The graph describes longitudinal (TR) and trasversal relaxation time (TE) (Schild and Laboratories, 1992).

These measures are different for each tissue. Tissues with more water content have longer T1 and T2. With the increase and decrease of the two orthogonal vectors of longitudinal and transversal magnetization, the resultant vector changes his inclination while he is rotating.

The vector describes a spiral in the space that reduces more and more his transversal dimension. This movement in the magnetic field is received by an antenna and the detected signal is called free induction decay (FID).

1.3.4 How to detect two different tissues

If there are two tissues with different T1 and T2 and a second impulse is sent in a short time so that the residual transversal magnetization still differs from the two tissues, than a higher signal will be received from the tissue with longer transversal relaxation time. A sequence of more impulses can be used with a certain repetition time (TR): the result is a T1 weighted image.

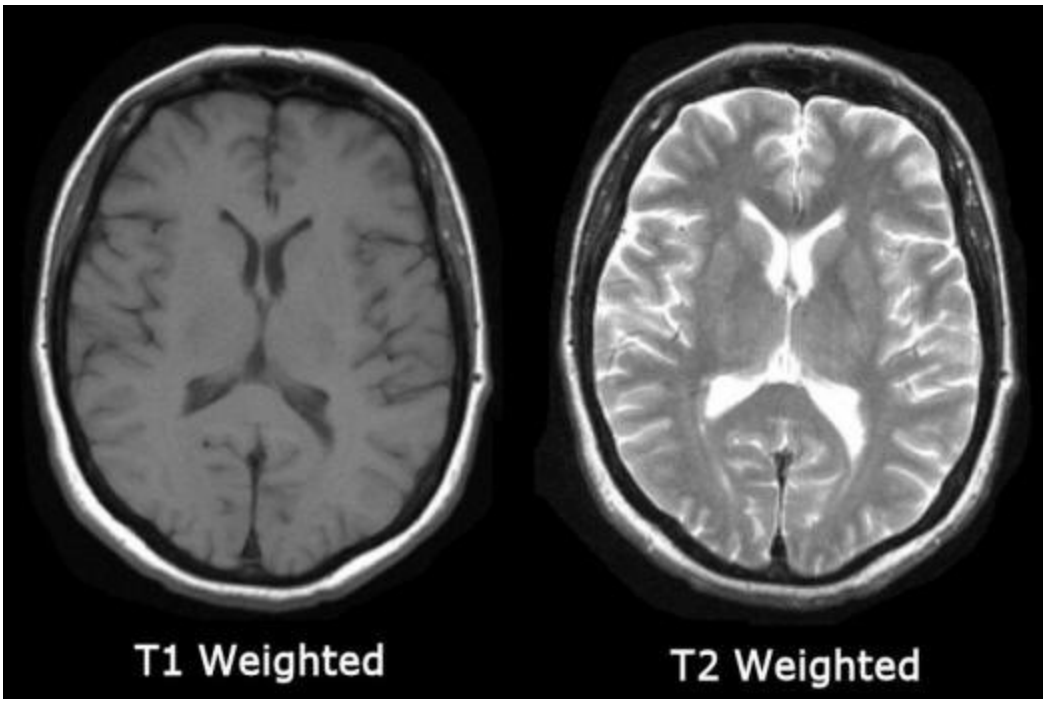

Figure 1.6. T1 and T2 weighted images.

T2 weighted images can be obtained detecting the proton density or spin density with a more complicate impulse sequence.

1.3.5 Blood flow effect

Between the moment when the impulse is sent and the moment when it is received there is a time lag during which protons move within the blood flow. So some adjustments must be applied.

1.3.6 Localization and slices dimensions

3D images are acquired by slices and localized using the magnetic gradient for two directions (Z and Y). For the third coordinate (X) a temporary magnetic field with a gradient is used to change the phase of protons with a different spatial distribution useful to localize the signal.

The voxel is the minimal unit of the image and is a rectangular parallelepiped; if the voxel is a cube is called isotropic. Some parameters describe the image dimensions, such as the field of view (FoV) that is the slice dimension (x-y) in millimeters or the slice thickness (z). These parameters are defined before the scan; with bigger voxels there is a worse resolution but a faster scan and an improved signal to noise ratio. Usually the size of a voxel is compared to the cortical thickness that is more or less 3-4 mm. Together with functional images is frequently acquired a high resolution anatomical image that is used as a base for functional images. BOLD signal can be few millimeters distant from neural

activation because the blood system is not punctually activated, so in order to solve this problem a spatial smoothing is performed by averaging the value of a voxel with that of the nearest voxels.

1.3.7 Scanner structure

The main component of the scanner is the principal magnet, which is capable of generating a magnetic field that generally is 1.5 or 3 Tesla, although with some scanners reach 7 Tesla. A Tesla is a magnetic measure unit equivalent to 10 Gauss; as comparison, the magnetic Earth field varies between 0.3 and 0.7 Gauss. Homogeneity of the magnetic field is very important for all the scanning process and can be calibrated with mechanical and electrical shimming. Most magnets are made of superconductor material kept at a temperature of -269° C, so that electricity can flow permanently and create a strong magnetic field. To maintain this coils' temperature helium and nitrogen are used.

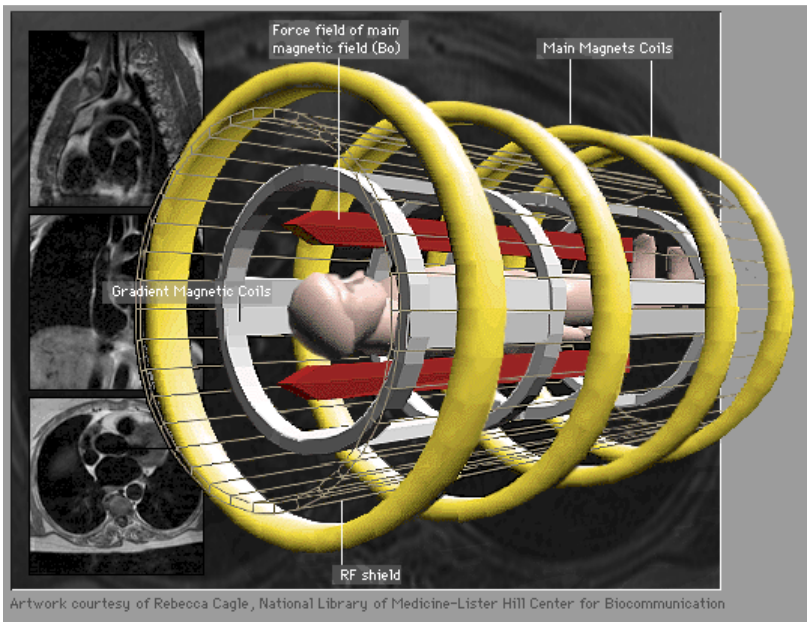

Figure 1.7. MRI scanner structure. (Cagle, n.d.)

Other components are the coils used to send and receive radio frequencies' impulses. For the brain a sort of helmet is used with a coil inside to receive the signal while the main coil transmits the impulse. To improve the magnetic field homogeneity there are other shim coils and finally other three coils create the magnetic gradient in the three directions of the space.

1.3.8 Anatomical techniques

MRI can be applied both for anatomical analysis investigating the brain structure as well as for functional analysis investigating cerebral activations. Most common anatomical analysis concerning brain/mind relation are morphometric analysis and diffusion analysis. In morphometric analysis anatomical features of cortical GM, or

white matter (WM) composed of neurons' axons, are measured. A typical application is comparing these measures between pathological and control subjects. The most diffuse anatomical analysis is the voxel-based morphometry that allows the measure of volume, thickness and density of both GM and WM. More sophisticated algorithms are applied for deformation-based morphometry or tensor-based morphometry.

Diffusion-weighted imaging (DTI) permits a fiber tracking analysis to obtain images of axonal bundles connecting different brain areas.

1.3.9 Functional techniques

In fMRI the assumption is that an increase in neuronal activity of a certain area is associated with an increase in the blood flow (and therefore a higher exchange of oxygen) in that area. Deoxyhemoglobin (without oxygen) and oxyhemoglobin (with oxygen) present different magnetic properties. The former, with presence of iron, is paramagnetic or more attracted by magnetic field, while the latter is diamagnetic or less attracted by magnetic fields. The ratio of oxygenated and deoxygenated hemoglobin changes the magnetic property of the blood, so that BOLD signal can be used to detect indirectly brain activity, both during the performance of tasks and at rest. For this kind of application sequences sensible to T*2 are applied.

Once acquired, data must be preprocessed.

1.3.10 Preprocessing

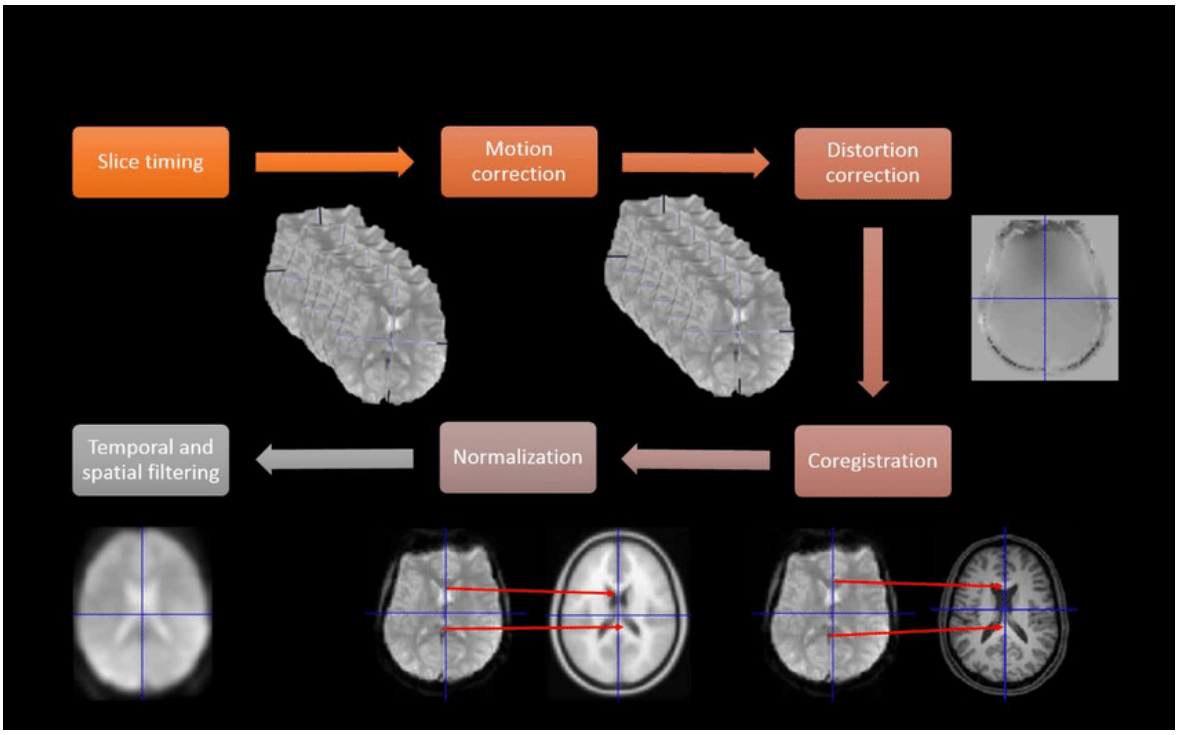

Figure 1.8. Preprocessing flow chart (Fengler, 2016).

Preprocessing and analysis of data are performed with the help of software, of which the most used are FSL, SPM, and Brainvoyager. For study 1 we used Brain Voyager (Brain Innovation Maastricht Holland). For Study 2 we used FSL (Analysis Group FMRIB, Oxford, UK), (Jenkinson et al., 2012a; Smith et al., 2004; Woolrich et al., 2009) and Matlab.

Also for functional analysis an anatomical base needs to be used, with a best image resolution. Both anatomical and functional data must be preprocessed.

Brain extraction consists in removing all tissue that is not cerebral.

Intensity inhomogeneity correction increases the accuracy of segmentation and coregistration by unifying the intensity of GM and WM in different parts of the brain, as original images could exhibit intensity inhomogeneity (Sled et al., 1998).

Segmentation separates GM, WM and cerebrospinal fluid (CSF) (Lim and Pfefferbaum, 1989). This is useful to determine the volume of CSF, GM, and WM in living human brain.

Movement correction. During the scan the subject may move and, as data are acquired by slices, a deviation may occur between two slices. This could be source of artifacts that reduce the quality of data. To manage this aspect, movements corrections are made on the 6 degrees of freedom in a rigid body, which means 3 translations and 3 rotations on axes X, Y and Z. A volume is chosen to register all the others volumes.

Slice timing correction. Each slice is scanned at a different time but BOLD effect involves more slices at the same time; this may cause differences between slices, not describing the real situation in that area. A solution is to apply a temporal interpolation to align all slices at time 0.

Spatial smoothing. As the activity of a voxel is linked to the activity of neighboring voxels, the single value of a voxel is substituted by a weighted average value of neighboring voxels. To do so, a Gaussian filter called kernel is typically used. In this way data are blurred but signal-to-noise-ratio is improved and it helps in case of multi-subjects analysis, where different brains show anatomical differences.

Temporal filtering. Some temporal noise could be present in a signal, caused by temporal drift from scanner and physiological cycles, such as cardiac and

respiratory fluctuations. Filtering at frequencies level is a way to remove some noise, although there is the risk of removing part of the signal.

Functional and anatomical coregistration. As already mentioned, to improve the spatial resolution of functional images, a coregistration with anatomical images is performed. For the coregistration, this procedure uses some specific reference anatomical points.

Spatial normalization. Spatial normalization allows comparing between individuals by mapping all the subjects' brains to a template brain; this is required for multi-subject experiment. In case of affine transformation there are 12 degrees of freedom: 3 rotations, 3 translations, 3 scalings, and 3 skewings. The most used templates are Talairach and Montreal Neurological Institute (MNI). Once normalized each point of the brain can be identified with the coordinates on the 3 axes. The origin (0,0,0) is the anterior commissure (AC). Positive or negative values on the x axis indicate positions on the right or on the left of the origin, respectively; positive or negative values on the y axis indicate anterior or posterior positions, respectively; positive or negative values on the z axis indicate superior or inferior positions, respectively. Spatial normalization may be difficult for subjects with lesions that have modified brain structure.

1.4 Autistic Spectrum Disorder:

The Diagnostic and Statistical Manual of Mental Disorders, fifth (American Psychiatric Association, 2013) defines ASD as a disorder in neurodevelopment with deficits in social interaction and communication, with repetitive behavior. These symptoms are present from early childhood with a negative effect on normal functioning. Currently ASD prevalence is about 1% of US population, with higher prevalence in males than females (Baron-Cohen, 2008).

ASD is a highly genetic disorder with concordance of 73-95% in monozygotic twins and an heritability of more than 90% (Bailey et al., 1995).

Within the label of ASD DSM-5 has collected what in the DSM-IV-TR was classified as Classic Autism, Asperger Syndrome (AS) and Pervasive Developmental Disorder-Not Otherwise Specified (PDD-NOS) (American Psychiatric Association, 2000).

ASD is now considered more as a continuum rather than a categorical pathology.

In fact more than one characteristic may coexist not only in patients but also in neurotypical conditions. Different levels of impact lead to different level of impairment with a high level of variability. In the clinical practice, on the basis of IQ scores, there is a distinction between high-functioning and low-functioning autistic individuals. Also a high-functioning variant of ASD, Asperger Syndrome, can be distinguished on the basis of IQ scores and good language development (Baron-Cohen, 2008).

To complicate the diagnosis possible comorbilities with other disorders can be present, such as epilepsy (Fombonne and Psych, 2005) or mental retardation (Srivastava and Schwartz, 2014).

1.4.1 Tests for diagnosis and research

Different tests can support the clinician's diagnosis of ASD, particularly the second version of Autism Diagnostic Observation Schedule (ADOS 2) and the Autism Diagnostic Interview-Revised (ADI-R).

The ADOS 2 uses standard tasks in an interactive way in order to evoke a particular behavior, such as psychoeducational or developmental tests (Gotham et al., 2009). This test evaluates the quality of social behavior and communication and differentiates scores in different domains, as a Social Affection and Repetitive Behavior. The ADI-R is an interview for the caregivers of autistic patients. Scores are divided into verbal and non-verbal communication, social skills, and repetitive behavior (Lord et al., 1994). An intelligence test, like the Wechsler Adult Intelligence Scale, the Wechster Abbreviated Scale of Intelligence (WASI) or the Differential Ability Scale (DAS-II) (Flanagan and Harrison, 2012), is normally performed to complete the diagnosis, particularly to identify high and low functioning autistic subjects. Furthermore the Behavior Rating Inventory of Executive Function (BRIEF) is used to evaluate the executive function impairment (Gioia et al., 2002). The Social Responsiveness Scale (SRS) is used to measure the level of social abilities (Constantino et al., 2003).Finally, the Vineland Adaptive

Behavior Scales (VABS) (Sparrow and Cicchetti, 1985) assesses the Adaptive Behavior (AB). All the previous tests are caregiver-based questionnaires.

1.4.2 Autistic Spectrum Disorder: Theories

ASD is a complex and heterogeneous disorder, mainly concerning higher cognitive functions. After the first description of autism in 1943 by Leo Kanner (Kanner, 1943), initially scientific literature described different types of behavioral dysfunctions. First in the 1960s the main psychological theory explained autism as a reaction of children to an abnormal relation with the mother (Bettelheim, 1959). This direction was investigated until mid 1980's (Tinbergen et al., 1985), but then this theory was dropped out.

Current theories explain autism from environmental, genetic, epigenetic, neurobiological and psychological points of view. I will focus on the psychological and neurobiological approaches.

Main researches on Autism during the late 1980s, based on the dysfunction in the theory of mind (ToM) development, came from Baron-Cohen, Leslie and Frith (Baron-Cohen et al., 1985; Frith, 1989). ToM indicates the understanding of feelings and thoughts of others and the capacity of assuming their intention and anticipating their behavior; this aspect is also referred to as mentalization (Premack and Woodruff, 1978). Children develop complete theory of mind skills at around 4 years old. On the contrary, autistic subjects show severe delay and impairment in developing social cognition skills, which would explain their reduced

capacity in social interaction and difficulties in verbal communication and empathy, without effect on visuospatial and mnestic functions (Baron-Cohen, 1990)

Consistently with this line of thought, Chris Frith has proposed the “weak central coherence theory”, according to which autistic symptoms could be caused by a dysfunction in the integration of information (Frith, 1989). From this point of view autistic subjects elaborate information coming from stimuli at an analytic and fragmented level rather than at the high level of meaning and context. This could explain the close attention to details, words or imagines as well as the incapacity of managing social situations. Also, sensory hypersensitivity could be linked to this aspect. Firth’s theory might explain the best performance of autistic children in finding a simple target in a larger picture (Embedded Figure Test), as well as their preference to observe local images instead of global pictures in the Navon test and bad performances in the homograph test, where a single stimulus must be decoded within a wider context (Baron-Cohen, 2008).

Research on ASD has also focused on the impairment of executive functions (Ozonoff and Strayer, 1997), which could be associated with an abnormal development of the prefrontal cortex.

Executive functions are involved in planning, action inhibition and problem solving; their dysfunction could explain why patients with ASD have difficulties in shifting attention and propensity to exclude different stimuli out of the focus of their attention. However, impairment in executive functions is not specific of ASD, although deficiency in the neuropsychological test of the Hanoi tower have been reported in ASD subjects (Ozonoff and Miller, 1995). A variant of this approach is

the Monotropism theory, which suggests that the impairment specifically affects the ability of multitasking (Murray et al., 2005).

The ToM theory has been criticized for being circular, as it implies that the impaired meta-representative ability is the cause of the dysfunction of mentalization. In contrast, critics have pointed out that dysfunction in this cognitive domain seems to be more the product of a reduced motivation than an inability *per se* (Boucher, 1989). For this reason ToM approaches have been revised; this has led to the proposal for the empathizing-systemizing (E-S) theory. Empathizing and systemizing are two psychological dimensions used to classify individuals. In patients with ASD the lack of empathy is balanced by an increase in systemizing, resulting in defined interests, repetitiveness and inclination to be creatures of habits. Notably, the difference between autistic and Asperger syndrome could reflect a different strength in systemizing (Baron-Cohen, 2008).

Specific aspects about neuroimaging and ASD will be examined in depth in the introduction of the second study but we can anticipate that cortical differences have been reported by comparing autistic patients with controls (Cauda et al., 2011b); (Cauda et al., 2012b); (Cauda et al., 2014).

These differences, which regard both cortical increase and decrease, have been detected in the brain areas that are involved in the ToM cognitive function, pain perception, speech production, social emotions, motor and cognitive tasks.

As to the functional connectivity, most of researchers agree on the fact that autistic subjects show an under-connectivity between frontal and posterior cortical areas (Just et al., 2012, 2004);on the contrary, the existence of over-connectivity is more controversial (Belmonte et al., 2004) (Hull et al., 2017; Picci et al., 2016).

Finally, at the level of brain networks differences between ASD patients and controls have been found principally in the DMN (Di Martino et al., 2014; Minshew and Keller, 2010; Monk et al., 2009; Weng et al., 2010) and in the salience network (Kleinhans et al., 2008; Uddin and Menon, 2010).

Study 1

The spatial distribution and physiological significance of autocorrelation in resting state BOLD signal

Ugo Vercelli[a b c], Andrea Nani[a b c], Stefano Moia[a b c], Jordi Manuello[a b c], Matteo Diano[a b c], Tommaso Costa[a b c], Sergio Duca[a], Franco Cauda[a b c]

[a] GCS fMRI, Koelliker Hospital, Turin, Italy

[b] Functional Neuroimaging and Neural Complex System Group, Department of Psychology, University of Turin, Turin, Italy

[c] Department of Psychology, University of Turin, Turin, Italy

2.1 Introduction

2.1.1 BOLD signal and noise

Since Biswal's seminal paper of 1995 the BOLD signal measured when the brain is at rest has been incrementally used to study the functional organization of the brain (Biswal et al. 1995). However, the first resting state studies were criticized because the measured signal was thought to be just noise, that is, a measurement not effectively caused by brain activation. For this reason, critics warned that autocorrelation (AC) ought always to be discarded (Aguirre et al., 1997; Bullmore et al., 2001). As a matter of fact, there are BOLD signal changes correlated with head movement, machine drift, breath, and cardiac pulsation. In particular, cardiac and breath pulsation show cyclic trends causing typical movements of the brain tissue as well as variations in the blood flow (Dagli et al., 1999). This problem, however, is (at least partially) solved by temporally filtering the signal (Biswal et al.,1996; Friston et al., 2000; Lowe et al., 1998).

Although certain studies pointed out the influence of physiological noise on functional connectivity signal (Birn et al., 2006; Chang et al., 2010; Shmueli et al., 2007; Van Buuren et al., 2009; Wise et al., 2004), other research demonstrated that the BOLD signal is correlated with neuronal activity (Biswal. et al., 1995; Buckner and Carroll, 2007; Maxim et al., 2005; Winket al.,2008). The fact that neuronal activity can account for the BOLD signal at rest has been further confirmed by finding that resting state networks (rsN) reflect the connections identified in task experiments (Greicius et al., 2003; Gusnard et al., 2001). What is

more, in the mouse the BOLD signal has been found to be clearly associated with cortical activity (Golanov et al., 1994), whereas in humans direct recording of neuronal spikes with intracranial electrodes during resting state has revealed that the spikes are correlated with the fluctuations of BOLD signal (Nir et al., 2008; Shmuel et al., 2002; Shmuel and Leopold, 2008). So, what was thought to be just autocorrelated noise is now considered as information about functional connectivity (Biswal, 2012). To date, given the well established evidence that neural activity at rest determines the BOLD signal, the issue that is yet unresolved is to understand how the physiological noise affects the signal.

2.1.2 Autocorrelation

Especially in the field of task-related imaging studies the BOLD signal AC was traditionally considered to be a noise effect (Aguirre et al., 1997; Bullmore et al., 2001; Lenoski et al., 2008; Lund et al., 2006; Purdon and Weisskoff, 1998; Zarahn et al., 1997). Thus, in order to correct it, several methods have been developed (Murphy et al., 2013). An autoregressive integrated moving average (ARIMA) model has been proposed as a pre-processing procedure (i.e., pre-whitening) (Granger and Newbold, 1974; Haugh, 1976). It has been pointed out that this pre-processing procedure could still be susceptible to bias (Friston et al., 2000). However, so far this approach for correcting AC has been applied with good results, especially in fMRI task-related studies. On the other hand, a recent paper

claimed that removing the effect of BOLD signal AC from real data seems to be negligible (Arbabshirani et al., 2014).

Especially with regard to the resting state condition the hypothesis that AC merely consists of noise, which cannot convey information about the neurophysiological substrate, can be unsupported by evidence. In fact several studies on BOLD signal persistence with the Hurst exponent (H) have shown that its distribution follows consistent anatomical patterns and is associated with physiological changes (Ciuciu et al., 2014; He, 2011; Sánchez Granero et al., 2008; Wink et al., 2008).

Indeed AC, along with other measures, (for instance H), can be thought of as an index of signal persistence or “memory”. On the one hand, this persistence can be caused by different noise sources, both physiological and not physiological (Birn et al., 2006; Chang et al., 2010; Shmueli et al., 2007; Van Buuren et al., 2009; Wise et al., 2004); on the other hand, it can be an intrinsic characteristic of the signal, due to particular aspects of the system, such as the capacity of associative areas to maintain memory of past information that can thereby be integrated with new information (He, 2011; Wink et al., 2008). In this case, the persistence of a signal may relate to how much the signal value, measured at a certain time, is correlated with another value of the same signal measured at a preceding time. In case of an output signal this property can be attributed to a particular feature of the system or to a characteristic of the input signal. As to the BOLD signal, its persistence may derive from brain activity (i.e., the system) or from the blood flow (i.e., the input signal).

From the theoretical point of view, if AC pattern is neurophysiologically significant, then this pattern should have a spatial distribution that is symmetrical and coherent with the function of brain areas. In particular, unimodal brain areas are supposed to show lower levels of AC, as they process information directly. In contrast, multimodal and associative brain areas are supposed to show higher levels of AC, as they need to process information coming from other brain regions in different time lags (Buckner and Carroll, 2007; Fuster, 1997; Hasson et al., 2009; Honey et al., 2013; Murray et al., 2014; Schacter et al., 2007).

Therefore, given both the preceding considerations and the fact that AC has been scarcely investigated as an informative parameter of BOLD signal, we decided to study the intrinsic properties of low frequency oscillations of the BOLD signal. In particular, we wanted to know: 1) if, in resting state data, the BOLD AC level is spatially distributed in a specific or meaningful pattern; 2) if different rsN have different AC levels; and 3) if unimodal and multimodal brain areas show different AC levels.

2.1.3 Hurst exponent

Hurts exponent (H) is a measure of long term memory of time courses and is used in many fields, from finance to hydrology. It has already been used to investigate the fractal dimension of resting state brain activity (He, 2011; Maxim et al., 2005; Park et al., 2010).

Mandelbrot demonstrated (Mandelbrot et al., 1997) that H values vary between 0 and 1; when H is more or less 0.5, it indicates that the time series on which was calculates has a random trend, which is to say that future is not influenced by the past and, consequently, there is no memory. When H is lower than 0.5, there is an anti-persistent walk, which means that the trend of the variable changes quite frequently; as a result, if the trend is growing there is a high probability that will decrease in the early future. An H value higher than 0.5 indicate persistence in the trend of the time series. The Hurst exponent is not obtained with a precise calculation but with estimation procedures, among which the Rescaled Range analysis is the most applied.

Given a time series X=(x_1,x_2, … , x_N), form a set of vectors

$$X_k^m = \left(x_{(k-1)m+1}, x_{(k-1)m+2}, \dots, x_{km}\right), m = 1,2, \dots . M \quad (4)$$

M is an integer indicating the maximal length of discrete time interval.

K=1,2,…., int (*N/m),* int(N/m) indicates the integer part of *N/m.*

The range *R* and standard deviation *S* of each interval can be defined as follows:

$$R_{k,m} = \max \sum_{i}^{m} (x_{(k-1)m+i} - \bar{x}_k) - \min \sum_{i}^{m} (x_{(k-1)m+i} - \bar{x}_k) \quad (5)$$

$$S_{k,m} = \sqrt{\frac{1}{m} \sum_{i}^{m} (x_{(k-1)m+i} - \bar{x}_k)^2} \quad (6)$$

where $\bar{x}_k = {}^{1}/_{m} \sum_{j=1}^{m} x_{(k-1)j+1}$ is the mean of each interval.

The mean of *R/S* is calculated as follows:

$$\frac{R_m}{S_m} = \frac{1}{\mathrm{int}({}^{N}/_{m})} \sum_{k=1}^{\mathrm{int}(N/m)} \frac{R_{k,m}}{S_{k,m}} \quad (7)$$

Finally, H is defined as the slope of the line that fits the pair (ln *m*, ln (R_m/S_m)) in a least-squares sense.

Persistence measured with H was investigated in subjects with early Alzheimer's disease. Compared to controls, patients showed higher H values, thus suggesting slower dynamics in BOLD signal (Maxim et al., 2005). In contrast, a decrease of persistence was detected in autistic subjects (Lai et al., 2010). Concerning normal

aging, a higher H was measured in the BOLD signal time courses of the hippocampus, bilaterally (Wink et al.,2006). Moreover, higher H values in the signal of the default mode network has been associated with a lower extraversion score (Lai et al., 2010).

Unfortunately, H has several drawbacks related to the estimation procedure, which depends on many factors as estimated on a random series the result could be a value that indicate a long memory (Sánchez Granero et al., 2008) and produces different results according to the different methods of estimation (Cannon et al., 1997; Poveda and Mesa, 1994). For these reasons we decided to explore the BOLD signal persistence with the more reliable and straightforward parameter of AC.

2.2 Materials and methods

2.2.1 Subjects

Fifteen healthy right-handed volunteers (8 females and 7 male; mean age M=29.6 years, SD=7.04), free of neurological or psychiatric disorders, without taking any medication known to alter brain activity and with no history of drug or alcohol abuse, were recruited. This study protocol was approved by the Ethics Committee of University of Torino and all clinical investigation were conducted according to the principles expressed in the Declaration of Helsinki. We obtained written informed consent from all participants involved in this study.

2.2.2 Image acquisition

Images were acquired during a resting state scan with a 1.5 Tesla INTERA™ scanner (Philips Medical Systems). Functional T2* weighted images were acquired using echoplanar sequence (TR=2000 ms, TE=50 ms, FA= 90°). The acquisition matrix was 64x64, with a 200 mm FoV. A total of 850 volumes were acquired: slice thickness was 4.5 mm; in-plane resolution was 3.1 mm. A set of three-dimensional high-resolution T1-weighted structural images was acquired,

using a Fast Field Echo sequence, with a 25 ms TR, an ultra-short TE, FA= 30°. Acquisition matrix was 256x256, and the FoV was 256 mm.

We used a long acquisition time in order to have a long time course for calculating more accurately both AC and H. Infact, following previous studies, calculation of H on longer data series are suggested in order to decrease error on estimation and to better capture the lower frequencies (Eke, et al., 2000; Herman et al, 2011; Rubin et al., 2013). Several studies pointed out that estimation of H for time series shorter than 256 are unreliable and bias and standard deviation of H estimates are less than 0.05 for series having more that 512 time points.(Bryce and Sprague, 2012; Cannon et al., 1997), this means that different fractal methods of calculation perform better with the increase of signal length.

To place these suggestions in the resting state fMRI context we must remember that a usual TR is 2 seconds. In our research we worked on a 850 volumes time course that means that the duration of the scan was more than 28 minutes that is a quite a long time for the subjects.

We think that is an acceptable tradeoff between practical scan procedures and methodologists suggestions.

2.2.3 Preprocessing

Datasets were analyzed using the BrainVoyager QX software (Brain Innovation, Maastricht, NL). Functional images were pre-processed to reduce artifacts, as

follows: (i) slice scan time; (ii) 3D motion correction; (iii) spatial smoothing (8 mm FWHM). Then time courses were temporally filtered (0.008 Hz and 0.08 Hz) and normalized (Thomas Yeo et al., 2015; Yeo et al., 2011). Subsequently, the dataset of each subject was transformed into the Talairach space (Talairach and Tournoux, 1988), the cerebrum was translated and rotated into the anterior/posterior commissures plane and its borders were identified. Finally, using the anatomo-functional coregistration matrix and the determined Talairach reference points, the functional time course of each subject was transformed into the Talairach space and the volume time course was created.

2.2.4 AC spatial distribution

AC is the correlation between elements of a series separated by an interval. In our case the series is the BOLD time course of a voxel and the interval is a time lag, multiple of the sampling rate (TR).

The AC formula is:

$$r_k = \frac{\sum_{t=k+1}^{n}(y_t - \bar{y})(y_{t-k} - \bar{y})}{\sum_{t=1}^{n}(y_t - \bar{y})^2} \quad (8)$$

where r_k is the autocorrelation for lag k.

AC is described by a graph called correlogram in which the variable on the horizontal axis is the temporal lag, while the variable on the vertical axis is the AC value for each time lag.

To obtain a map of the AC spatial distribution we computed voxel wise the AC at different time lags and then considered its sum at lag 1 and lag 2, which was then attributed to each voxel respectively. We repeated this calculation for every time course of the BOLD signal for each voxel of every subject. We subsequently computed the average AC and summarized the results using a one sample t test. The threshold was $q<0.05$, Bonferroni corrected for multiple comparisons.

To define the nodes showing the highest and lowest AC values we modified the threshold so that only the 10% highest and lowest peaks were visualized. On each of these peaks we designed a 10 mm spherical ROI. Anatomical labels relative to high and low AC ROIs were identified with the Talairach Client software (Lancaster et al., 2000, 1997) (Tab.2.1).

Roi	Talairach			MNI			Talairach Client	Lag 1+ Lag 2	Ring	AC
	x	y	z	x	y	z				
Pcun	6	-57	33	8	-60	2	Precuneus, BA 7	1,059	PTF	high
FPole	5	60	4	6	66	-7	Medial Frontal Gyrus, BA 10	0,988	PTF	high
SMGr	50	52	25	55	60	17	Supramarginal Gyrus, Brodmann area 40	0,95	PTF	high
SMGl	-51	-55	21	-54	-55	25	Supramarginal Gyrus, Brodmann area 40	0,949	PTF	high
BA10l	-40	42	13	-42	47	6	Middle Frontal Gyrus, BA 10	0,904	PTF	high
dACC	-1	30	32	0	37	28	Cingulate Gyrus, BA 32	0,786	PTF	high
BA3l	-20	-29	59	-20	-30	1	Postcentral Gyrus, BA 3	0,647	VSA	low
MDNr	11	-16	15	13	-14	13	Thalamus Medial dorsal Nucleus	0,632	Subcor	low
BA3r	21	-26	59	25	-26	59	Postcentral Gyrus, BA 3	0,586	VSA	low
MDNl	-11	-14	15	-11	-12	14	Thalamus Medial dorsal Nucleus	0,582	Subcor	low
SNl	-17	-4	-4	-17	-3	-8	Lentiform Nucleus, Medial Globus Pallidus	0,542	Subcor	low
BA6l	-28	-1	44	-29	5	45	Middle Frontal Gyrus, BA 6	0,441	VSA	low
BA6r	35	-5	44	39	1	44	Middle Frontal Gyrus, BA 6	0,427	VSA	low
SNr	15	-5	-4	17	-4	-9	Lentiform Nucleus, Medial Globus Pallidus	0,426	Subcor	low

Table 2.1. List of ROIs, with Talairach coordinates, as described in Talairach Client, and their corrispondence to the dual ring architecture, AC value and level.

To verify the degree of similarity of the autocorrelograms between the ROIs we employed a hierarchical clustering. The optimal number of cluster was determined using the silhouette method (Rousseeuw, 1987). For each of the high and low AC ROIs we averaged temporal signal of all the voxel included in the ROI and calculated the correlogram or autocorrelation function (ACF) of the averaged timecourse. An example of two ACFs is illustrated in Fig. 2.1.

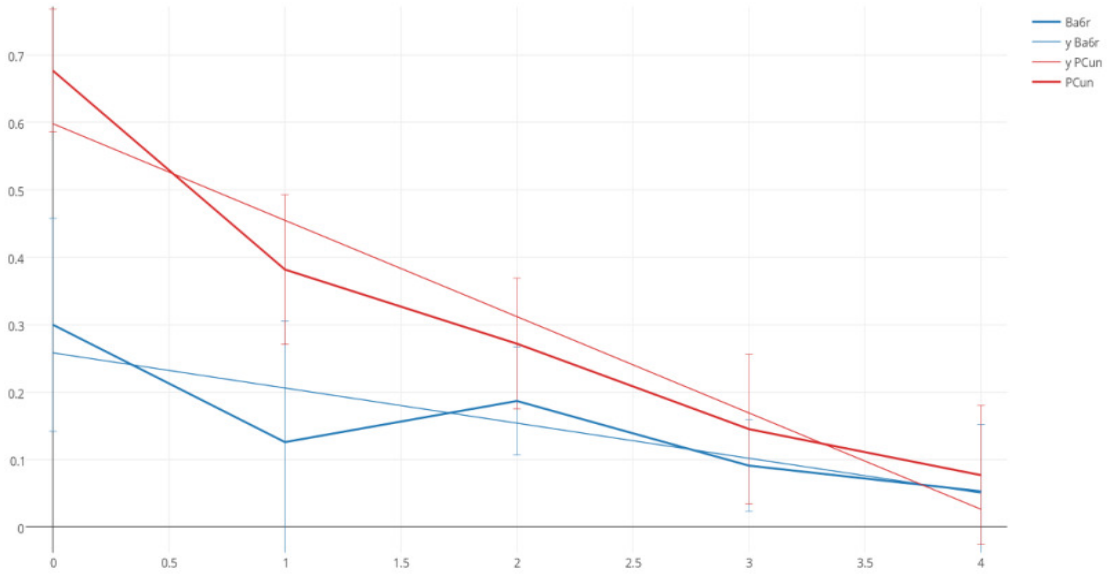

Fig. 2.1. Autocorrelation functions.Two examples of autocorrelation function. The red line is obtained from the signal of precuneus, which is the brain area with the highest AC level, the blue line is obtained from the signal of Brodmann area 6, which is the brain area with a lowest AC level.

The aforementioned process was repeated for all the subjects. The first 5 lag points of all the correlograms were then fitted with a line and the angular coefficient was considered as a parameter to measure the AC level of the BOLD signal in that ROI. To verify the statistical difference between angular coefficients of every couple of ROIs we performed a t test.

To understand from a network perspective the spatial distribution of the AC values, we employed the 20 large-scale brain networks subdivision provided by Biswal in a previous study (Biswal et al., 2010). For each of the 20 networks we calculated the number of voxels showing an 1+2 AC that was significantly different from the mean (one sample t test $p < 0.05$, Bonferroni corrected). In order to exclude the possibility that the signal-to-noise-ratio (SNR) could influence the results of AC spatial distribution, we calculated voxel-wise the SNR and compared its spatial distribution with that of the AC.

To our knowledge only another study considered the spatial distribution of AC in resting state BOLD signal and Lag 1+2 was the parameter used (Kaneoke et al., 2012). We also calculated the correlation between AC of Lag 1 plus Lag 2 and the sum of AC from Lag 1 to Lag 5, for each subject and each ROI, the result is a correlation of 0,90. This demonstrates that AC at lag 1 plus lag 2 is a good and parsimonious parameter to confront AC level in different voxels.

Finally, in order to further verify our results, we also measured the persistence of the signal using H as parameter (Hurst, 1950). For a description of the method, refer to Peng et al. (Peng et al., 1994).

2.3 Results

2.3.1 Voxel-wise analysis

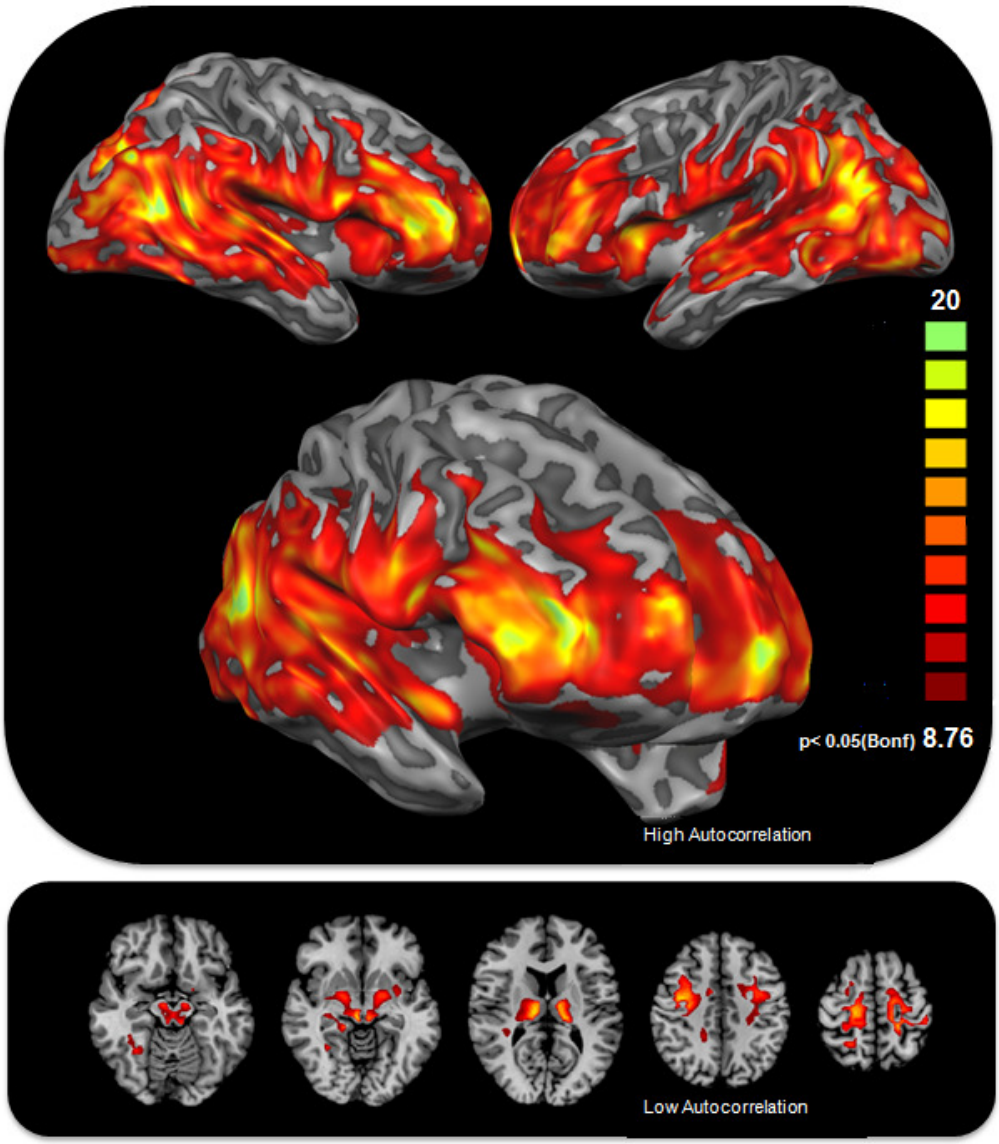

Fig. 2.2. Autocorrelation spatial distribution. The upper panel illustrates the statistical map of the ROIs with higher AC in the frontoparietal areas, anterior insula and cingulate cortex. The lower panel illustrates an axial view of ROIs with lower AC in sensorimotor areas, thalamic and pontine subcortical regions.

Once obtained the statistical parametric map describing the spatial distribution of the AC level in BOLD signal, we observed that AC is symmetrically distributed across hemispheres. This pattern is illustrated by Fig. 2.2: the upper panel illustrates the statistical map of the ROIs with higher AC in the frontoparietal areas, anterior insula and cingulate cortex; the lower panel illustrates an axial view of ROIs with lower AC in sensorimotor areas, thalamic and pontine subcortical regions.

We found that frontoparietal areas, anterior insula and cingulate cortex exhibit statistically significant higher AC levels compared to average. In contrast, sensorimotor areas, thalamic and pontine subcortical regions exhibit statistically significant lower AC levels compared to average. The ROIs with higher AC are the following: left Brodmann area 10 (BA10l); dorsal anterior cingulate cortex (dACC); frontal pole (FP); precuneus (Pcun); left supramarginal gyrus (SMGl); right supramarginal gyrus (SMGr) (Fig. 2.3).

This AC spatial distribution closely resembles the DMN and part of the ventral attentional network (VAN) and frontoparietal network (Biswal. et al., 1995; Biswal and Ulmer, 1999; De Luca et al., 2006; Dosenbach et al., 2007; Fox et al., 2006; Greicius, 2008; Greicius et al., 2003; D.S. Margulies et al., 2007; Mckeown et al., 1998; Seeley et al., 2007).

The ROIs with lower AC are the following: left Brodmann Area 6 (BA6l); right Brodmann area 6 (BA6r); left Brodmann area 3 (BA3l); right Brodmann area 3(BA3r); left medial dorsal nucleus of the thalamus (MDNl); right medial dorsal nucleus of the thalamus (MDNr); left superior nucleus of the thalamus (SNl); right superior nucleus of the thalamus (SNr).

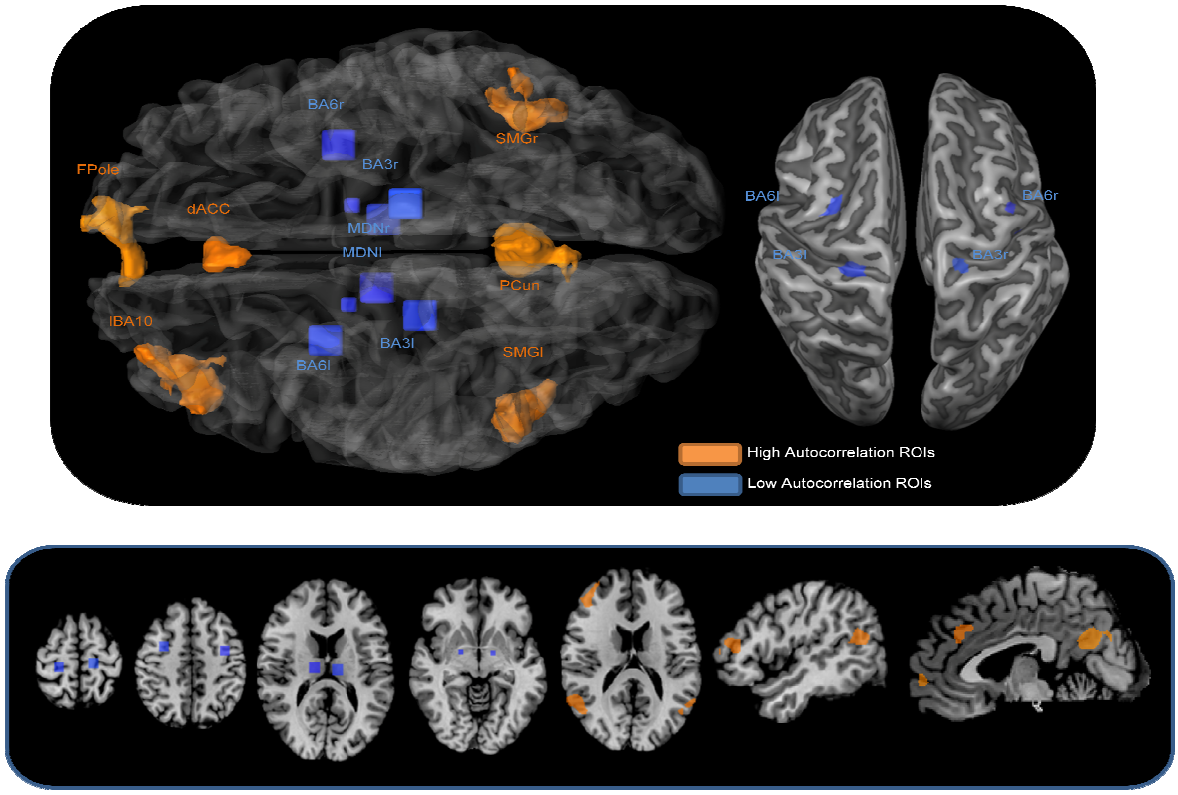

Fig. 2.3. ROIs location. ROIs with higher AC are colored in orange, while ROIs with lower AC are colored in blue. BA10l: left Brodmann area 10; dACC: dorsal anterior cingulate cortex; FP: frontal pole; Pcun: precuneus; SMGl: left supramarginal gyrus; SMGr: right supramarginal gyrus; BA6l: left Brodmann Area 6; BA6r: right Brodmann area 6; BA3l: left Brodmann area 3; BA3r: right Brodmann area 3; MDNl: left medial dorsal nucleus of the thalamus; MDNr: right medial dorsal nucleus of the thalamus; SNl: left superior nucleus of the thalamus; SNr: right superior nucleus of the thalamus.

2.3.2 Clustering

The markedly symmetrical distribution across hemispheres of the AC spatial pattern is evident if a hierarchical clustering algorithm is applied to the correlograms acquired from the ROIs (Fig. 2.4). In fact, two homologous areas of the hemispheres compose the first level of clustering; this occurs both for ROIs with higher AC levels and for ROIs with lower AC levels.

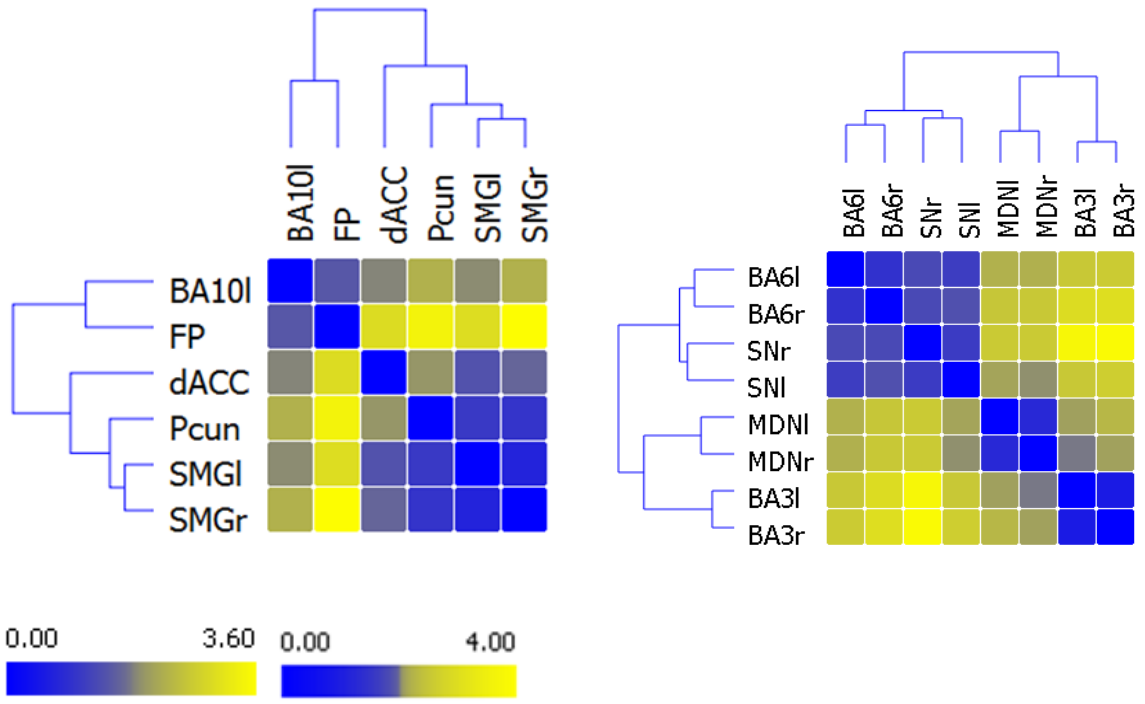

Fig.2.4.ROIs clustering. The left dendrogram describes the hierarchical clustering of the ROIs with lower AC, while the right dendrogram describes the hierarchical clustering of the ROIs with higher AC.

At the second level of clustering, areas with lower AC are grouped into three clusters: one composed of sensorimotor areas (BA 3 and 6), the other two composed of subcortical areas. In turn, areas with higher AC are also grouped into three clusters: one cluster composed of posterior areas (left and right supramarginal gyri and precuneus), one composed of just the anterior cingulate cortex (ACC) and another composed of frontal areas (left BA10l and frontal pole). Of note, at a third level of clustering, the ACC is grouped with the posterior areas.

This analysis confirms and better specifies the statistical differences between ROIs with high and low AC. Fig. 2.5 illustrates the results of the t test between the ROIs. A few exceptions aside (dACC-BA3l, dACC-MDNr, BA10l-MDNr, FP-MDNr, FP-MDNl, FP-BA3l, FP-BA3r, FP-SNl), differences between areas with higher AC and areas with lower AC are statistically significant. On the contrary, differences

between homologous areas are not statistically significant; this result is intuitively consistent as it can indicate a sort of symmetry in the AC distribution. Notably, within the brain regions with higher AC, frontal areas exhibit less AC level than posterior ones. Finally, among the posterior areas, the precuneus shows the highest AC level. This region has been related to important associative functions and is one of the essential parts of the DMN (Cavanna and Trimble, 2006).

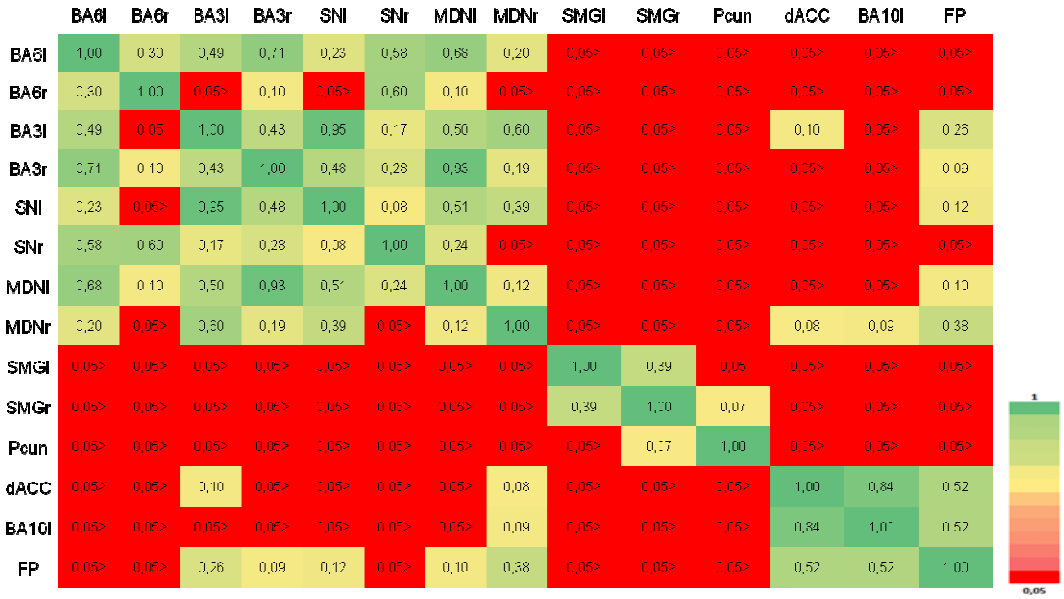

Fig.2.5. AC t test results. The figure shows the probability values of the paired samples t test on the angular coefficients of line fitting the first 5 lags of the autocorrelation function. When there is a significant difference between the two angular coefficients (Sig. 2-tailed) < 0.05, the cell color is red, otherwise is cool. Rows and columns are ordered in such a way that all ROIs with lower AC are closer. Also ROIs with higher AC are close to each other. Frontal ROIs and posterior ROIs occupy consecutive rows/columns so as to create modules.

2.3.3 High AC voxels in brain networks

For each brain network the calculation of the number of voxels with higher AC yielded the following results. The DMN appears to be the network with the highest number of higher AC voxels, followed by VAN and frontoparietal network (Fig. 2.6). This results confirms what has already been described in the statistical parametric map (Fig. 2.2), and accords well with all the others previous observations.

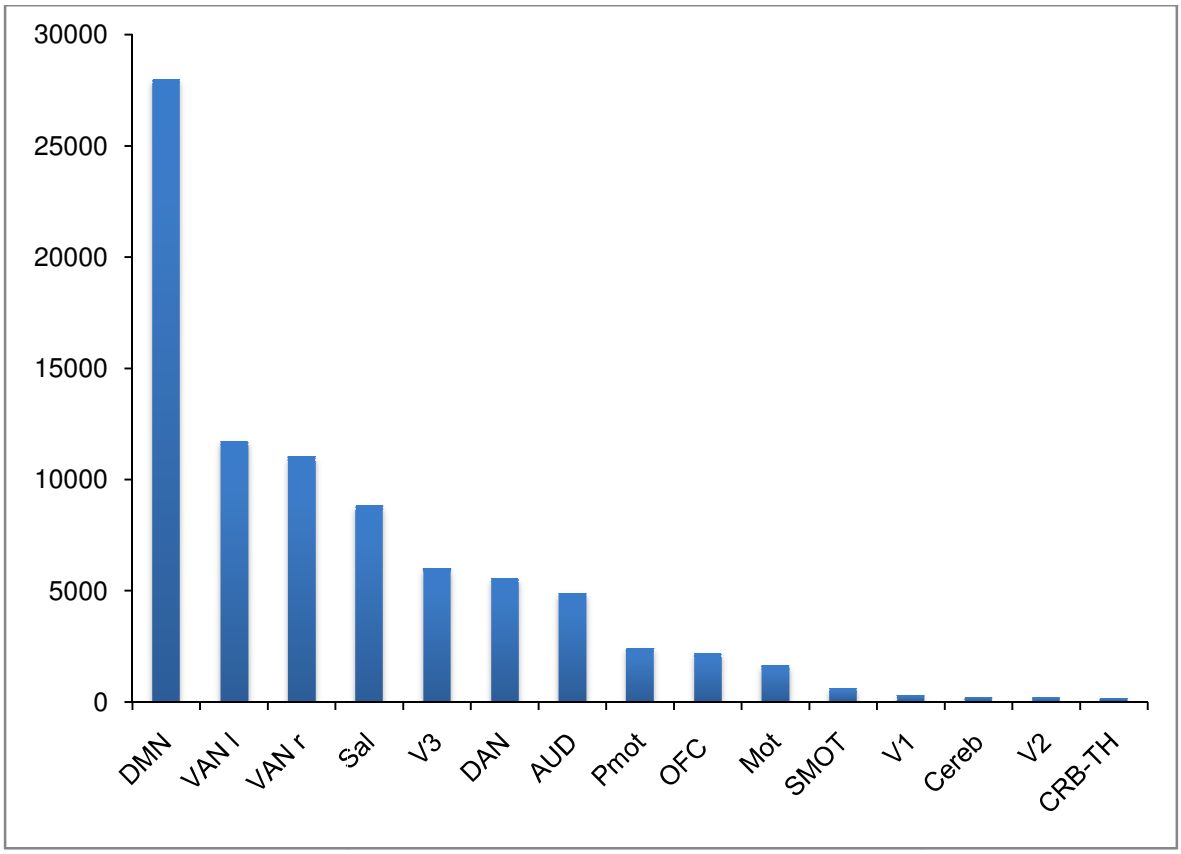

Fig.2.6. AC in brain networks. Different brain networks ordered by numbers of voxels with higher AC (Lag1+Lag2). These are the networks put forward by Biswal. DMN: default mode network, VANl: ventral attentional network left, VANr: ventral attentional network right, Sal: salience network, V3: third visual cortex, DAN: dorsal attentional network, AUD: auditive cortex, Pmot: premotor cortex, OFC: orbitofrontal cortex, Mot: motor cortex, SMOT: somatomotor cortex, V1: first visual cortex, Cereb: cerebellum, V2: second visual cortex, CRB-TH:

2.3.4 Comparison with the Hurst Exponent

We also measured the BOLD signal persistence using H as parameter. The Detrended Fluctuation Analysis (H) was used to estimate the Hurst parameter (Peng et al., 1994). Notably, the comparison between AC values and those

obtained with H produced similar results, even though with H many differences between ROIs were no longer statistically significant (Fig. 2.7).

	BA6l	BA6r	BA3l	BA3r	SNl	SNr	MDNl	MDNr	SMGl	SMGr	Pcun	dACC	BA10l	FP
BA6l	1,00	0,24	0,73	0,84	0,94	0,28	0,52	0,73	0,59	0,72	0,90	0,28	0,05>	0,13
BA6r	0,24	1,00	0,96	0,85	0,36	0,80	0,89	0,19	0,40	0,31	0,31	0,08	0,05>	0,10
BA3l	0,73	0,96	1,00	0,67	0,70	0,85	0,98	0,66	0,57	0,61	0,66	0,40	0,09	0,05>
BA3r	0,84	0,85	0,67	1,00	0,80	0,70	0,87	0,76	0,65	0,70	0,77	0,44	0,07	0,05>
SNl	0,94	0,36	0,70	0,80	1,00	0,22	0,50	0,82	0,54	0,75	0,94	0,33	0,05>	0,12
SNr	0,28	0,80	0,85	0,70	0,22	1,00	0,74	0,32	0,18	0,23	0,24	0,05>	0,05>	0,05>
MDNl	0,52	0,89	0,98	0,87	0,50	0,74	1,00	0,23	0,34	0,37	0,40	0,20	0,05>	0,06
MDNr	0,73	0,19	0,66	0,76	0,82	0,32	0,23	1,00	0,83	0,93	0,87	0,44	0,05>	0,22
SMGl	0,59	0,40	0,57	0,65	0,54	0,18	0,34	0,83	1,00	0,84	0,51	0,50	0,05>	0,26
SMGr	0,72	0,17	0,61	0,70	0,75	0,23	0,37	0,93	0,84	1,00	0,71	0,37	0,05>	0,23
Pcun	0,90	0,31	0,66	0,77	0,94	0,24	0,40	0,87	0,51	0,71	1,00	0,31	0,05>	0,14
dACC	0,28	0,08	0,40	0,44	0,33	0,05>	0,20	0,44	0,50	0,37	0,31	1,00	0,15	0,36
BA10l	0,05>	0,05>	0,09	0,07	0,05>	0,05>	0,05>	0,05>	0,05>	0,05>	0,05>	0,15	1,00	0,78
FP	0,13	0,10	0,05>	0,05>	0,12	0,05>	0,06	0,22	0,26	0,23	0,14	0,36	0,78	1,00

Fig.2.7. Hurst t test results. The figure shows the probability values of the paired samples t test on the Hurst exponent (H). When there is a significant difference between H and AC (Sig. 2-tailed)< 0.05, the cell color is red, otherwise is cool.

2.4 Discussion

Our analysis provides evidence that AC could be an interesting index to explore voxel-wise the memory level or persistence of the BOLD signal. In fact, we observed: i) that the pattern of AC level distributes symmetrically across hemispheres; ii) that the AC spatial distribution reflects the patterns of certain large-scale resting state networks; iii) and that unimodal and multimodal areas exhibit lower and higher AC levels, respectively. These findings suggest that the BOLD signal AC during resting state is not exclusively the result of physiological noise but also the result of functional brain organization.

In particular, we found evidence that the spatial distribution of AC level reflects the distinction between primary (or unimodal) and secondary (or multimodal or associative) brain areas. The former (auditory, visual and somatic areas) exhibit lower AC levels, while the latter (associative regions of the frontal, parietal, and temporal lobes) exhibit higher AC levels. It is worth noting that this distinction strongly resembles the functional organization described as “dual intertwined rings architecture” (Mesmoudi et al., 2013). In this model, somatosensory regions (visual, somatic, and auditory) form one ring, called VSA, while parietal, temporal and frontal areas form the other ring, called PTF. Notably, we found that the brain areas with higher AC levels are parts of the PTF ring, while the brain areas with lower AC levels are within the VSA ring.

It has been suggested that two different timings characterize the integration process within the two rings, so that the brain could achieve a multi-temporal

integration of sensory stimuli with past and present information and use it to adopt different and appropriate courses of action (Mesmoudi et al., 2013). Thus, in this perspective, a persistent BOLD signal might be indicative that the brain is maintaining information in order to connect past, present and future events (He, 2011; Wink et al., 2008).

We also analyzed the distribution of voxels with high AC in the different rsN, and found that most of these voxels are part of the DMN, VAN and the salience network. This provides further evidence for the previous observation about the dual ring different timing. Remarkably AC level in V1,V2 and V3 reflects the hierarchical organization of primary and secondary sensory visual areas (Wandell et al., 2007), as compared to V1 and V2the higher presence of voxels with high AC level in V3 reveals a persistence in BOLD signal that could be an implication of higher level of information processing in that area.

In previous studies, analyses of the BOLD signal and its persistence have been carried out with the parameters of the frequency spectrum and H, resulting in a strong correlation between the H and the power spectrum, described with a power-law exponent.

The first inspection of the persistence of the BOLD signal, performed using H as parameter, has revealed that the BOLD signal coming from GM exhibits higher persistence values than the BOLD signal coming from WM or CSF (Biswal et al., 2010; Maxim et al., 2005; Wink et al., 2008; Zuo et al., 2010). Moreover, the long memory of the signal measured with H decreases during task conditions compared to rest (He, 2011), so much so that higher H values have been reported within the DMN, whereas lower H values have been reported within the salience,

attentional and visual networks, with the lowest H values observed in motor and subcortical networks (Ciuciu et al., 2014). All these results are in line with our findings, which argue for the hypothesis that, compared to associative brain regions, unimodal areas are supposed to have lower AC levels in virtue of their less complex functional organization.

However, although a study sustained that with H it is possible to obtain evidence of long memory in random series (Sánchez Granero et al., 2008), the calculation of this parameter presents difficulties (Cannon et al., 1997). In fact, in order to calculate H, temporal series must be appreciably long. And it has been pointed out that the estimation of H is less reliable for values around 0.5 (Schepers et al., 2002).

Interestingly, it has been found that the BOLD signal coming from regions that are part of cognitive networks has a frequency spectrum with more power on the lower frequency compared to the values of perceptual networks (Ding et al., 2011; Salvador et al., 2008; Zuo et al., 2010). Given the relation between AC and the power spectrum, described by the Wiener-Khinchin theorem, these findings further support our results, as a signal with a power that is more distributed on lower frequencies is supposed to show higher AC levels than a signal with a power that is less distributed on lower frequencies, and this signal longer persistence could be the necessary support to cognitive functions.

To our best knowledge, only one study has thus far investigated the AC spatial distribution of BOLD signal in resting state (Kaneoke et al., 2012). This paper points out that the AC spatial distribution somehow reflects the pattern of the DMN (Buckner et al., 2008). Here we found that the ROIs with higher AC levels are

parts of the DMN as well as of the VAN and frontoparietal network. The study of Kaneoke et al. used AC to spot differences between precuneus and posterior cingulate cortex (PCC). Intriguingly, in their analysis the BOLD signal of the cognitive and associative subareas of precuneus exhibited a higher AC level than the BOLD signal of the visual and somatosensory subareas (Margulies et al., 2007; Margulies et al., 2009). What is more, AC levels were found to be higher in the ventral PCC (vPCC) compared with those of the dorsal PCC; notably, vPCC is the most connected subarea of PCC within the DMN. The DMN is known to be active during tasks involving internal focusing, such as autobiographical memory or elaboration of future plans (Buckner et al., 2008; Shannon and Buckner, 2004; Vincent et al., 2006; Wheeler and Buckner, 2004). Coherently, the vPCC is active during tasks involving autobiographical memory (Svoboda et al., 2006) as well as future planning (Schacter et al., 2007). Of note, lesions of vPCC can cause amnesia (Leech et al., 2011; Valenstein et al., 1987).

Another study has associated the BOLD signal with higher AC levels with brain areas characterized by a higher number of both long-range and short-range synaptic connections (Baria et al., 2013; Baria et al., 2011). What is more, the AC cortical pattern distribution is similar to the pattern distribution of the myelin content, and it is known that unimodal areas have a higher myelin content than multimodal associative regions (Fuster, 1997; Glasser and Van Essen, 2011). In fact, associative regions have a higher neuronal density with more extended dendritic ramifications and synapses (Collins, et al., 2010). Given that the main function of myelin is to speed up the axonal impulse, it should be extremely interesting to investigate this aspect in relation to the BOLD signal persistence.

All the aforementioned studies are not only consistent with each other but also with a recent paper showing that certain brain areas appear to have a BOLD signal at rest characterized by scale-free behavior and a Lévy flight course (Costa et al., 2016).

The BOLD signal has well known neurophysiological underpinnings (He et al., 2008; Lauritzen and Gold, 2003; Palva and Palva, 2012) and at this level interesting research has been done on its persistence. For instance, AC of the electrode signal at rest was studied in humans with recorded electrocorticography (ECoG). AC level was found to be higher in prefrontal and other associative areas, and lower in auditory and visual areas, but, intriguingly, in these sensory areas it showed a tendency to increase from primary areas to more integrative areas (Honey et al., 2013). Similar results were found by analyzing single neuron spike trains in primate cortex, which showed higher AC levels in prefrontal areas, average AC levels in parietal associative areas and lower AC levels in sensory areas (Murray et al., 2014).

Furthermore, another study explored the relationship between the temporal properties of large-scale networks and the co-expression of human genes. Congruence was found between expression of subsets of genes, temporal properties of the proteins coded by these genes, and the functional organization of different brain areas. In particular, genes coding for proteins associated with faster neural transmission were more co-expressed in unimodal areas, whereas genes coding for proteins associated with slower and sustained neural activation were more co-expressed in multimodal associative areas (Cioli et al., 2014).

These results seem to be in agreement with our findings showing a higher persistence of the BOLD signal in higher-order cortical areas. Future investigations are nonetheless needed in order to confirm this intriguing relationship between genetic expression and brain functional organization.

Other worthwhile directions for future research are the issues of how the AC level distribution differs within pathological and control subjects, as well as of how it changes during the human life cycle, particularly in healthy aging subjects. In patients with Alzheimer's disease, for instance, the regions showing accumulation of with beta-amyloid plaques are the same regions that compose the DMN (Bartzokis et al., 2007, Buckner and Vincent, 2007). Furthermore, most of the other neurodegenerative diseases present atrophy in regions that are parts of the DMN, salience and executive control networks (Ahmed et al., 2016). And these important networks have also been found to be altered in a variety of psychiatric conditions (Goodkind et al., 2015; McTeague et al., 2016).

In line with our analysis, the involvement of large-scale networks of associative areas in brain disorders might suggest a decrease in AC levels within those areas. More findings on this important issue will positively impact on clinical practice, as the BOLD signal AC may be discovered to be a significant biomarker for both neurological and psychiatric conditions.

2.5 Conclusion

Although part of BOLD signal AC is noise, another part, especially during the resting state condition, can convey relevant neurophysiological information. This type of information can be related to the processing memory or persistence of brain functional organization (Ball et al., 2011; Buckner et al., 2008; Buckner and Carroll, 2007; Fuster, 1997; Fuster and Bressler, 2012; Gusnard et al., 2001; Raichle et al., 2001; Schacter et al., 2007; Strogatz, 2001). In fact, analyses carried out in this study provide evidence that 1) the BOLD signal AC level appears to be spatially distributed in specific or meaningful patterns; 2) different AC levels characterize different rsN; and, finally, 3) unimodal (or sensory) and multimodal (or associative) brain areas show different AC levels. In particular, multimodal regions exhibit higher memory or persistence values in the BOLD signal compared to unimodal and subcortical regions. This suggests a relationship between higher AC values and higher-order cognitive functions, so that the BOLD signal AC in resting state may be considered as a potential parameter to measure the capacity for storing and processing information across different brain areas, which opens the possibility of future use of this parameter in clinical contexts.

2.6 Foreword Study 2

While in the first study we aimed to validate AC as a good method to measure BOLD signal persistence, in the second study we aimed to verify the possibility of using AC as a biomarker for brain disease. We chose to investigate AC in ASD because cognitive theories about this disorder involve the role of those areas that we already observed to have a high persistence in BOLD signal.

Thus, the research questions of study 2 were the following: concerning BOLD signal persistence, are there differences between individuals with ASD and controls? In case of positive answer, can these differences be located in the brain areas that, according to the cognitive theories about ASD, play a role in the development of this condition? And, finally, is AC pattern informative enough to help distinguish between autistic and healthy individuals?

Study 2

Autocorrelation of BOLD signal used as a parameter to classify autistic subjects

Ugo Vercelli[1,2,3], Stefano Moia[1,2,3], Jordi Manuello[1,2,3], Andrea Nani[1,2,3],

Tommaso Costa[1,2,3], Karina Tatu[1,2,3], Sergio Duca[1,3], Franco Cauda[1,2,3]

1 GCS fMRI, Koelliker Hospital and University of Turin, Turin, Italy

2 Department of Psychology, University of Turin, Turin, Italy

3 FOCUS Lab, Department of Psychology, University of Turin, Turin, Italy

3.1 Introduction

3.1.1 Persistence of BOLD signal measured with autocorrelation

In study 1 (Vercelli et al., 2017) we investigated the AC of fMRI BOLD signal at rest and found that a higher level of AC is measured in the BOLD signal coming from heteromodal areas (associated with the higher cognitive functions) compared to a lower AC measured in unimodal/somatosensory and subcortical cortices. A higher AC means that the BOLD signal is more persistent, which is to say that the signal level fluctuates slowly. What is the physiological meaning of this dynamic is not as yet clear but a possibility is that a higher level of information integration needs more permanence of the signal. In his seminal paper, published in 1998, Mesulam refers to the temporal expansion that is needed to integrate asynchronous information, that is, information coming at different times (Mesulam, 1998). According to his hypothesis, different information must be “kept on line” to construct a coherent and integrated picture of reality. Thus, given that the persistent reverberation of neuronal spiking activity is assumed as a correlate of working memory (Amit, 1995), and that BOLD signal is an indirect measure of neuronal activity, we can hypothesize that also the persistence of BOLD signal might be connected with the process of working memory.

3.1.2 Neuroimaging and ASD

Neuroimaging made possible non-invasive research with better accuracy compared to the past. Techniques like structural MRI, functional MRI and diffusion MRI have been applied to study both the normal and the pathological brain. Also ASD has been investigated as to GM and WM differences and abnormal functional connectivity of patients compared to normal subjects. In particular, the creation of a specific database with MRI and behavioral data about autistic subjects has been a concrete help for research in the quest for studying ASD (Di Martino et al., 2014).

Compared to normal subjects, structural MRI investigations have reported cortical differences (GM decreases and GM increases) in patients with ASD. On the basis of the results of a meta-analysis (Cauda et al., 2011b) including 16 papers and 728 subjects, differences were detected in regions involved in the ToM cognitive function; GM increases and GM decreases were especially reported in the middle temporal gyrus, posterior cingular cortex, precuneus and amygdala. Other significant differences were detected in the cerebellum and in the insula, a brain region involved in important functions ranging from pain perception and speech production to social emotions (Cauda et al., 2012b), including the conscious monitoring of the body's condition via the integration of different unconscious stimuli (both external and internal) with emotional processes, as well as the conscious detection of error (Cauda et al., 2012a, 2011a; Klein et al., 2013; Nieuwenhuys, 2012; Vercelli et al., 2014; Wylie and Tregellas, 2010). Finally, modifications were also detected in the caudate nucleus, a part of the basal

ganglia involved both in motor and cognitive tasks (Haber, 2016). A further meta-analysis investigated WM abnormalities and found accordance between GM and WM alterations (Cauda et al., 2014).

As to the functional connectivity, several studies investigated the functional changes in patients with ASD in the light of the cognitive theories of this condition.

The main cognitive theories of ASD focus on two closely related aspects: the theory of mind and executive dysfunctions (Austin et al., 2014). However, studies that have investigated these aspects with fMRI techniques did not produced homogeneous results (Margulies et al., 2009; Naughtin et al., 2017; Prat et al., 2016; Sharfitz, 2015; Spunt and Adolphs, 2017).

Conversely, there is a good general agreement on the so-called “under-connectivity theory”, which suggests that autistic subjects exhibit a reduced cortico-cortical connectivity, particularly between frontal and posterior cortical areas(Just et al., 2012, 2004).

It is worth noting that, in addition to the under-connectivity theory, also an over-connectivity theory has been proposed (Belmonte et al., 2004), which suggests that over-connectivity patterns may be present at cortical local level; on this aspect, however, there is no consensus yet (Hull et al., 2017; Picci et al., 2016).

Dysfunction in brain networks have been repeatedly found in patients with ASD, particularly in the DMN (Di Martino et al., 2014; Minshew and Keller, 2010; Monk et al., 2009; Weng et al., 2010) and salience network areas (Kleinhans et al., 2008; Uddin and Menon, 2010).

In addition to these anatomical and functional findings, study 2 was aimed to test the hypothesis that also AC could be altereted in the BOLD signal patterns of autistic subjects, and, if so, whether AC could be used as a parameter to discriminate between autistic and control subjects.

3.2 Materials and methods

3.2.1 Subjects

Subjects' data for this study were obtained from the open access database of the Autism Brain Imaging Data Exchange (ABIDE) consortium (Di Martino et al., 2014). ABIDE is a database focused on autism and is composed of two databases, ABIDE I and ABIDEII. The existence of this database was another good reason to choose this condition to test AC as a possible biomarker.

In our study we selected subjects from ABIDE I, that is composed of 1112 subjects, 539 with ASD and 573 typical controls. Age is between 7 and 64, with a median of 14.7 years. Datasets come from 20 different sites. Anatomical and functional resting state imaging data are available together with phenotypic datasets. Although extremely useful, this database is quite heterogeneous; acquisition are done with subjects keeping eyes sometimes open, sometimes closed, with different models of scanners of different producers and, above all, different scanning sequences.

As we plan to use the data for classifying with a sample vector machine (SVM), we followed the recommendation to select subjects with a longer acquisition time. In fact, as we can see in Fig. 3.1, longer acquisition times improve classification accuracy.

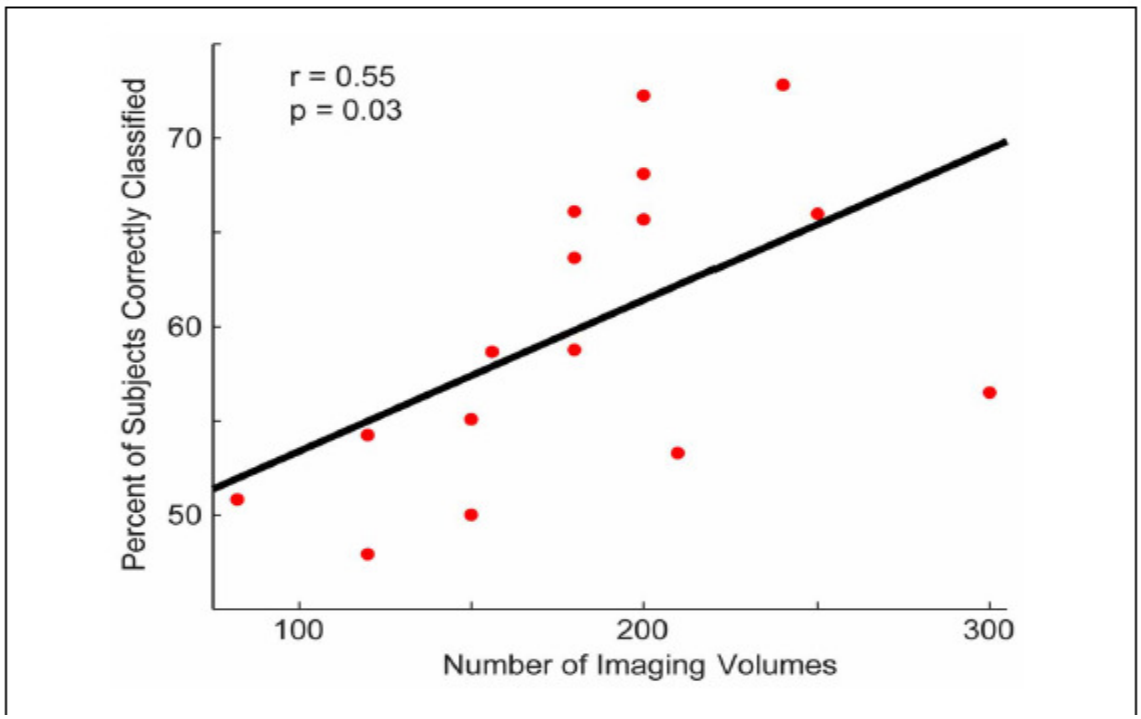

Fig.3.1.Classification accuracy increases with the increase of volumes acquired (Nielsen et al., 2013).

Therefore we only selected the ABIDE studies with an acquisition time of (at least) 180 volumes (6 minutes). This choice was due not only to improve the classification accuracy but also to have a better evaluation of AC (Herman et al., 2011).

The final selection consisted of resting state data of 792 subjects: 385 with ASD (age range 7-64 yo, mean=17.13±8.05 yo) and 407 neurotypical controls (NC) (age range 6.47-42 yo, mean=17±7 yo).

These data were obtained from 14 sites.

Site	Control	Autistic	Asperger	PDD-NOS	M	F	Age Mean	Age SD
CMU	13	14			21	6	26,6	5,7
LEAUV1	15	14			29		22,6	3,5
LEAUV2	20	15			27	8	14,1	1,6
MAX	6	2	8		16		14,8	10,4
NYU	105	53	21	5	147	37	15,3	6,6
OLI	16	20			31	5	16,8	3,5
PTT	27	29			48	8	18,9	6,9
SBL	15	2	7	6	30		34,4	8,6
SOSU	24	3	7	2	29	7	14,5	1,9
STAN	20	20			32	8	9,9	1,5
UM1	57	45	7	1	84	26	13,4	2,8
UM2	22	10	3	1	33	2	16,1	3,4
USM	43	57		1	101		22,1	7,7
YALE	28	6	8	14	40	16	12,8	2,9

Table3.1. Subjects for site: number of controls, of autistic patients, Asperger and PDD-NOS, males, females, mean age and standard deviation age.

Different assessment tools were employed across sites to measure Full Intelligence Quotient (FIQ): Differential Ability Scales II-School age (DAS-II), Wechsler Abbreviated Scales of Intelligence (WASI), Wechsler Intelligence Scale for Children, (WISC), Wechsler Adult Intelligence Scales (WAIS), Hamburg-Wechsler Intelligence test for Children (HAWIK-IV), Wortschatz test (WST). All these scales have a minimum of 50 and a maximum of 160 scores, save for DAS-II that has 30 and 170 as extreme scores. So we assumed that all scores are almost comparable.

3.2.2 MRI data analysis

A custom script, based on FMRIB Software (FSL); (Jenkinson et al., 2012b) and Analysis of Functional NeuroImage (AFNI); (Cox, 1996) was used for the preprocessing of the MRI volumes. It consisted in: anatomical reorientation and skull stripping, functional reorientation, motion correction, functional brain extraction, non-linear normalization computation, segmentation, CSF and WM signal extraction, spatial smoothing (6 mm FWHM), nuisance, grand mean scaling, detrending, volumes normalization.

To take into account magnetization instability, the first 10 timepoints of the rs-fMRI were discarded before the functional reorientation. The detrending, both linear and quadratic, was made using fsl_regfilt command. No temporal filtering, prewithening or Global Signal Regression were applied.

3.2.3 First level analysis

The smoothness of the BOLD signal was computed voxelwise for every subject, obtaining one Brain Smoothness Map (BSm) per subject. The computation was performed in MATLAB® (MathWorks, 2012)·, averaging the value of the autocorrelation value at lag 1 and lag 2, and expressing it as the hyperbolic arctangent of the result (as a z-Fisher transformed map).

Given a vector Xt and its variation at lag 1 (Xt+1) and at lag 2 (Xt+2):

$$X_t = \{x_1, x_2, \ldots, x_n\}$$
$$X_{t+1} = \{x_{2,} x_3, \ldots, x_n\}$$
$$X_{t+2} = \{x_{3,} x_4, \ldots, x_n\}$$

Smoothness can be computed as:

$$S = \tanh^{-1}\left[\frac{corr(X_t, X_{t+1}) + corr(X_t, X_{t+2})}{2}\right] \quad (9)$$

3.2.3 Second Level Analysis

Before the second level analysis, to take into account the age range of the sample, age was treated as a non-explanatory covariate and regressed from the Bsm volumes with fsl_regfilt.

A standard non-parametric test was performed using FSL's tool randomize (Winkler et al., 2014) with 5000 permutations. TFCE corrected p values maps were obtained and a threshold was applied in order to have statistical significant maps ($p<=0.05$). Only the contrast NC > ASD was found significant. The obtained map is displayed in fig. 3.3.

3.2.4 Classification with SVM

To classificate ASD and control subjects we employed a multi-voxel pattern analysis (MVPA), a technique capable of searching through data to identify patterns of features that are highly predictive of different conditions. For a review see (Mahmoudi et al., 2012). SVM performs classification by constructing the best multidimensional hyperplane that separates the data into two categories.

To explain the algorithm we can hipotize that each subject has just two voxels X and Y. Each voxel has a AC value and is positioned in a Cartesian plan where the 2 axes are the AC values of the 2 voxels.

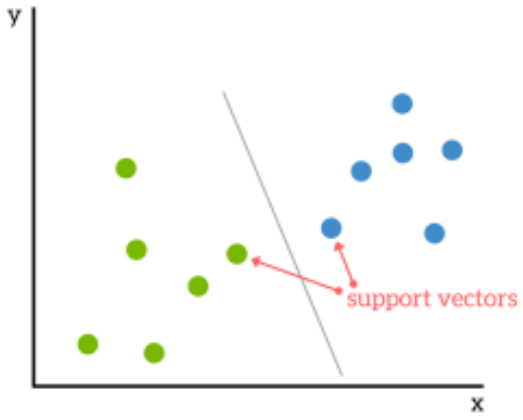

Fig. 3.2.http://www.kdnuggets.com/2016/07/support-vector-machines-simple-explanation.html

In this sample a straight line can divide the subjects into two groups.

When the voxels are 3, the plain becomes a 3D space and the line becomes a plane, with more voxels we can talk of hyperspace and hyperplane.

Each example is an input vector $x_i(i = 1, \dots, N)$, the features M (i.e. x_i in R^M) in our case are the number of voxels, and each subject can be associated with two classes y=1 or +1, in our case -1 is the autistic class and +1 the control class.

The data points closer to the hyperplane are called “support vectors” and are those that determine the shape of the best hyperplane. The distance between the support vectors and the hyperplane is called “margin” and the higher it is, the better the classification.

The discriminating function with the highest margin is

$$f(x) = w \cdot x + b. \tag{10}$$

Where w is the normal weight vector of the hyperplane, b is the bias and translates the origin of the feature space.

We can also write:

$$w \cdot x = \sum_{j=1}^{M} w^{(j)} x^{(j)} \tag{11}$$

SVM tries to find the best hyperplane$w \cdot x + b = 0$ that can maximize the margin $2/\|w\|$

The problem to solve is:

$$\min_{w,b} \frac{1}{2}\|w\|^2 \tag{12}$$

with the constraints:

$$y_i(x_i \cdot w + b) \geq 1, \forall i \in \{1, \ldots., N\}$$

In case data do not allow for a clearly separating hyperplane, a slack variable is introduced: $\xi_i \geq 0$ for all $i \in \{1, \ldots, N\}$,

$$y_i(x_i \cdot w + b) \geq 1 - \xi_i \tag{13}$$

When $\xi_i = 0$, no training errors are permitted and this situation is called “hard margin”.

With $0 \leq \xi_i \leq 1$, some subjects can be located in the margin.

With $\xi_i \geq 1$, some errors are permitted and this case is described as “soft margin”. To optimize the complexity of the hyperplane and the number of errors, a penalty factor C is introduced.

With this factor the problem is:

$$\min_{w,b,\xi} \frac{1}{2}\|w\|^2 + C\sum_{i=1}^{N}\xi_i \quad (14)$$

With the constraints $y_i(x_i \cdot w + b) - 1 + \xi_i \geq 0$

$$, \forall i \in \{1, \ldots., N\}, \quad \xi_i \geq 0$$

There are 2 steps in the procedure of a classification. First the SVM is trained on a set, and then it is validated on another set.

As in most of the applications of SVM in fMRI, the number of features (voxels) is much higher than the number f examples (subjects), M>N. This problem is described as “the curse of dimensionality”. With the increase of dimensions the space increases so much that the data become sparse and this is a problem for any method demanding statistical significance. To avoid it, “cross validation” can be used, and following Kohavi we applied a ten-fold cross validation (Kohavi, 1995)

The data were divided in 10 parts, 9 were used as training set, one as validation set, and this was repeated 10 times, changing the validation set each time.

The 10 results were averaged to obtain a single accuracy estimation.

We applied the SVM to all subjects together and also when they were divided into three categories.

The 3 categories were the data base site, the age category and the cognitive level.

3.4 Results

3.4.1 Differences between ASD and NC subjects at group level

Once obtained, the statistical map (Fig. 3.3) with the contrast between ASD and NC subjects (NC> ASD) was examined for statistically significant differences concerning BOLD signal AC level.

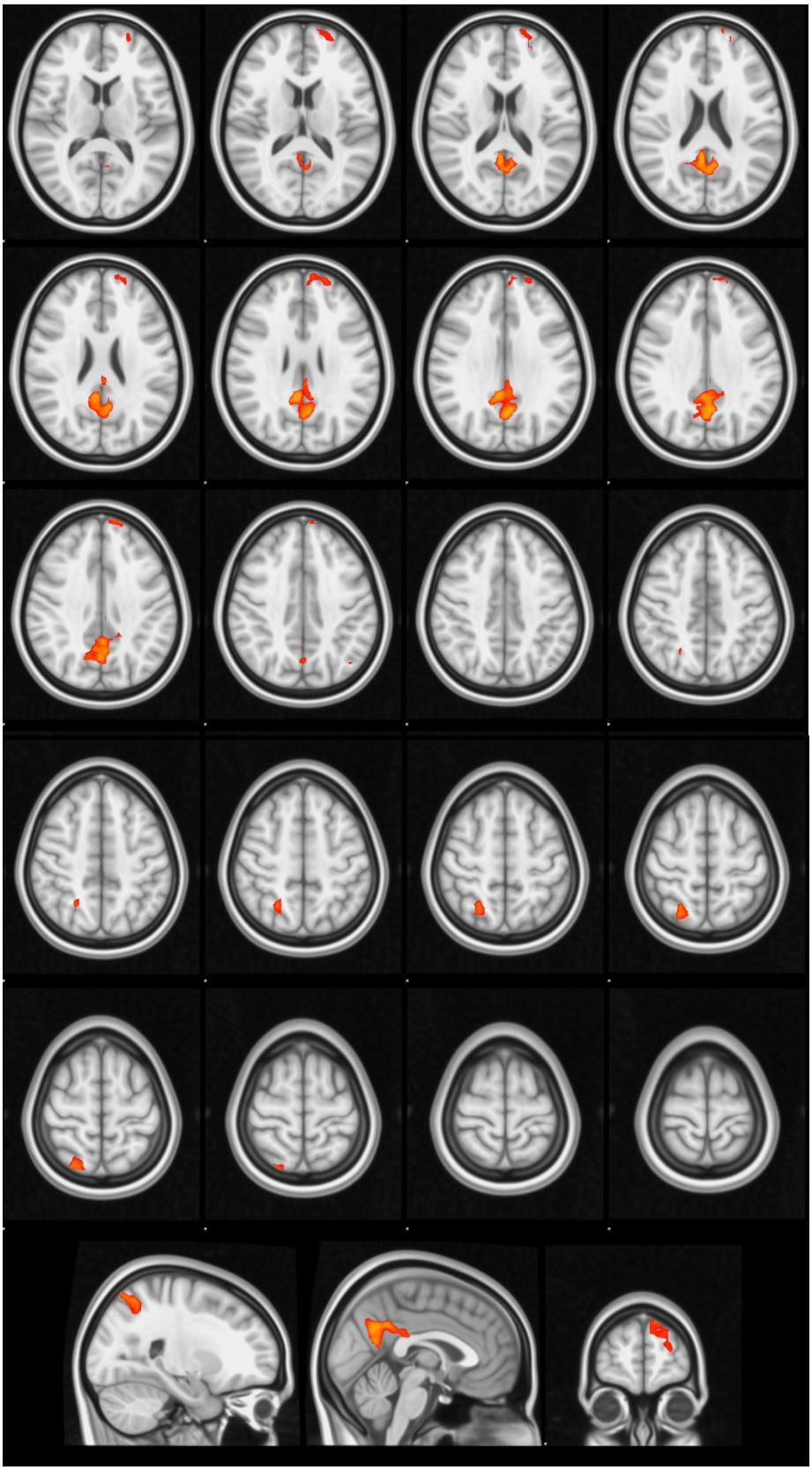

Fig.3.3.Brain areas with a significant statistically higher AC level in control subjects compared to ASD subjects.

Only the contrast NC > ASD was found significant, as ASD subjects exhibit a lower AC in the areas of prefrontal, posterior medial and posterior parietal cortices.

Tab. 3.2 illustrates the main statistics obtained with Mango (Research Imaging Institute, n.d.) concerning the main clusters of the statistical map.

Description	Mean	SD	Size (mm)	Voxels	
Cluster 1 of 7	0,969	0,0095	8856	328	
Cluster 2 of 7	0,957	0,0030	2106	78	
Cluster 3 of 7	0,962	0,0068	1836	68	
Cluster 4 of 7	0,951	0,0000	54	2	
Cluster 5 of 7	0,952	NaN	27	1	
Cluster 6 of 7	0,951	NaN	27	1	

Table 3.2. Brain areas (clusters) with mean statistically significance, standard deviation of significance, size of the clustering (mm) and in number of voxels.

As we can see, there are 3 consistent clusters, as the others are quite small and located closely to the bigger 3.

Cluster	Value		X	Y	Z	Label 1	Label 2	Label 3
1	0.985	Max	6	-45	27	Right Cerebrum	Limbic Lobe	Pos Cingulate
1	0.953	Min	3	-69	39	Right Cerebrum	Parietal Lobe	Precuneus
1	0.947	Centr	0	-51	30	Left Cerebrum	Limbic Lobe	Cingulate Gyrus
2	0.964	Max	-12	60	36	Left Cerebrum	Frontal Lobe	Sup Frontal Gyrus
2	0.951	Min	-9	60	39	Left Cerebrum	Frontal Lobe	Sup Frontal Gyrus
2	0.962	Centr	-18	60	27	Left Cerebrum	Frontal Lobe	Sup Frontal Gyrus
3	0.974	Max	24	-60	57	Right Cerebrum	Parietal Lobe	Precuneus
3	0.951	Min	24	-60	60	Right Cerebrum	Parietal Lobe	Sup Parietal Lob
3	0.968	Centr	21	-63	57	Right Cerebrum	Parietal Lobe	Precuneus

Table 3.3. Clusters' significance values; location in MNI coordinates and labels refer to the MNI (Nearest grey matter) as Mango output (Collins et al., 1995; Mazziotta et al., 2001).

To label and locate at group level the areas where AC level is statistically different between autistic and control subjects, as well as to define the cognitive functions of these areas in an objective way, we used Neurosynth. For an exhaustive explanation see (Yarkoni et al., 2011). Neurosynth is a platform for automatically synthesizing the results of more than 11000 neuroimaging studies. Starting from the statistical map with the contrast between ASD and NC subjects (NC> ASD) we introduced in Neurosynth the coordinates of the three more relevant locations. Fig. 3.4 shows the map of functional connectivity related to the first location, which is the posteromedial part of the DMN.

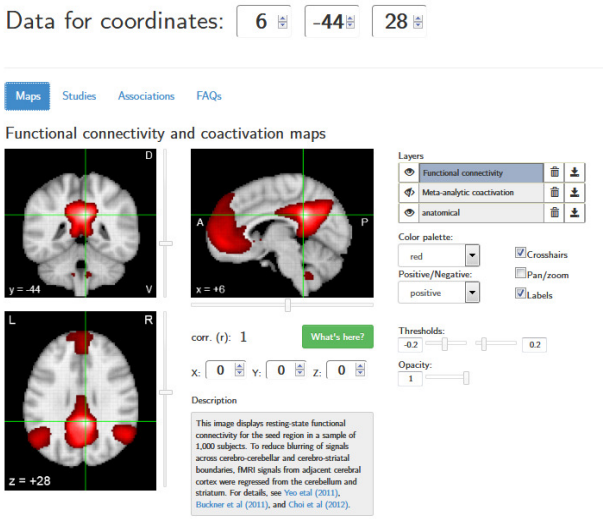

Fig. 3.4. The Neurosynth coactivations map of the first location.

The decoding result gives a list of cognitive terms; posterior cingulate, resting state, precuneus, medial prefrontal, deactivation, default mode.

Most of them just describe the position while other terms refer to the fact that this is the pattern of the DMN.

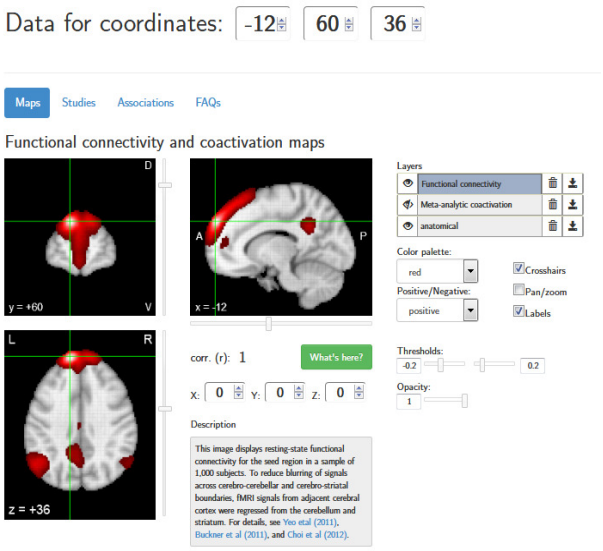

Fig.3.5. The Neurosynth coactivations map of the second location.

The functional connectivity map of the second location (in a prefrontal position) resembles the DMN pattern and the related cognitive terms are “mental states”, “mind”, ”self”, ”mentalizing”, also terms related to the DMN functions (Fig. 3.6).

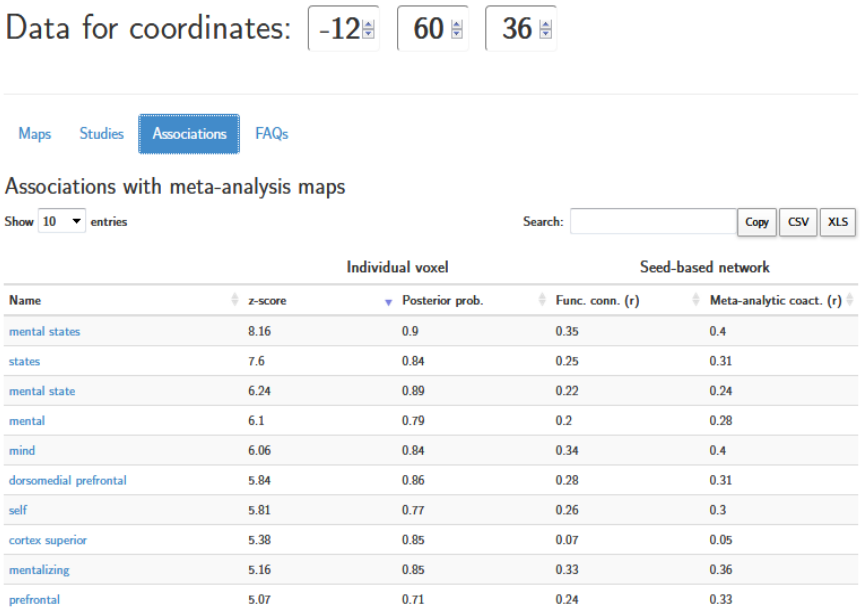

	Individual voxel		Seed-based network	
Name	z-score	Posterior prob.	Func. conn. (r)	Meta-analytic coact. (r)
mental states	8.16	0.9	0.35	0.4
states	7.6	0.84	0.25	0.31
mental state	6.24	0.89	0.22	0.24
mental	6.1	0.79	0.2	0.28
mind	6.06	0.84	0.34	0.4
dorsomedial prefrontal	5.84	0.86	0.28	0.31
self	5.81	0.77	0.26	0.3
cortex superior	5.38	0.85	0.07	0.05
mentalizing	5.16	0.85	0.33	0.36
prefrontal	5.07	0.71	0.24	0.33

Fig. 3.6. List of cognitive domains related to the second location’s local maxima.

If we look at the terms related to the centroid of the second location, we find also “mind ToM” cognitive domain (Fig. 3.7).

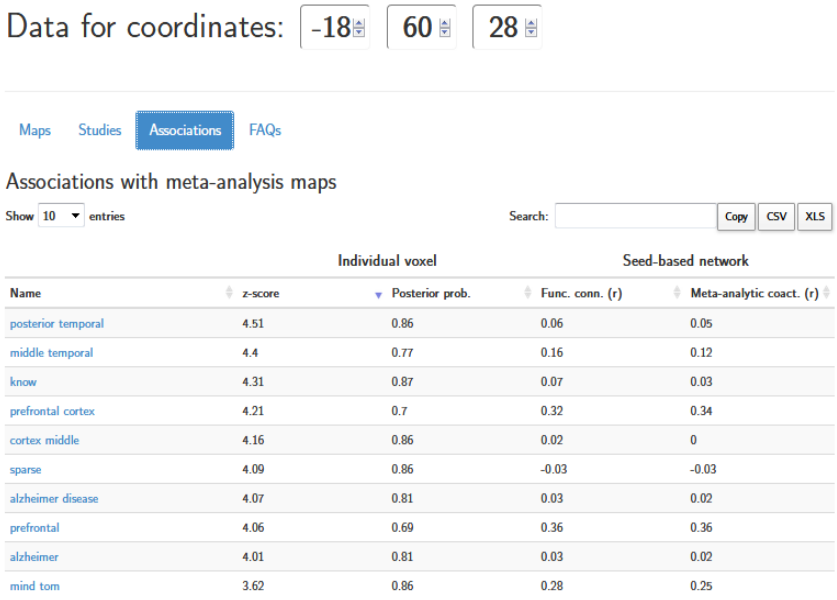

Data for coordinates: -18 60 28

Maps Studies Associations FAQs

Associations with meta-analysis maps

Show 10 entries Search: Copy CSV XLS

	Individual voxel		Seed-based network	
Name	z-score	Posterior prob.	Func. conn. (r)	Meta-analytic coact. (r)
posterior temporal	4.51	0.86	0.06	0.05
middle temporal	4.4	0.77	0.16	0.12
know	4.31	0.87	0.07	0.03
prefrontal cortex	4.21	0.7	0.32	0.34
cortex middle	4.16	0.86	0.02	0
sparse	4.09	0.86	-0.03	-0.03
alzheimer disease	4.07	0.81	0.03	0.02
prefrontal	4.06	0.69	0.36	0.36
alzheimer	4.01	0.81	0.03	0.02
mind tom	3.62	0.86	0.28	0.25

Fig. 3.7. List of cognitive domains related to the second location’s centroid.

Infact if we introduce in Neurosynth the cognitive term “ToM”, the related map describing the meta-analysis is illustrated by Fig 3.8, a pattern rather similar to that of the DMN.

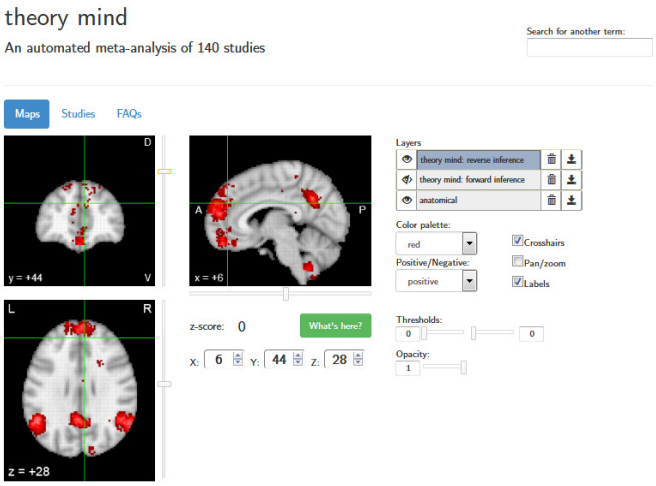

Fig. 3.8. The map is the result of a meta-anaysis about the ToM cognitive domain.

The third location, identified with the MNI atlas used in Mango, appears to be the precuneus, another essential part of the DMN (Utevsky et al., 2014).

However, the result of Neurosynth (fig 3.11) provides a different identification, describing this third location as a part of the dorsal attention network (DAN), a network composed by the inferior parietal sulcus (IPS) and the frontal eye field (FEF) (Vossel et al., 2014). Along with the ventral attention network, DAN is in charge of attention control and particularly the dorsal part seems to be implicated in the top down, voluntary attentional control. If we compare the coactivations map of the third location (Fig. 3.9) and the DAN pattern (Fig.3.10), we can appreciate the similarity between the two patterns.

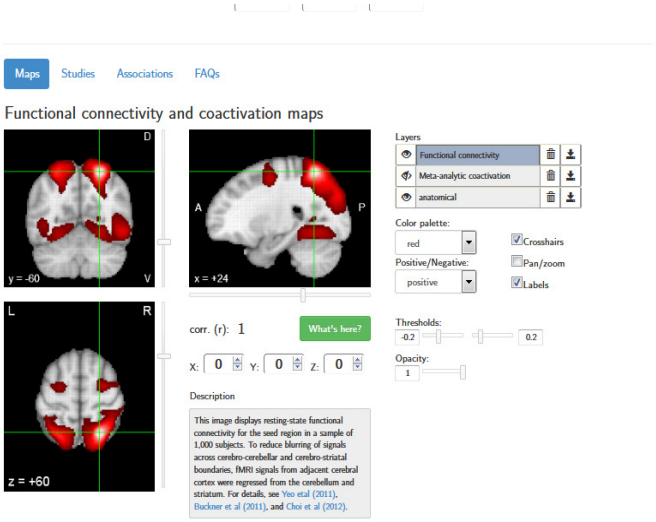

Fig. 3.9.TheNeurosynth coactivations map of the third location.

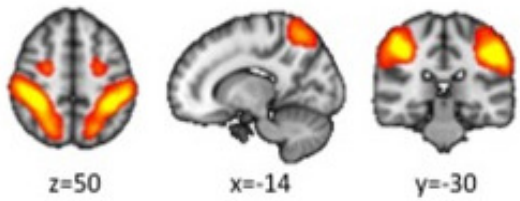

Fig. 3.10. The dorsal attentional network (DAN) (Mueller et al., 2013).

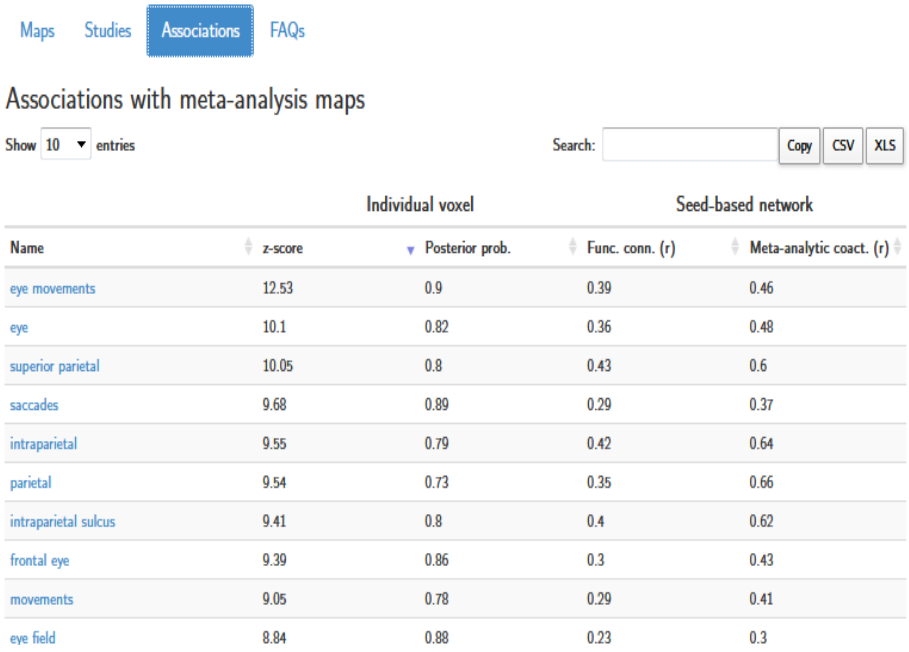

Maps Studies Associations FAQs

Associations with meta-analysis maps

Show 10 entries Search: Copy CSV XLS

		Individual voxel	Seed-based network	
Name	z-score	Posterior prob.	Func. conn. (r)	Meta-analytic coact. (r)
eye movements	12.53	0.9	0.39	0.46
eye	10.1	0.82	0.36	0.48
superior parietal	10.05	0.8	0.43	0.6
saccades	9.68	0.89	0.29	0.37
intraparietal	9.55	0.79	0.42	0.64
parietal	9.54	0.73	0.35	0.66
intraparietal sulcus	9.41	0.8	0.4	0.62
frontal eye	9.39	0.86	0.3	0.43
movements	9.05	0.78	0.29	0.41
eye field	8.84	0.88	0.23	0.3

Fig. 3.11. List of cognitive domains related to the third location's local maxima.

Significant cognitive terms related to the pattern of coactivations of the third location are "intraparietal", "eyes movement", "frontal eye", "eye field". The frontal eye field regions are involved in top down control of attention and sustaining attention and are part of the DAN (Grosbras and Paus, 2003; Hung et al., 2011; Silvanto et al., 2006), therefore this is another confirmation that the pattern refers to the DAN.

3.4.2 Differences between ASD and NC subjects at single subject level.

Concerning the single subject classification, the result of SVM applied to all subjects is a classification with an accuracy of 64.3%, a sensitivity of 63.4%, and a specificity of 65.1% and an AUC of 68.6%.

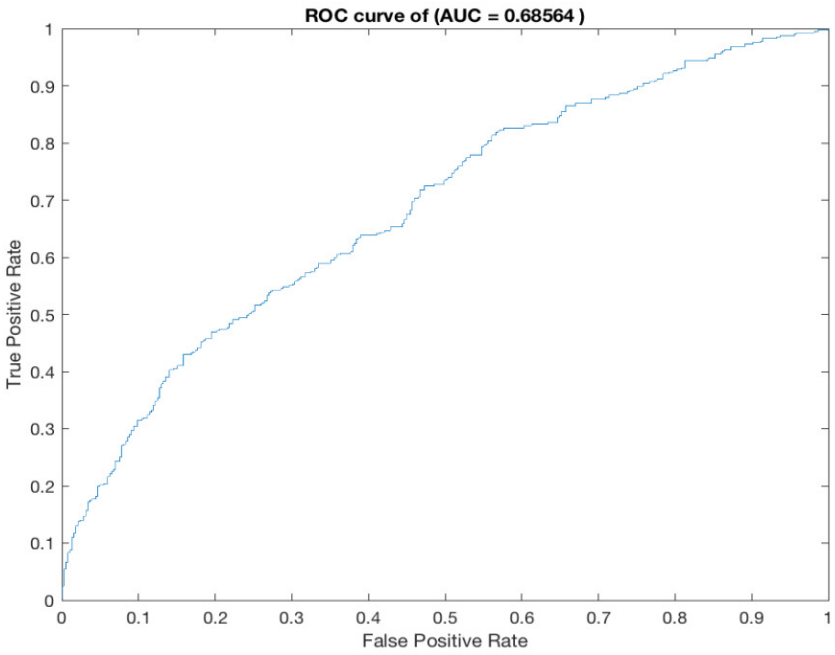

Fig. 3.12. This is the ROC curve resulting from the classification of all subjects.

Cluster	X	Y	Z	Brain area
1	-22	-70	60	Intraparietal
2	24	56	26	Prefrontal
3	42	-70	36	Precuneus
4	10	58	36	Prefrontal
5	0	-60	32	Precuneus
6	-6	-48	18	Precuneus
7	54	-70	-10	Occipitotemporal
8	48	36	12	Prefrontal

Tab.3.4.The coordinates are in MNI and refer to the maxima of each cluster.

Tab.3.4 lists the locations of the main clusters of the pattern used to perform the single-subject classification (as to this pattern see Fig. 3.17 in the Discussion).

We also applied the classification to single different datasets (coming from different Universities), to different age categories and to different FIQ levels.

Performances in classification were quite heterogeneous, particularly on different sites (Tab. 3.5).

	Accuracy	AUC	ASD n.	NC n.	Eyes	Age	Scanner type
Yale	0.929	0.950	40	42	open	7-17.8	SIEMENS MAGNETOM Atrio Tim syngo MR B17
Cmu	0.926	0.808	14	13	closed	19-40	SIEMENS MAGNETOM Verio syngo MR B17
Sdsu	0.917	0.961	14	22	open	8.7-17.2	GEMR7503T
Max	0.861	0.893	24	33	closed	7-58	SIEMENS MAGNETOM Verio syngo MR B17
Pitt	0.842	0.865	30	27	closed	9.3-35.2	SIEMENS MAGNETOM Allegra syngo MR A30
Olin	0.833	0.900	20	16	open	10-24	SIEMENS MAGNETOM Allegra syngo MR B2004A
Stanford	0.775	0.755	20	20	closed	7.5-12.9	GE SIGNA 3T
Um1	0.709	0.793	55	55	open	8.2-19.2	GE SIGNA 3T
Nyu	0.685	0.739	79	105	open	6.5-39.1	SIEMENS MAGNETOM Allegra syngo MR B2004A
Um2	0.629	0.301	13	22	open	12.8-28.8	GE SIGNA 3T
Usm	0.614	0.631	58	43	open	8.8-50.2	SIEMENS MAGNETOM Atrio Tim syngo MR B17
Leuven 1	0.586	0.486	14	15	open	18-32	PHILIPS INTERA 3T
Leuven 2	0.571	0.550	15	20	open	12.1-16.9	PHILIPS INTERA 3T
Sbl	0.567	0.253	15	15	closed	20-64	PHILIPS INTERA 3T

Tab. 3.5. The following abbreviation where used to indicate the database site: Yale: Yale Child Study Center, Cmu: Carnagie Mellon University, Sdsu: San Diego State University, Max: Ludwig Maximilians University Munich, University of Pittsburg, School of Medicine, Olin: Olin,Institute of Living at Hartford Hospital, Stanford: Stanford University, Um1: University of Michigan Sample 1, Nyu: NYU Langone Medical center, Um2: University of Michigan Sample 2, Usm: University of Utah School of Medicine, Leuven 1: University of Leuven: Sample 1, Leuven 2: University of Leuven: Sample 2, Sbl: Social Brain Lab BCN NIC UMC Groningen and Netherlands Institute for Neuroscience. As measures of classification performance, Accuracy and area under the curve (AUC) are indicated. Other information regards the eyes, if open or closed during the acquisition, the age range of subjects and the kind of scanner machine used. ASD n. refers to the number of autistic subjects, NC n. refers to the number of control subjects.

	Accuracy	Sensivity	Specificity	AUC
age_00_09	0.780	0.750	0.810	0.835
age_10_11	0.723	0.680	0.773	0.685
age_12_13	0.504	0.500	0.500	0.431
age_14_17	0.636	0.677	0.589	0.665
age_18_19	0.532	0.511	0.532	0.411
age_20_26	0.613	0.641	0.574	0.666
age_27_64	0.677	0.671	0.683	0.616

Tab.3.6.Classification of results between age categories.

Concerning age category, the classification performance is higher for the two younger categories and decreases for the other older categories (Tab. 3.6).

	Accuracy	Sensivity	Specificity	AUC
FIQ_100_115	0.695	0.737	0.635	0.693
FIQ_116_148	0.618	0.633	0.588	0.651

Tab.3.7.Classification of results between levels of full intelligence quotient (FIQ).

Concerning the classification of different level of full Intelligence quotient, it was applied only to the two categories where the control subjects were available (Tab. 3.7).

3.4.3 High variation in single subject classification performance

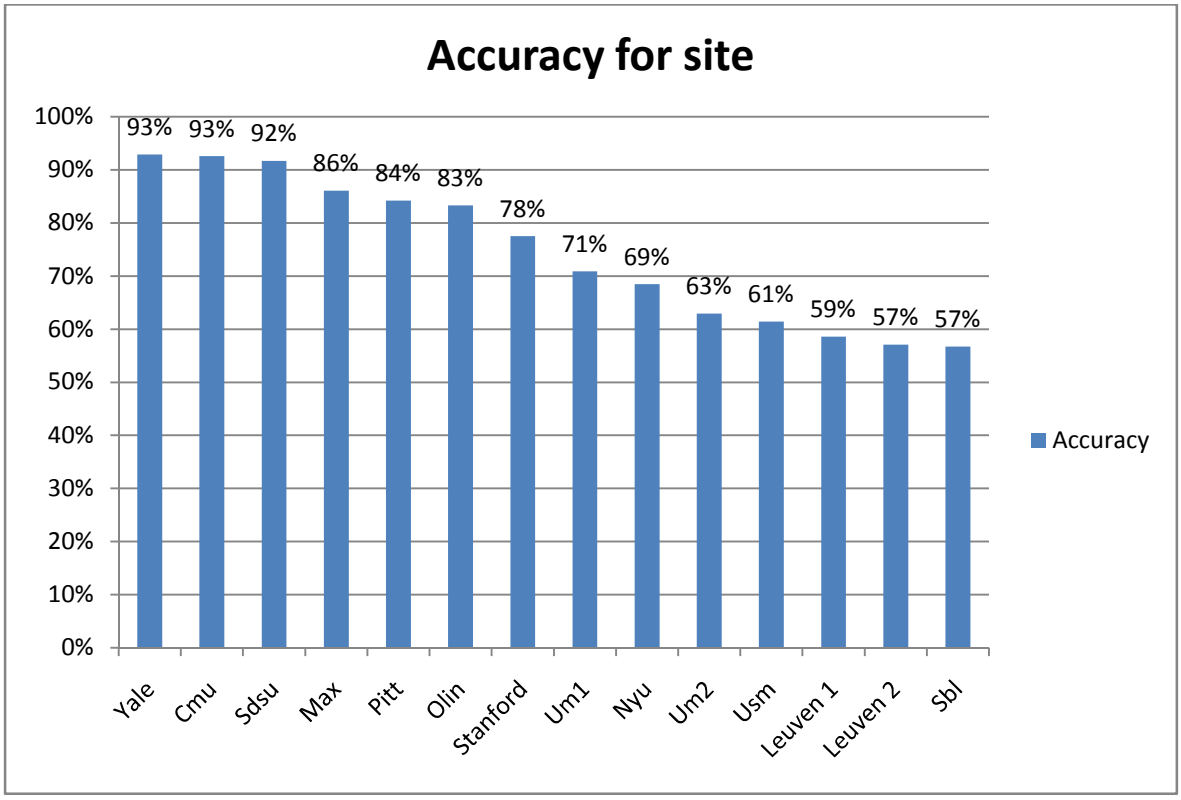

Fig. 3.13.Accuracy performances for different sites.

Concerning the subject level classification, if the classification of all subjects together performs with an accuracy of 64.3%, at single site level results are quite heterogeneous (Fig.3.13), with 6 sites out of 14 where the classification has an accuracy higher than 80%, reaching excellent results for 3 sites with an accuracy of 93% and 92%.

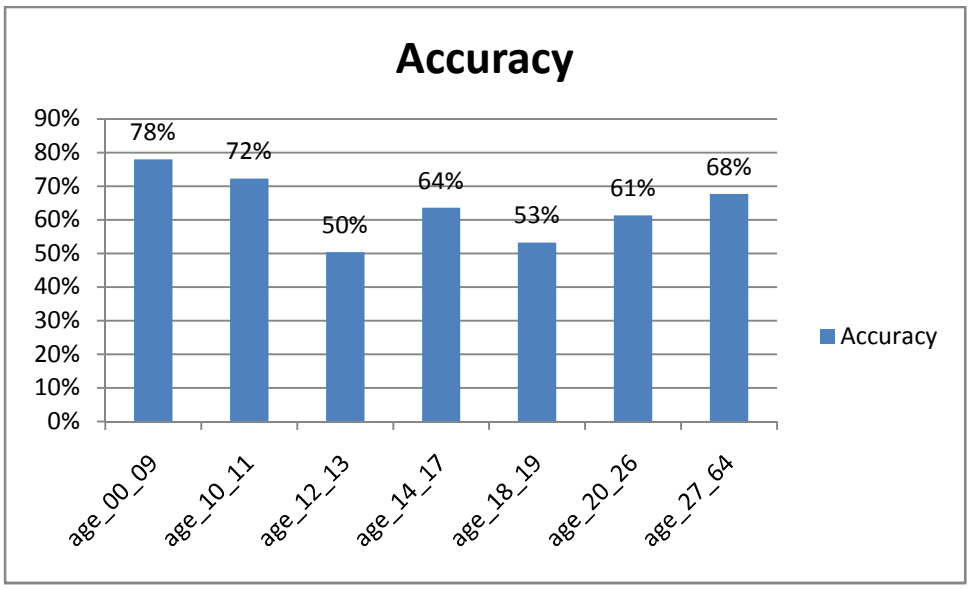

Fig. 3.14. Accuracy performances for different age categories.

Also if differentiation is made for categories of age, results are quite different (Fig. 3.14), with the best accuracy of 78% for subjects till 9 years old and the worst performance with a 50% accuracy for subjects of 12 and 13 years old.

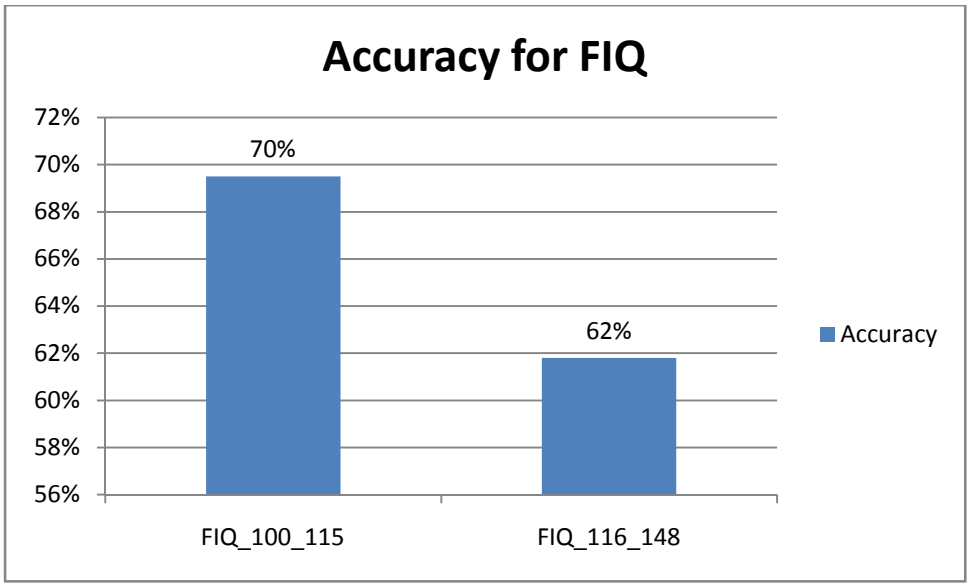

Fig.3.15. Accuracy performances for different FIQ categories.

Some differences also emerge between subjects with different FIQ level, with a 70% accuracy for subjects with FIQ between a score of 100 and 115, and a 62% of accuracy for subjects with FIQ between a score of 116 and 148 (Fig. 3.15).

Subjects with FIQ lower than 100 where not considered in this sub classification, as no control subject with FIQ lower than 100 was available.

3.5 Discussion

3.5.1 Differences between ASD and control at group level

The results show statistical differences between ASD and control group in AC level mainly in three locations. The first two locations are part of the DMN; this is in line with the cognitive theory that relates ASD to a dysfunction in the ToM.

The third location could be considered as either part of DMN or of DAN.

If we consider this location as another part of the DMN, we can conclude that all differences at group level between ASD subjects and controls are all located in the DMN. But the possibility to consider the third location as part of the DAN makes it possible to examine the hypothesis about the connection between ASD and an impairment of the attentional networks. Indeed, the function of directing attention to an object is involved in the social cognition (Corbetta et al., 2008). For example, the Relational Frame Theory (RFT) describes the joined attention (JA) and social referencing (SR) as the two precursors of the derived relational responding (DRR). These are fundamental abilities for the children-caregiver interaction as well as the subsequent development of language and higher cognitive functions (Hayes et al., 2001; Pelaez, 2009). JA is the capacity of using the visual contact and the gaze to coordinate the attention with another person so as to share an experience, such an object or an interesting event (Mundy et al., 1994). JA starts to develop between 9 and 12 months, beginning with the gaze shift between an object and a caregiver (Bakeman and Adamson, 1984). The role of JA seems quite important for its relation with ASD (Carpenter et al., 2002),so much so that it has been proposed that an impairment in JA be a necessary and sufficient condition for

recognizing ASD in infants (Dawson et al., 2004). Indeed, many autistic children do not shift their attention to sounds or other social stimuli and JA impairment has been associated with language deficits (Charman et al., 1997). Evidence suggests that the intraparietal sulcus (IPS) together with the left fusiform gyrus (LFG), superior temporal sulcus, (STS) and inferior occipital gyrus (IOG) responds more to faces than to different pictures (Hoffman and Haxby, 2000; Puce et al., 1998; Wicker et al., 1998). Some studies showed hyperactivity during process of facial expressions (Baron-Cohen et al., 2000; Critchley et al., 2000) in IPS areas, such as the peristriate visual cortex and precuneus. Moreover, it has been investigated the connection between deficits in ToM processing, the relative impaired social cognition and the dysfunctional eye gaze processing (Baron-Cohen, 2001; Baron-Cohen et al., 2000, 1999; Mundy, 2003). Although many aspects of the relation of gaze and autistic brain are still unclear, a number of studies describe an atypical functionality during facial perception in ASD subjects (Adolphs, 2003; Baron-Cohen et al., 2000; Hadjikhani et al., 2007; Humphreyset al., 2009; Kliemann et al., 2010; Klin et al., 2002; Pelphrey et al., 2002; Pierce et al., 2001; Scherf, 2010; Schultz, 2005).

As the top-down function of the DAN is characterized by an involvement of both working memory (Downing, 2000; Woodman and Luck, 2007) and long-term memory (Moores et al., 2003), it is not surprising that in the DAN brain areas the BOLD signal persistence has a higher AC and that, as a result of its disfunctioning, this AC could decrease in ASD subjects.

To sum up, the ASD group shows a reduced AC in areas that are part of the DMN and the DAN. These two networks are essential systems of brain functional organization. The DMN organizes introspection and auto referential thoughts,

while the DAN controls the external environment involving perception and action (Fox et al., 2005; Golland et al., 2007), and, as showed in Fig. 3.16, when one is activated, the other is deactivated (Fox et al., 2006; Fransson, 2005; Nir et al., 2006).

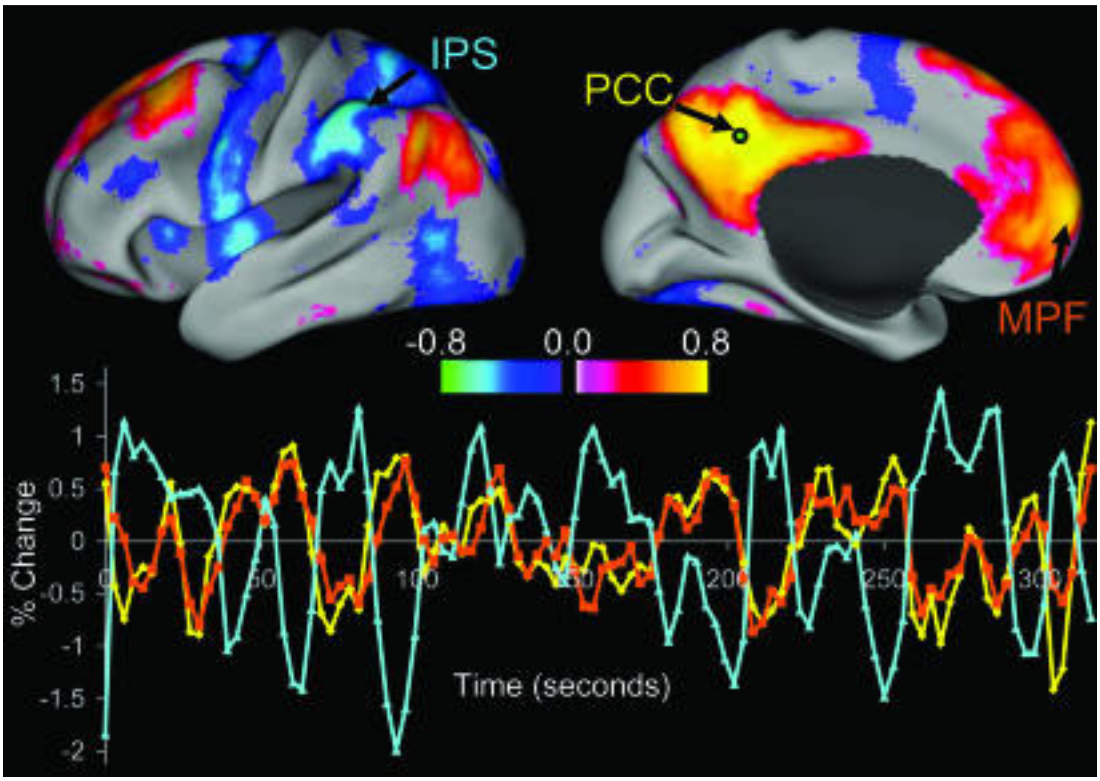

Fig.3.16.The red time course refers to the posterior part of the DMN and the blue one to the DAN (Fox et al., 2005).

So, at group level, brain areas exhibiting a lower AC in autistic subjects are located in cortical regions involved in the integration of information (ToM and somatosensory integration), which are parts of DMN and DAN.

AC results are consistent with the main cognitive theories on ASD, which focus on the dysfunction of the multimodal and integrative areas involved in ToM and

executive functions. In fact, in patients with ASD these brain regions show a reduced anterior posterior inter-connectivity as well as long range under-connectivity and are characterized by low levels of AC, whereas in normal subjects they typically exhibit a high persistence of the BOLD signal.

3.5.2 Single subject classification pattern

The pattern that can classify autistic subjects is mainly formed by prefrontal, posteromedial and parietal areas; areas that we have seen are crucial parts of the DMN and DAN.

These findings confirm the group level results. Infact, the areas with a statistical difference at group level are also part of the classification pattern at single subject level.

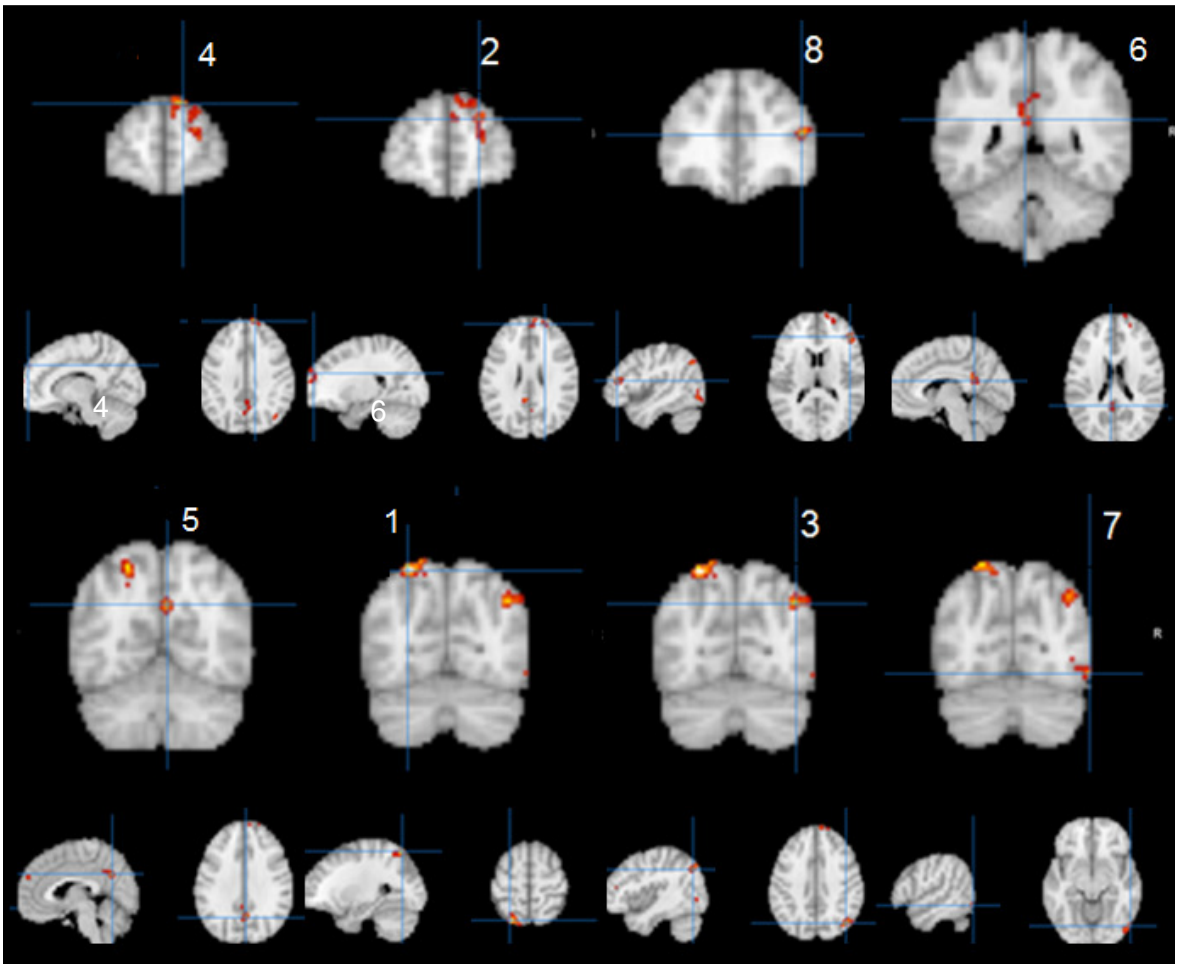

Fig. 3.17.Clusters of voxels that influence more the classification accuracy, numbers refer to the number of cluster inTab.3. 4.

In a very recent study a ‘Fukunaga–Koontz’ transform was applied to connectivity matrices obtained from the same ABIDE database used here. Subsequently, authors employed a SVM classifier and found out the brain regions that better separate ASD subjects from controls (Subbaraju et al., 2017). The results where divided in adults and adolescents. Figure 3.18 illustrates the results concerning adolescents (<18 age).

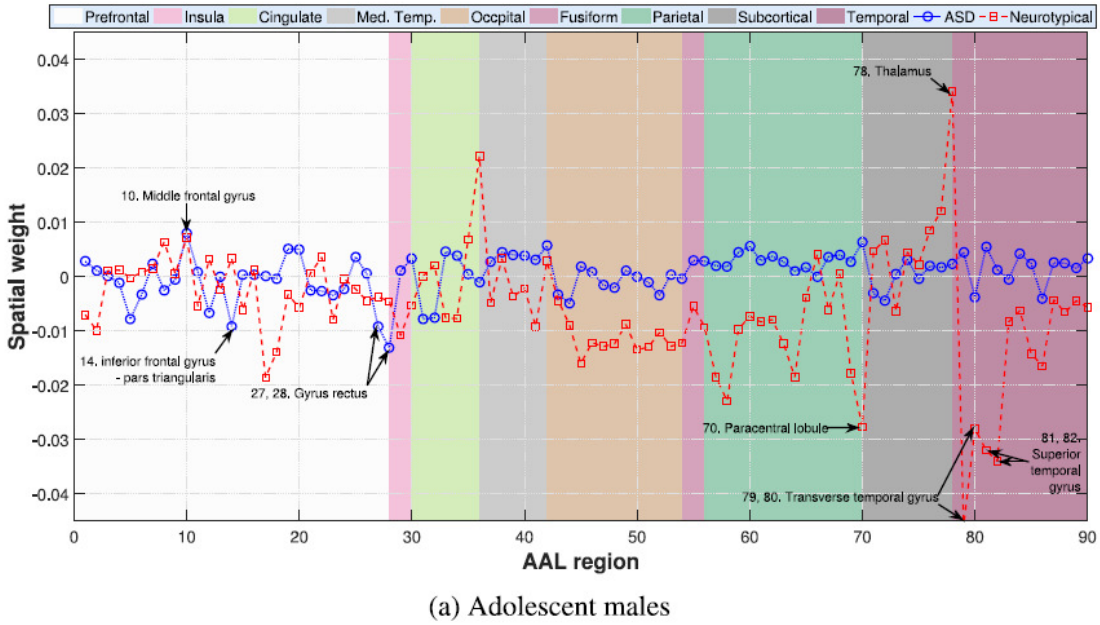

(a) Adolescent males

Fig.3.18.Spatial weight in classification of adolescent autistic males subjects (Subbaraju et al., 2017). AAL: Automated Anatomical Labeling.

Prefrontal, parietal, temporal and subcortical areas are highlighted in both classes, but in adults some occipital areas are also involved. Significantly, these results are not in contrast with ours. Curiously, in adolescents it is not specified the second positive higher peak of weight that refers to AAL region 36, which is the right posterior cingulate gyrus.

3.5.3 Heterogeneity in classification

Significant differences in classification accuracy were found due to different sites. These results lead to think that the quality of data, the scan procedures, sequences and scanner machine characteristics could influence the classification performance.

At a level group, autistic subjects have high differences from controls using AC as parameter, but when we tried to classify subjects a classification rate of 64.3% was achieved. So, a highly significant group difference does not necessarily translate into a strong classification result. This is because the range of values for AC level is highly overlapping for the two groups, as shown in the Fig. 3.19 case A.

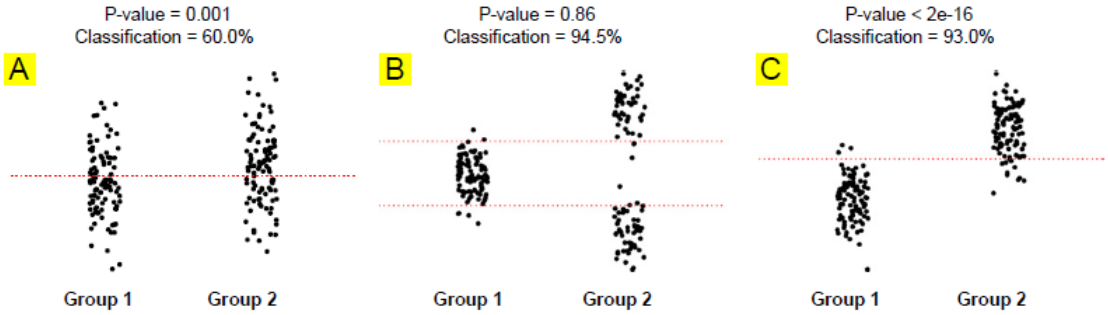

Fig. 3.19. Case A is an example of good results in a t-test at group level and less performance in single subject classification, case B describes the opposite situation and case C show the situation with strong group differences and good classification accuracy (Arbabshirani et al., 2017)

Our classification results, with many good performances at single site level and less good performance on classifying all subject together, is not unusual, as it an interesting review (Arbabshirani et al., 2017) suggests an inverse relationship between accuracy and sample size (Fig.3.20).

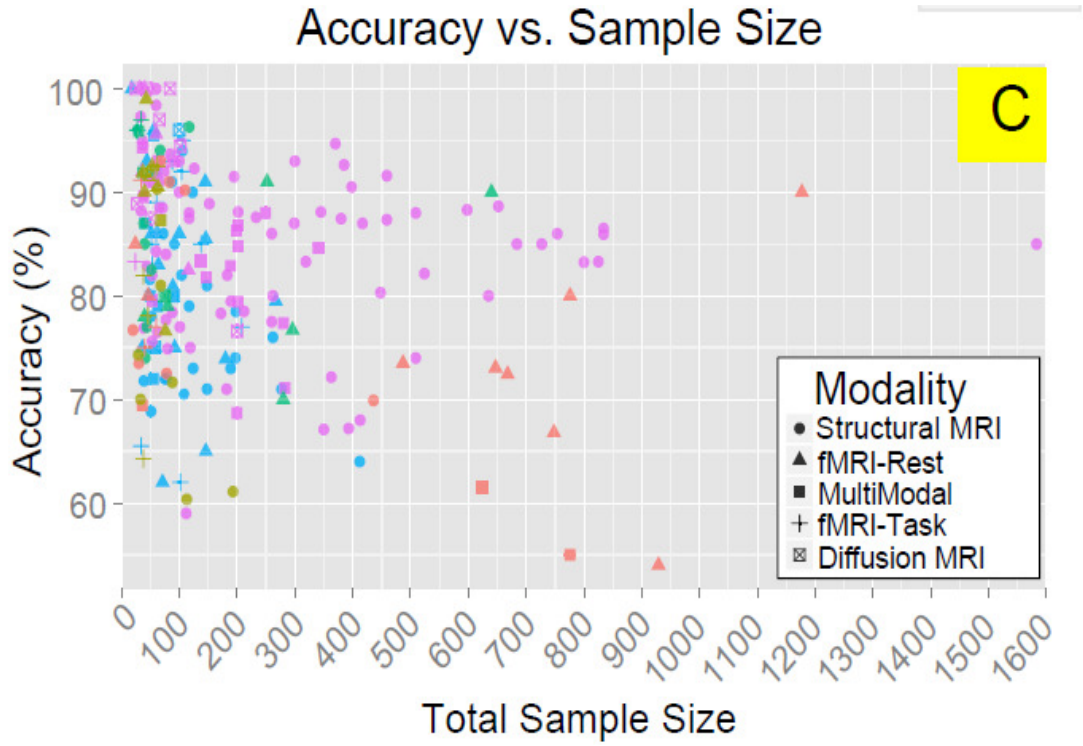

Fig. 3.20. Classification accuracy and total sample size in classification studies on neuroimaging MRI data (Arbabshirani et al., 2017).

According to this review, most of experiments of classification based on MRI data used less than 200 subjects. The present research, in contrast, is one of the few that was based on a far larger sample (around 800 subjects).

3.6 Conclusion

The present study aimed to verify whether the dynamics of fMRI BOLD signal at rest, and particularly its persistence, can differentiate autistic from control subjects.

A second issue was to investigate these differences to better understand the neurophysiological meaning of BOLD signal persistence.

We used AC as parameter to measure persistence, a simple and reliable parameter used in signal analysis.

Results confirm the reliability of AC: in fact differences at group and single subject level were found.

These differences are almost all located in prefrontal, posteromedial and intraparietal areas. At network level most of these areas are part of DMN and of DAN. These results are in line with the main cognitive theories of ASD, particularly with the ToM theory and the long-range under-connectivity theory.

Much remains to understand about the changes in neural activity that cause a reduction of persistence in BOLD signal. For example, further investigations are needed to comprehend whether the reduced AC is a result of functional or structural changes in those areas, or both.

Given the disparities of classification performance between data sites, it would be interesting to investigate the differences in scan procedures and sequences to verify how much a better classification depends on different choices in these parameters.

A recent study has demonstrated that, by reducing the features to 90 brain regions, accuracy of classification increases (Iidaka, 2015). Also another research has suggested that, compared to neurotypical subjects, classification of individuals with ASD achieves better performance with the reduction of the number of features (Subbaraju et al., 2017).

On the basis of these results, an improvement of the analysis carried out in this study could be the application of the same method to a reduced number of variables.

A future aim is also to apply the same analyses about BOLD signal AC to other brain disorders with abundant and available datasets, such as Alzheimer's disease and schizophrenia, so as to verify similarities and differences between neuropathological conditions as well as improve our understanding of the AC variations of the BOLD signal.

4 Thesis conclusions

Rather than being a mere repetition of the conclusions of the previous studies, this wants to be a concluding remark about my PhD research. If I had to condense these years in a word, I would choose “uncertainty”.

In my first study I discuss how in fMRI BOLD signal analysis AC has been considered, at least at the beginning, a pure noise to be filtered in order to detect the signal.

However, it is now undisputed that by filtering the signal to eliminate noise, a part of the information is lost as well. In addition, a study on functional connectivity estimates has showed that correcting for AC does not change much the results of

t tests, which are the important analyses for scientific research (Arbabshirani et al., 2014).

It has also been demonstrated that the frequently used filtering to reduce endogenous AC can create an induced AC (Davey et al., 2013).

The traditional analysis of time series applies two kinds of methods: time domain analysis (like AC) and frequencies domain analysis (like power spectrum analysis). Other tools were developed after Mandelbrot’s works on economic time series (Mandelbrot et al., 1997). These tools refer to the fractal dimension of time series, of which an example is the Hurst exponent estimation with the rescale range analysis (Schepers et al., 2002; Shumway and Stoffer, 2011).

Many researchers have used fractal parameters and power spectrum analysis to investigate fMRI BOLD signal dynamics (Ciuciu et al., 2014; He, 2011; Maxim et al., 2005; Palva and Palva, 2012; Salvador et al., 2008; Wink et al., 2008).

However, Hurst exponent estimation procedure has several drawbacks, such as it can indicate the existence of a long memory in a random series (Sánchez Granero et al., 2008) and produces different results according to the different methods of calculation (Cannon et al., 1997; Poveda and Mesa, 1994).

As to the power spectrum analysis, the Wiener-Khinchin (Wiener, 1930) theorem relates it with the AC function in that the energy spectral density of a signal corresponds to the Fourier transform of the AC function of the same signal. Nevertheless, before my research, only one study used AC to investigate brain dynamics (Kaneoke et al., 2012).

Concerning the topological distribution of the level of persistence of the fMRI BOLD signal, most of researchers agree that, with the help of the above mentioned methods, heteromodal areas show higher signal persistence compared to unimodal, limbic and subcortical areas. But nonetheless, to create uncertainty a study has claimed exactly the opposite, enunciating the general principle that in heteromodal areas the signal detected has a higher component of high frequencies (Baria et al., 2013).

With regard to my second study, the results are quite promising, as AC seems to discriminate well at group level between autistic and control subjects, and the most relevant areas are consistent with the main cognitive theories on ASD. At single subject level, classification accuracy reaches 92% for some database sites and just 57% for others. Still, these uncertain results are in line with the known pitfalls

of single subject classification based on neuroimaging data (Arbabshirani et al., 2017; Nielsen et al., 2013).

So, more often than not, uncertainty is the keyword to explain the neural correlates of persistence of the fMRI BOLD signal at rest.

To reduce this level of uncertainty I proposed (pag.30) to link AC BOLD persistence with information integration. Future research is therefore needed, especially at single neuron level and single cortical layer of neuron, in order to investigate the interaction of groups of neurons within cortical layers. Also new findings in computational neuroscience will help to understand the inner neuronal activity that generates different levels of persistence.

I hope that my research on the spatial distribution of AC BOLD persistence and its variation in pathological subjects will be a little step forward to address these future issues.

5 Bibliography

Adolphs, R., 2003. Cognitive neuroscience of human social behaviour. Nat.Rev.Neurosci. 4, 165–178. doi:10.1038/nrn1056

Aguirre, G.K., Zarahn, E., D'Esposito, M., 1997. Empirical analyses of BOLD fMRI statistics. II. Spatially smoothed data collected under null-hypothesis and experimental conditions. Neuroimage 5, 199–212. doi:10.1006/nimg.1997.0263

Ahmed, R.M., Devenney, E.M., Irish, M., Ittner, A., Naismith, S., Ittner, L.M., Rohrer, J.D., Halliday, G.M., Eisen, A., Hodges, J.R., Kiernan, M.C., 2016. Neuronal network disintegration: common pathways linking neurodegenerative diseases. J. Neurol. Neurosurg. Psychiatry jnnp-2014-308350. doi:10.1136/jnnp-2014-308350

Amaral, D.G., Schumann, C.M., Nordahl, C.W., 2018. Neuroanatomy of autism. Trends Neurosci. 31, 137–145. doi:10.1016/j.tins.2007.12.005

American Psychiatric Association, 2013. DSM-V, American Journal of Psychiatry. doi:10.1176/appi.books.9780890425596.744053

American Psychiatric Association, 2000. DSM-IV, Diagnostic and Statistical Manual of Mental Disorders 4th edition TR. doi:10.1176

Amit, D.J., 1995. The Hebbian paradigm reintegrated: Local reverberations as internal representations. Behav. Brain Sci. 18, 617–657. doi:10.1017/S0140525X0004022X

Anderson, C.M., Lowen, S.B., Renshaw, P.F., 2006. Emotional task-dependent

low-frequency fluctuations and methylphenidate: Wavelet scaling analysis of 1/f-type fluctuations in fMRI of the cerebellar vermis. J. Neurosci. Methods 151, 52–61. doi:10.1016/j.jneumeth.2005.09.020

Arbabshirani, M.R., Damaraju, E., Phlypo, R., Plis, S., Allen, E., Ma, S., Mathalon, D., Preda, A., Vaidya, J.G., Adali, T., Calhoun, V.D., 2014. Impact of autocorrelation on functional connectivity. Neuroimage 102, 294–308. doi:10.1016/j.neuroimage.2014.07.045

Arbabshirani, M.R., Plis, S., Sui, J., Calhoun, V.D., 2017. Single subject prediction of brain disorders in neuroimaging: Promises and pitfalls. Neuroimage 145, 137–165. doi:10.1016/j.neuroimage.2016.02.079

Austin, G., Groppe, K., Elsner, B., 2014. The reciprocal relationship between executive function and theory of mind in middle childhood: a 1-year longitudinal perspective. Front. Psychol. 5, 655. doi:10.3389/fpsyg.2014.00655

Bailey, A., Le Couteur, A., Gottesman, I., Bolton, P., Simonoff, E., Yuzda, E., Rutter, M., 1995. Autism as a strongly genetic disorder: Evidence from a British twin study. Psychol. Med. 25, 63. doi:10.1017/S0033291700028099

Bakeman, R., Adamson, L.B., 1984. Coordinating Attention to People and Objects in Mother-Infant and Peer-Infant Interaction. Child Dev. 55170219, 1278–1289. doi:10.2307/1129997

Ball, G., Stokes, P.R., Rhodes, R. a, Bose, S.K., Rezek, I., Wink, A.-M., Lord, L.-D., Mehta, M. a, Grasby, P.M., Turkheimer, F.E., 2011. Executive functions and prefrontal cortex: a matter of persistence? Front. Syst. Neurosci. 5, 3.

doi:10.3389/fnsys.2011.00003

Baria, A.T., Baliki, M.N., Parrish, T., Apkarian, A.V., 2011. Anatomical and functional assemblies of brain BOLD oscillations. J. Neurosci. 31, 7910–9. doi:10.1523/JNEUROSCI.1296-11.2011

Baria, A.T., Mansour, A., Huang, L., Baliki, M.N., Cecchi, G.A., Mesulam, M.M., Apkarian, A. V., 2013. Linking human brain local activity fluctuations to structural and functional network architectures. Neuroimage 73, 144–155. doi:10.1016/j.neuroimage.2013.01.072

Baron-Cohen, S., 2008. Theories of the autistic mind. Psychologist 21, 112–116. doi:http://dx.doi.org/10.1016%2F0010-0277%2885%2990022-8

Baron-Cohen, S., 2001. Theory of mind and autism: A review. Spec. Issues Int. Rev. Res. Ment. Retard. 23, 169–184. doi:http://dx.doi.org/10.1016/S0074-7750(00)80010-5

Baron-Cohen, S., 1990. Autism: A Specific Cognitive Disorder of & lsquo;Mind-Blindness'. Int. Rev. Psychiatry 2, 81–90. doi:10.3109/09540269009028274

Baron-Cohen, S., Baron-Cohen, S., Ring, H.A., Ring, H.A., Wheelright, S., Wheelright, S., Bullmore, E.T., Bullmore, E.T., Brammer, M.J., Brammer, M.J., Simmons, A.M., Simmons, A.M., Williams, S.C., Williams, S.C., 1999. Social intelligence in the normal and autisitic brain: an fMRI study. Eur. J. Neurosci. 11, 1891–1898. doi:10.1046/j.1460-9568.1999.00621.x

Baron-Cohen, S., Leslie, A.M., Frith, U., 1985. Does the autistic child have a "theory of mind" ? Cognition 21, 37–46. doi:https://doi.org/10.1016/0010-0277(85)90022-8

Baron-Cohen, S., Ring, H.A., Bullmore, E.T., Wheelwright, S., Ashwin, C., Williams, S.C.R., 2000. The amygdala theory of autism. Neurosci. Biobehav. Rev. 24, 355–364. doi:10.1016/S0149-7634(00)00011-7

Bartzokis, G., Lu, P.H., Mintz, J., 2007. Human brain myelination and amyloid beta deposition in Alzheimer's disease. Alzheimer's Dement. 3, 122–125. doi:10.1016/j.jalz.2007.01.019

Belmonte, M.K., Allen, G., Beckel-Mitchener, A., Boulanger, L.M., Carper, R.A., Webb, S.J., 2004. Autism and Abnormal Development of Brain Connectivity. J. Neurosci. 24, 9228 LP-9231.

Bettelheim, B., 1959. Joey. Sci. Am. 200, 116–130.

Birn, R.M., Diamond, J.B., Smith, M.A., Bandettini, P.A., 2006. Separating respiratory-variation-related fluctuations from neuronal-activity-related fluctuations in fMRI. Neuroimage 31, 1536–1548. doi:10.1016/j.neuroimage.2006.02.048

Biswal., B., Yetkin, F.Z., Hautong, V.M., Hyde, J.S., 1995. - Functional connectivity in the motor cortex of resting human brain using. Magn Reson Med 34, 537–541. doi:10.1002/mrm.1910340409

Biswal, B., DeYoe, E.A., Hyde, J.S., 1996. Reduction of physiological fluctuations in fMRI using digital filters. Magn. Reson. Med. 35, 107–113. doi:10.1002/mrm.1910350114

Biswal, B., Mennes, M., Zuo, X., Gohel, S., Kelly, C., Smith, S.M., Beckmann, C.F., Adelstein, J.S., Buckner, R.L., Colcombe, S., Dogonowski, A., Ernst, M., Fair, D., Hampson, M., Hoptman, M.J., Hyde, J.S., Kiviniemi, V.J., Kötter, R.,

Li, S., Lin, C., Lowe, M.J., Mackay, C., Madden, D.J., Madsen, K.H., Margulies, D.S., Mayberg, H.S., McMahon, K., Monk, C.S., Mostofsky, S.H., Nagel, B.J., Pekar, J.J., Peltier, S.J., Petersen, S.E., Riedl, V., Rombouts, S.A.R.B., Rypma, B., Schlaggar, B.L., Schmidt, S., Seidler, R.D., Siegle, G.J., Sorg, C., Teng, G., Veijola, J., Villringer, A., Walter, M., Wang, L., Weng, X., Whitfield-Gabrieli, S., Williamson, P., Windischberger, C., Zang, Y., Zhang, H., Castellanos, F.X., Milham, M.P., 2010. Toward discovery science of human brain function. Proc Natl Acad Sci U S A 107, 4734–9. doi:10.1073/pnas.0911855107

Biswal, B.B., 2012. Resting state fMRI: A personal history. Neuroimage 62, 938–944. doi:10.1016/j.neuroimage.2012.01.090

Biswal, B.B., Ulmer, J.L., 1999. Blind Source Separation of Multiple Signal Sources of f{MRI} data sets using independent component analysis. J.\ Comput. Assist. Tomogr. 23, 265–271.

Boucher, J., 1989. The theory of mind hypothesis of autism: Explanation, evidence and assessment. Br. J. Disord. Commun. 24, 181–198. doi:10.3109/13682828909011955

Bryce, R.M., Sprague, K.B., 2012. Revisiting detrended fluctuation analysis. Sci. Rep. 2. doi:10.1038/srep00315

Buckner, R.L., Andrews-Hanna, J.R., Schacter, D.L., 2008. The brain's default network: Anatomy, function, and relevance to disease. Ann. N. Y. Acad. Sci. 1124, 1–38. doi:10.1196/annals.1440.011

Buckner, R.L., Carroll, D.C., 2007. Self-projection and the brain. Trends Cogn. Sci.

11, 49–57. doi:10.1016/j.tics.2006.11.004

Buckner, R.L., Vincent, J.L., 2007. Unrest at rest: Default activity and spontaneous network correlations. Neuroimage 37, 1091–1096. doi:10.1016/j.neuroimage.2007.01.010

Bullmore, E., Long, C., Suckling, J., Fadiwj, J., Calvertl, G., Zelaya, F., Carpenter, A., Brammers, M., 2001. Colored noise and computational inference in fMRI time series analysis : resampling methods in time and wavelet domains SInstitute of Psychiatry KCL , London UK. Hum. Brain Mapp. 12, 2001.

Cagle, R., n.d. Force field of main magnetic field [WWW Document]. Bethesda Natl. Libr. Med. List. Hill Cent. Biocommunication;

Cannon, M.J., Percival, D.B., Caccia, D.C., Raymond, G.M., Bassingthwaighte, J.B., 1997. Evaluating scaled windowed variance methods for estimating the Hurst coefficient of time series. Physica A 241, 606–626. doi:10.1016/S0378-4371(97)00252-5

Carpenter, M., Pennington, B., Rogers, S.J., 2002. Interrelations among social-cognitive skills in young children with autism. J. Autism Dev. Disord. 32, 91–106. doi:10.1023/A:1014836521114

Cauda, F., Costa, T., Palermo, S., D'Agata, F., Diano, M., Bianco, F., Duca, S., Keller, R., 2014. Concordance of white matter and gray matter abnormalities in autism spectrum disorders: A voxel-based meta-analysis study. Hum. Brain Mapp. 35, 2073–2098. doi:10.1002/hbm.22313

Cauda, F., Costa, T., Torta, D.M.E., Sacco, K., D'Agata, F., Duca, S., Geminiani, G., Fox, P.T., Vercelli, A., 2012a. Meta-analytic clustering of the insular cortex

Characterizing the meta-analytic connectivity of the insula when involved in active tasks. Neuroimage 62, 343–355. doi:10.1016/j.neuroimage.2012.04.012

Cauda, F., D'Agata, F., Sacco, K., Duca, S., Geminiani, G., Vercelli, A., 2011a. Functional connectivity of the insula in the resting brain. Neuroimage 55, 8–23. doi:https://doi.org/10.1016/j.neuroimage.2010.11.049

Cauda, F., Geda, E., Sacco, K., D'Agata, F., Duca, S., Geminiani, G., Keller, R., 2011b. Grey matter abnormality in autism spectrum disorder: an activation likelihood estimation meta-analysis study. J. Neurol. Neurosurg. & Psychiatry 82, 1304 LP-1313.

Cauda, F., Torta, D.M.-E., Sacco, K., Geda, E., D'Agata, F., Costa, T., Duca, S., Geminiani, G., Amanzio, M., 2012b. Shared "Core" Areas between the Pain and Other Task-Related Networks. PLoS One 7, e41929.

Cavanna, A.E., Trimble, M.R., 2006. The precuneus: A review of its functional anatomy and behavioural correlates. Brain. doi:10.1093/brain/awl004

Chang, C., Cunningham, J.P., Glover, G.H., 2010. Function. Respiration 44, 857–869. doi:10.1016/j.neuroimage.2008.09.029.Influence

Charman, T., Swettenham, J., Baron-Cohen, S., Cox, a, Baird, G., Drew, a, 1997. Infants with autism: an investigation of empathy, pretend play, joint attention, and imitation. Dev. Psychol. 33, 781–789. doi:10.1037/0012-1649.33.5.781

Cioli, C., Abdi, H., Beaton, D., Burnod, Y., Mesmoudi, S., 2014. Differences in human cortical gene expression match the temporal properties of large-scale functional networks. PLoS One 9, 1–28. doi:10.1371/journal.pone.0115913

Ciuciu, P., Abry, P., He, B.J., 2014. Interplay between functional connectivity and scale-free dynamics in intrinsic fMRI networks. Neuroimage 95, 248–263. doi:10.1016/j.neuroimage.2014.03.047

Ciuciu, P., Varoquaux, G., Abry, P., Sadaghiani, S., Kleinschmidt, A., 2012. Scale-free and multifractal time dynamics of fmri signals during rest and task. Front. Physiol. 3 JUN, 1–18. doi:10.3389/fphys.2012.00186

Collins, C.E., Airey, D.C., Young, N.A., Leitch, D.B., Kaas, J.H., 2010. Neuron densities vary across and within cortical areas in primates. Proc. Natl. Acad. Sci. 107, 15927–15932. doi:10.1073/pnas.1010356107

Collins, D.L., Holmes, C.J., Peters, T.M., Evans, A.C., 1995. Automatic 3-D model-based neuroanatomical segmentation. Hum. Brain Mapp. 3, 190–208. doi:10.1002/hbm.460030304

Constantino, J.N., SA, D., RD, T., MK, S., MM, G., SL, B., LM, M., CS, S., Splinter, R., Reich, W., 2003. Validation of a brief quantitative measure of autistic traits: comparison of the Social Responsiveness Scale with the Autism Diagnostic Interview-Revised. J. Autism Dev. Disord. 33, 427–433.

Corbetta, M., Patel, G., Shulman, G.L., 2008. The Reorienting System of the Human Brain: From Environment to Theory of Mind. Neuron 58, 306–324. doi:10.1016/j.neuron.2008.04.017

Costa, T., Boccignone, G., Cauda, F., Ferraro, M., 2016. The Foraging brain: Evidence of L??vy dynamics in brain networks. PLoS One 11, 1–16. doi:10.1371/journal.pone.0161702

Cox, R.W., 1996. AFNI: Software for Analysis and Visualization of Functional

Magnetic Resonance Neuroimages. Comput. Biomed. Res. 29, 162–173. doi:http://dx.doi.org/10.1006/cbmr.1996.0014

Critchley, H.D., Daly, E.M., Bullmore, E.T., Williams, S.C.R., Amelsvoort, T. Van, Robertson, D.M., Rowe, A., Phillips, M., McAlonan, G., Howlin, P., Murphy, D.G.M., 2000. The functional neuroanatomy of social behaviour: Changes in cerebral blood flow when people with autistic disorder process facial expressions. Brain 123, 2203–2212. doi:10.1093/brain/123.11.2203

Dagli, M.S., Ingeholm, J.E., Haxby, J. V, 1999. Localization of cardiac-induced signal change in fMRI. Neuroimage 9, 407–415. doi:10.1006/nimg.1998.0424

Davey, C.E., Grayden, D.B., Egan, G.F., Johnston, L.A., 2013. Filtering induces correlation in fMRI resting state data. Neuroimage 64, 728–740. doi:http://dx.doi.org/10.1016/j.neuroimage.2012.08.022

Dawson, G., Toth, K., Abbott, R., Osterling, J., Munson, J., Estes, A., Liaw, J., 2004. Early social attention impairments in autism: social orienting, joint attention, and attention to distress. Dev. Psychol. 40, 271–83. doi:10.1037/0012-1649.40.2.271

De Luca, M., Beckmann, C.F., De Stefano, N., Matthews, P.M., Smith, S.M., 2006. fMRI resting state networks define distinct modes of long-distance interactions in the human brain. Neuroimage 29, 1359–1367. doi:10.1016/j.neuroimage.2005.08.035

Di Martino, A., Yan, C.-G., Li, Q., Denio, E., Castellanos, F.X., Alaerts, K., Anderson, J.S., Assaf, M., Bookheimer, S.Y., Dapretto, M., Deen, B., Delmonte, S., Dinstein, I., Ertl-Wagner, B., Fair, D.A., Gallagher, L., Kennedy,

D.P., Keown, C.L., Keysers, C., Lainhart, J.E., Lord, C., Luna, B., Menon, V., Minshew, N.J., Monk, C.S., Mueller, S., Muller, R.-A., Nebel, M.B., Nigg, J.T., O'Hearn, K., Pelphrey, K.A., Peltier, S.J., Rudie, J.D., Sunaert, S., Thioux, M., Tyszka, J.M., Uddin, L.Q., Verhoeven, J.S., Wenderoth, N., Wiggins, J.L., Mostofsky, S.H., Milham, M.P., 2014. The autism brain imaging data exchange: towards a large-scale evaluation of the intrinsic brain architecture in autism. Mol Psychiatry 19, 659–667.

Ding, J.R., Liao, W., Zhang, Z., Mantini, D., Xu, Q., Wu, G.R., Lu, G., Chen, H., 2011. Topological fractionation of resting-state networks. PLoS One 6. doi:10.1371/journal.pone.0026596

Dosenbach, N.U.F., Fair, D. a, Miezin, F.M., Cohen, A.L., Wenger, K.K., Dosenbach, R. a T., Fox, M.D., Snyder, A.Z., Vincent, J.L., Raichle, M.E., Schlaggar, B.L., Petersen, S.E., 2007. Distinct brain networks for adaptive and stable task control in humans. Proc. Natl. Acad. Sci. U. S. A. 104, 11073–8. doi:10.1073/pnas.0704320104

Downing, P.E., 2000. Interactions between visual working memory and selective attention. Psychol. Sci. 11, 467–473. doi:10.1111/1467-9280.00290

Eke, A., Herman, P., Bassingthwaighte, J.B., Raymond, G.M., Percival, D.B., Cannon, M., Balla, I., Ikrenyi, C., 2000. Physiological time series : distinguishing fractal noises from motions. Eur. J. phisiology 403–415.

Fengler, A., 2016. How the brain attunes to sentence processing. University of Lipzig.

Filippi, M., 2009. fMRI Techniques and Protocols, 1st ed. Humana press.

Flanagan, D.P., Harrison, P.L., 2012. Contemporary Intellectual Assessment: Theories, Tests, and Issues. Guilford Publications.

Fombonne, E., Psych, F.R.C., 2005. Epidemiology of Autistic Disorder and Other Pervasive Developmental Disorders. J Clin Psychiatry 66, 3–8.

Fox, M.D., Corbetta, M., Snyder, A.Z., Vincent, J.L., Raichle, M.E., 2006. Spontaneous neuronal activity distinguishes human dorsal and ventral attention systems. Proc. Natl. Acad. Sci. 103, 10046–10051. doi:10.1073/pnas.0604187103

Fox, M.D., Snyder, A.Z., Vincent, J.L., Corbetta, M., Van Essen, D.C., Raichle, M.E., 2005. The human brain is intrinsically organized into dynamic, anticorrelated functional networks. Proc. Natl. Acad. Sci. U. S. A. 102, 9673–8. doi:10.1073/pnas.0504136102

Fransson, P., 2005. Spontaneous low-frequency BOLD signal fluctuations: An fMRI investigation of the resting-state default mode of brain function hypothesis. Hum. Brain Mapp. 26, 15–29. doi:10.1002/hbm.20113

Friston, K.J., Josephs, O., Zarahn, E., Holmes, A.P., Rouquette, S., Poline, J.-B., 2000. To Smooth or Not to Smooth? Neuroimage 12, 196–208. doi:10.1006/nimg.2000.0609

Frith, U., 1989. A new look at language and communication in autism. Int. J. Lang. Commun. Disord. 24, 123–150. doi:10.3109/13682828909011952

Fuster, J.M., 1997. Fuster - Network memory. Trends Neurosci. 20, 451–459.

Fuster, J.M., Bressler, S.L., 2012. Cognit activation. a mechanism enabling

temporal integration in working memory. Trends Cogn. Sci. 16, 207–218. doi:10.1016/j.tics.2012.03.005

Gioia, G.A., Isquith, P.K., Kenworthy, L., Barton, R.M., 2002. Profiles of Everyday Executive Function in Acquired and Developmental Disorders. Child Neuropsychol. 8, 121–137. doi:10.1076/chin.8.2.121.8727

Glasser, M.F., Van Essen, D.C., 2011. Mapping human cortical areas in vivo based on myelin content as revealed by T1- and T2-weighted MRI. J. Neurosci. 31, 11597–616. doi:10.1523/JNEUROSCI.2180-11.2011

Golanov, E. V, Yamamoto, S., Reis, D.J., 1994. Spontaneous waves of cerebral blood flow associated with a pattern of electrocortical activity. Am. J. Physiol. 266, R204–R214.

Golland, Y., Bentin, S., Gelbard, H., Benjamini, Y., Heller, R., Nir, Y., Hasson, U., Malach, R., 2007. Extrinsic and intrinsic systems in the posterior cortex of the human brain revealed during natural sensory stimulation. Cereb. Cortex 17, 766–777. doi:10.1093/cercor/bhk030

Goodkind, M., Eickhoff, S.B., Oathes, D.J., Jiang, Y., Chang, A., Jones-Hagata, L.B., Ortega, B.N., Zaiko, Y. V, Roach, E.L., Korgaonkar, M.S., Grieve, S.M., Galatzer-Levy, I., Fox, P.T., Etkin, A., 2015. Identification of a common neurobiological substrate for mental illness. JAMA psychiatry 72, 305–315. doi:10.1001/jamapsychiatry.2014.2206

Gotham, K., Pickles, A., Lord, C., 2009. Standardizing ADOS Scores for a Measure of Severity in Autism Spectrum Disorders. J. Autism Dev. Disord. 39, 693–705. doi:10.1007/s10803-008-0674-3

Granger, C.W.J., Newbold, P., 1974. Spurious Regressions in Econometrics. J. Econom. 2, 111–120.

Greicius, M., 2008. Resting-state functional connectivity in neuropsychiatric disorders. Curr. Opin. Neurol. 21, 424–30. doi:10.1097/WCO.0b013e328306f2c5

Greicius, M.D., Krasnow, B., Reiss, A.L., Menon, V., 2003. Functional connectivity in the resting brain: a network analysis of the default mode hypothesis. Proc. Natl. Acad. Sci. U. S. A. 100, 253–8. doi:10.1073/pnas.0135058100

Grosbras, M.-H., Paus, T., 2003. Transcranial magnetic stimulation of the human frontal eye field facilitates visual awareness. Eur. J. Neurosci. 18, 3121–3126. doi:10.1111/j.1460-9568.2003.03055.x

Gusnard, D., Akbudak, E., Shulman, G., Raichle, M.E., Louis, S., 2001. Role of Medial Prefrontal Cortex in a Default Mode of Brain Function 2001.

Haar, S., Berman, S., Behrmann, M., Dinstein, I., 2016. Anatomical Abnormalities in Autism? Cereb. Cortex 26, 1440–1452.

Haber, S.N., 2016. Corticostriatal circuitry. Dialogues Clin. Neurosci. 18, 7–21.

Hadjikhani, N., Joseph, R.H., Snyder, J., Tager-Flusberg, H., 2007. Abnormal activation of the social brain during face perception in autism. Hum. Brain Mapp. 28, 441–449. doi:10.1002/hbm.20283

Hasson, U., Yang, E., Vallines, I., Heeger, D.J., Rubin, N., 2009. NIH Public Access. New York 28, 2539–2550. doi:10.1523/JNEUROSCI.5487-07.2008.A

Haugh, L., 1976. Checking the independence of two covariance-stationary time

series: a univariate residual cross-correlation approach. J. Am. Stat. Assoc. 71, 378–385. doi:10.1080/01621459.1976.10480353

Hayes, S.C., Fox, E., Gifford, E. V, Wilson, K.G., Barnes-Holmes, D., Healy, O., 2001. Derived Relational Responding as Learned Behavior BT - Relational Frame Theory: A Post-Skinnerian Account of Human Language and Cognition, in: Hayes, S.C., Barnes-Holmes, D., Roche, B. (Eds.), . Springer US, Boston, MA, pp. 21–49. doi:10.1007/0-306-47638-X_2

He, B.J., 2011. Scale-free properties of the functional magnetic resonance imaging signal during rest and task. J. Neurosci. 31, 13786–95. doi:10.1523/JNEUROSCI.2111-11.2011

He, B.J., Snyder, A.Z., Zempel, J.M., Smyth, M.D., Raichle, M.E., 2008. Electrophysiological correlates of the brain's intrinsic large-scale functional architecture. Proc Natl Acad Sci U S A 105, 16039–16044. doi:10.1073/pnas.0807010105

Herman, P., Sanganahalli, B.G., Hyder, F., Eke, A., 2011. Fractal analysis of spontaneous fluctuations of the BOLD signal in rat brain. Neuroimage 58, 1060–1069. doi:10.1016/j.neuroimage.2011.06.082

Hoffman, E. a, Haxby, J. V, 2000. Distinct representations of eye gaze and identity in the distributed human neural system for face perception. Nat. Neurosci. 3, 80–84. doi:10.1038/71152

Honey, C.J., Thesen, T., Donner, T.H., Silbert, L.J., Carlson, E., Devinsky, O., Doyle, W.K., Rubin, N., Heeger, D.J., 2013. NIH Public Access. Neuron 76, 423–434. doi:10.1016/j.neuron.2012.08.011.Slow

Hull, J. V., Jacokes, Z.J., Torgerson, C.M., Irimia, A., Van Horn, J.D., Aylward, E., Bernier, R., Bookheimer, S., Dapretto, M., Gaab, N., Geschwind, D., Jack, A., Nelson, C., Pelphrey, K., State, M., Ventola, P., Webb, S.J., 2017. Resting-state functional connectivity in autism spectrum disorders: A review. Front. Psychiatry 7. doi:10.3389/fpsyt.2016.00205

Humphreys, K., Hasson, U., Avidan, G., Minshew, N., & Behrmann, M., 2009. Places and Objects in Adults with Autism. Autism Res. 1, 52–63. doi:10.1002/aur.1.Cortical

Hung, J., Driver, J., Walsh, V., 2011. Visual Selection and the Human Frontal Eye Fields: Effects of Frontal Transcranial Magnetic Stimulation on Partial Report Analyzed by Bundesen's Theory of Visual Attention. J. Neurosci. 31, 15904 LP-15913.

Hurst, H.E., 1950. Long-term Storage Capacity of Reservoirs. American Society of Civil Engineers.

Iidaka, T., 2015. Resting state functional magnetic resonance imaging and neural network classified autism and control. Cortex 63, 55–67. doi:10.1016/j.cortex.2014.08.011

Jenkinson, M., Beckmann, C.F., Behrens, T.E.J., Woolrich, M.W., Smith, S.M., 2012a. Fsl. Neuroimage 62, 782–790. doi:10.1016/j.neuroimage.2011.09.015

Jenkinson, M., Beckmann, C.F., Behrens, T.E.J., Woolrich, M.W., Smith, S.M., 2012b. FSL. Neuroimage 62, 782–790. doi:http://dx.doi.org/10.1016/j.neuroimage.2011.09.015

Just, M.A., Cherkassky, V.L., Keller, T.A., Minshew, N.J., 2004. Cortical activation

and synchronization during sentence comprehension in high-functioning autism: evidence of underconnectivity. Brain 127, 1811–1821.

Just, M.A., Keller, T.A., Malave, V.L., Kana, R.K., Varma, S., 2012. Autism as a neural systems disorder: A theory of frontal-posterior underconnectivity. Neurosci. Biobehav. Rev. 36, 1292–1313. doi:http://dx.doi.org/10.1016/j.neubiorev.2012.02.007

Kaneoke, Y., Donishi, T., Iwatani, J., Ukai, S., Shinosaki, K., Terada, M., 2012. Variance and autocorrelation of the spontaneous slow brain activity. PLoS One 7, 3–12. doi:10.1371/journal.pone.0038131

Kanner, L., 1943. Autistic disturbances of affective contact. Nerv. Child. doi:10.1105/tpc.11.5.949

Klein, T.A., Ullsperger, M., Danielmeier, C., 2013. Error awareness and the insula: links to neurological and psychiatric diseases. Front. Hum. Neurosci. 7, 14. doi:10.3389/fnhum.2013.00014

Kleinhans, N.M., Richards, T., Sterling, L., Stegbauer, K.C., Mahurin, R., Johnson, L.C., Greenson, J., Dawson, G., Aylward, E., 2008. Abnormal functional connectivity in autism spectrum disorders during face processing. Brain 131, 1000–1012.

Kliemann, D., Dziobek, I., Hatri, A., Steimke, R., Heekeren, H.R., 2010. Atypical reflexive gaze patterns on emotional faces in autism spectrum disorders. J. Neurosci. 30, 12281–7. doi:10.1523/JNEUROSCI.0688-10.2010

Klin, A., Jones, W., Schultz, R., Volkmar, F., Cohen, D., 2002. Visual fixation patterns during viewing of naturalistic social situations as predictors of social

competence in individuals with Autism. Arch. Gen. Psychiatry 59, 809–816. doi:10.1001/archpsyc.59.9.809

Kohavi, R., 1995. A Study of Cross-Validation and Bootstrap for Accuracy Estimation and Model Selection 5.

Lai, M.C., Lombardo, M. V., Chakrabarti, B., Sadek, S.A., Pasco, G., Wheelwright, S.J., Bullmore, E.T., Baron-Cohen, S., Suckling, J., 2010. A shift to randomness of brain oscillations in people with autism. Biol. Psychiatry 68, 1092–1099. doi:10.1016/j.biopsych.2010.06.027

Lancaster, J.L., Rainey, L.H., Summerlin, J.L., Freitas, C.S., Fox, P.T., Evans, A.C., Toga, A.W., Mazziotta, J.C., 1997. Automated labeling of the human brain: A preliminary report on the development and evaluation of a forward-transform method. Hum. Brain Mapp. 5, 238–242. doi:10.1002/(SICI)1097-0193(1997)5:4<238::AID-HBM6>3.0.CO;2-4

Lancaster, J.L., Woldorff, M.G., Parsons, L.M., Liotti, M., Freitas, C.S., Rainey, L., Kochunov, P. V., Nickerson, D., Mikiten, S.A., Fox, P.T., 2000. Automated Talairach Atlas labels for functional brain mapping. Hum. Brain Mapp. 10, 120–131. doi:10.1002/1097-0193(200007)10:3<120::AID-HBM30>3.0.CO;2-8

Lauritzen, M., Gold, L., 2003. Brain function and neurophysiological correlates of signals used in functional neuroimaging. J. Neurosci. 23, 3972–80.

Leech, R., Kamourieh, S., Beckmann, C.F., Sharp, D.J., 2011. Fractionating the default mode network: distinct contributions of the ventral and dorsal posterior cingulate cortex to cognitive control. J. Neurosci. 31, 3217–24. doi:10.1523/JNEUROSCI.5626-10.2011

Lenoski, B., Baxter, L.C., Karam, L.J., Maisog, J., Debbins, J., 2008. On the performance of autocorrelation estimation algorithms for fMRI analysis. IEEE J. Sel. Top. Signal Process. 2, 828–838. doi:10.1109/JSTSP.2008.2007819

Lim, K.O., Pfefferbaum, A., 1989. Segmentation of MR brain images into cerebrospinal fluid spaces, white and gray matter. J. Comput. Assist. Tomogr. 13, 588–593.

Lord, C., Rutter, M., A, L.C., 1994. Autism Diagnostic Interview-Revised: a revised version of a diagnostic interview for caregivers of individuals with possible pervasive developmental disorders. J. Autism Dev. Disord. 24, 659–685.

Lowe, M.J., Mock, B.J., Sorenson, J.A., 1998. Functional Connectivity in Single and Multislice Echoplanar Imaging Using Resting-State Fluctuations. Neuroimage 7, 119–132. doi:10.1006/nimg.1997.0315

Lund, T.E., Madsen, K.H., Sidaros, K., Luo, W.L., Nichols, T.E., 2006. Non-white noise in fMRI: Does modelling have an impact? Neuroimage 29, 54–66. doi:10.1016/j.neuroimage.2005.07.005

Mahmoudi, A., Takerkart, S., Regragui, F., Boussaoud, D., Brovelli, A., 2012. Multivoxel pattern analysis for fMRI data: A review. Comput. Math. Methods Med. 2012. doi:10.1155/2012/961257

Mandelbrot, B., Fisher, A., Calvet, L., 1997. A Multifractal Model of Asset Returns. Work. Pap. -- Yale Sch. Manag. Econ. Res. Netw. 1. doi:10.1016/j.physa.2004.05.061

Margulies, D.S., Kelly, A.M., Uddin, L.Q., Biswal, B.B., Castellanos, F.X., Milham, M.P., 2007. Mapping the functional connectivity of anterior cingulate cortex.

Neuroimage 37, 579–588. doi:10.1016/j.neuroimage.2007.05.019

Margulies, D.S., Vincent, J.L., Kelly, C., Lohmann, G., Uddin, L.Q., Biswal, B.B., Villringer, A., Castellanos, F.X., Milham, M.P., Petrides, M., 2009. Precuneus shares intrinsic functional architecture in humans and monkeys. Proc. Natl. Acad. Sci. U. S. A. 106, 20069–20074. doi:10.1073/pnas.0905314106

MathWorks, 2012. Bioinformatics Toolbox: User's Guide (R2012a). Retrieved July 14, 2012.

Maxim, V., Şendur, L., Fadili, J., Suckling, J., Gould, R., Howard, R., Bullmore, E., 2005. Fractional Gaussian noise, functional MRI and Alzheimer's disease. Neuroimage 25, 141–158. doi:10.1016/j.neuroimage.2004.10.044

Mazziotta, J., Toga, A., Evans, A., Fox, P., Lancaster, J., Zilles, K., Woods, R., Paus, T., Simpson, G., Pike, B., Holmes, C., Collins, L., Thompson, P., MacDonald, D., Iacoboni, M., Schormann, T., Amunts, K., Palomero-Gallagher, N., Geyer, S., Parsons, L., Narr, K., Kabani, N., Le Goualher, G., Boomsma, D., Cannon, T., Kawashima, R., Mazoyer, B., 2001. A probabilistic atlas and reference system for the human brain: International Consortium for Brain Mapping (ICBM). Philos. Trans. R. Soc. London. Ser. B 356, 1293–1322. doi:10.1098/rstb.2001.0915

Mckeown, M.J., Makeig, S., Brown, G.G., Jung, T., Kindermann, S.S., Bell, A.J., Sejnowski, T.J., 1998. <McKeown1998_ICA.pdf> 188, 160–188.

McTeague, L.M., Goodkind, M.S., Etkin, A., 2016. Transdiagnostic impairment of cognitive control in mental illness. J. Psychiatr. Res. 83, 37–46. doi:10.1016/j.jpsychires.2016.08.001

Mesmoudi, S., Perlbarg, V., Rudrauf, D., Messe, A., Pinsard, B., Hasboun, D., Cioli, C., Marrelec, G., Toro, R., Benali, H., Burnod, Y., 2013. Resting State Networks' Corticotopy: The Dual Intertwined Rings Architecture. PLoS One 8. doi:10.1371/journal.pone.0067444

Mesulam, M.M., 1998. From sensation to cognition. [Review] [274 refs]. Brain 121, 1013–1052.

Minshew, N.J., Keller, T.A., 2010. The nature of brain dysfunction in autism: functional brain imaging studies. Curr. Opin. Neurol. 23.

Monk, C.S., Peltier, S.J., Wiggins, J.L., Weng, S.-J., Carrasco, M., Risi, S., Lord, C., 2009. Abnormalities of intrinsic functional connectivity in autism spectrum disorders,. Neuroimage 47, 764–772. doi:http://dx.doi.org/10.1016/j.neuroimage.2009.04.069

Moores, E., Laiti, L., Chelazzi, L., 2003. Associative knowledge controls deployment of visual selective attention. Nat. Neurosci. 6, 182–189. doi:10.1038/nn996

Mueller, S., Wang, D., Fox, M.D., Yeo, B.T.T., Sepulcre, J., Sabuncu, M.R., Shafee, R., Lu, J., Liu, H., 2013. Individual Variability in Functional Connectivity Architecture of the Human Brain. Neuron 77, 586–595. doi:10.1016/j.neuron.2012.12.028

Mundy, P., 2003. Annotation: The neural basis of social impairments in autism: The role of the dorsal medial-frontal cortex and anterior cingulate system. J. Child Psychol. Psychiatry Allied Discip. 44, 793–809. doi:10.1111/1469-7610.00165

Mundy, P., Sigman, M., Kasari, C., 1994. Joint attention, developmental level, and symptom presentation in autism. Dev. Psychopathol. 6, 389. doi:10.1017/S0954579400006003

Murphy, K., Birn, R.M., Bandettini, P.A., 2013. Resting-state fMRI confounds and cleanup. Neuroimage 80, 349–359. doi:10.1016/j.neuroimage.2013.04.001

Murray, D., Lesser, M., Lawson, W., 2005. Attention, monotropism and the diagnostic criteria for autism. Autism 9, 139–156. doi:10.1177/1362361305051398

Murray, J.D., Bernacchia, A., Freedman, D.J., Romo, R., Wallis, J.D., Cai, X., Padoa-Schioppa, C., Pasternak, T., Seo, H., Lee, D., Wang, X.-J., 2014. A hierarchy of intrinsic timescales across primate cortex. Nat. Neurosci. 17, 1661–3. doi:10.1038/nn.3862

Naughtin, C.K., Horne, K., Schneider, D., Venini, D., York, A., Dux, P.E., 2017. Do implicit and explicit belief processing share neural substrates? Hum. Brain Mapp. 4772, 4760–4772. doi:10.1002/hbm.23700

Nielsen, J., Zielinski, B., Fletcher, P., Alexander, A., Lange, N., Bigler, E., Lainhart, J., Anderson, J., 2013. Multisite functional connectivity MRI classification of autism: ABIDE results . Front. Hum. Neurosci. .

Nieuwenhuys, R., 2012. Chapter 7 - The insular cortex: A review, in: Hofman, M.A., Falk, D.B.T.-P. in B.R. (Eds.), Evolution of the Primate Brain. Elsevier, pp. 123–163. doi:https://doi.org/10.1016/B978-0-444-53860-4.00007-6

Nir, Y., Hasson, U., Levy, I., Yeshurun, Y., Malach, R., 2006. Widespread functional connectivity and fMRI fluctuations in human visual cortex in the

absence of visual stimulation. Neuroimage 30, 1313–1324. doi:10.1016/j.neuroimage.2005.11.018

Nir, Y., Mukamel, R., Dinstein, I., Privman, E., Harel, M., Fisch, L., Gelbard-Sagiv, H., Kipervasser, S., Andelman, F., Neufeld, M.Y., Kramer, U., Arieli, A., Fried, I., Malach, R., 2008. Interhemispheric correlations of slow spontaneous neuronal fluctuations revealed in human sensory cortex. Nat. Neurosci. 11, 1100–8.

Ozonoff, S., JN, M., 1995. Teaching theory of mind: a new approach to social skills training for individuals with autism. J. Autism Dev. Disord. 25, 415–433.

Ozonoff, S., Strayer, D.L., 1997. Inhibitory function in nonretarded children with autism. J. Autism Dev. Disord. 27, 59–78. doi:10.1023/A:1025821222046

Palva, J.M., Palva, S., 2012. Infra-slow fluctuations in electrophysiological recordings, blood-oxygenation-level-dependent signals, and psychophysical time series. Neuroimage 62, 2201–2211. doi:10.1016/j.neuroimage.2012.02.060

Park, C., Lazar, N.A., Ahn, J., Sornborger, A., 2010. A multiscale analysis of the temporal characteristics of resting-state fMRI data. J. Neurosci. Methods 193, 334–342. doi:10.1016/j.jneumeth.2010.08.021

Pelaez, M., 2009. Joint attention and social referencing in infancy as precursors of derived relational responding. Deriv. relational responding Appl. Learn. with autism other Dev. Disabil. A Progress. Guid. to Chang. 63–78.

Pelphrey, K.A., Sasson, N.J., Reznick, J.S., Paul, G., Goldman, B.D., Piven, J., 2002. Visual Scanning of Faces in Autism. J. Autism Dev. Disord. 32, 249–

261. doi:10.1023/A:1016374617369

Peng, C.K., Buldyrev, S. V., Havlin, S., Simons, M., Stanley, H.E., Goldberger, A.L., 1994. Mosaic organization of DNA nucleotides. Phys. Rev. E 49, 1685–1689. doi:10.1103/PhysRevE.49.1685

Picci, G., Gotts, S.J., Scherf, K.S., 2016. A theoretical rut: revisiting and critically evaluating the generalized under/over-connectivity hypothesis of autism. Dev. Sci. 19, 524–549. doi:10.1111/desc.12467

Pierce, K., Müller, R.A., Ambrose, J., Allen, G., Courchesne, E., 2001. Face processing occurs outside the fusiform “face area” in autism: evidence from functional MRI. Brain a J. Neurol. 124, 2059–2073. doi:10.1093/brain/124.10.2059

Poveda, G., Mesa, O.J., 1994. Estimation of the Hurst Exponent h and Geos Diagrams for a Non-Stationary Stochastic Process BT - Stochastic and Statistical Methods in Hydrology and Environmental Engineering: Time Series Analysis in Hydrology and Environmental Engineering, in: Hipel, K.W., McLeod, A.I., Panu, U.S., Singh, V.P. (Eds.), . Springer Netherlands, Dordrecht, pp. 409–420. doi:10.1007/978-94-017-3083-9_29

Prat, C.S., Stocco, A., Neuhaus, E., Kleinhans, N.M., 2016. Basal ganglia impairments in autism spectrum disorder are related to abnormal signal gating to prefrontal cortex. Neuropsychologia 91, 268–281. doi:10.1016/j.neuropsychologia.2016.08.007

Premack, D., Woodruff, G., 1978. Does the chimpanzee have a theory of mind? Behav. Brain Sci. 4.

Puce, a, Allison, T., Bentin, S., Gore, J.C., McCarthy, G., 1998. Temporal cortex activation in humans viewing eye and mouth movements. J. Neurosci. 18, 2188–2199.

Purdon, P.L., Weisskoff, R.M., 1998. Effect of temporal autocorrelation due to physiological noise and stimulus paradigm on voxel-level false-positive rates in fMRI. Hum. Brain Mapp. 6, 239–249. doi:10.1002/(SICI)1097-0193(1998)6:4<239::AID-HBM4>3.0.CO;2-4

Raichle, M.E., MacLeod, A.M., Snyder, A.Z., Powers, W.J., Gusnard, D.A., Shulman, G.L., 2001. A default mode of brain function. Proc. Natl. Acad. Sci. U. S. A. 98, 676–82. doi:10.1073/pnas.98.2.676

Research Imaging Institute, U., n.d. Mango.

Rousseeuw, P.J., 1987. Silhouettes: A graphical aid to the interpretation and validation of cluster analysis. J. Comput. Appl. Math. 20, 53–65. doi:10.1016/0377-0427(87)90125-7

RSuckling, J., Wiank, A.M., Bernard, F.A., Barnes, A., Bullmore, E., 2008. Endogenous multifractal brain dynamics are modulated by age, cholinergic blockade and cognitive performance. J. Neurosci. Methods 174, 292–300. doi:10.1016/j.jneumeth.2008.06.037

Rubin, D., Fekete, T., Mujica-Parodi, L.R., 2013. Optimizing Complexity Measures for fMRI Data: Algorithm, Artifact, and Sensitivity. PLoS One 8. doi:10.1371/journal.pone.0063448

Salvador, R., Mart??nez, A., Pomarol-Clotet, E., Gomar, J., Vila, F., Sarr??, S., Capdevila, A., Bullmore, E., 2008. A simple view of the brain through a

frequency-specific functional connectivity measure. Neuroimage 39, 279–289. doi:10.1016/j.neuroimage.2007.08.018

Sánchez Granero, M.A., Trinidad Segovia, J.E., García Pérez, J., 2008. Some comments on Hurst exponent and the long memory processes on capital markets. Phys. A Stat. Mech. its Appl. 387, 5543–5551. doi:10.1016/j.physa.2008.05.053

Schacter, D.L., Addis, D.R., Buckner, R.L., 2007. Remembering the past to imagine the future: the prospective brain. Nat. Rev. Neurosci. 8, 657–661. doi:10.1038/nrn2213

Schepers, H.E., van Beek, J.H.G.M., Bassingthwaighte, J.B., 2002. Four Methods to Estimate the Fractal Dimension from Self-Affine Signals. IEEE Eng. Med. Biol. Mag. 11, 57–64. doi:10.1109/51.139038

Scherf, 2010. Location, location, location: alterations in the functional topography of face- but not object- or place-related cortex in adolescents with autism. Front. Hum. Neurosci. 4, 1–16. doi:10.3389/fnhum.2010.00026

Schild, H.H., Laboratories., B., 1992. MRI made easy (... well almost). Berlex Laboratories, Wayne, NJ.

Schultz, R.T., 2005. Developmental deficits in social perception in autism: The role of the amygdala and fusiform face area. Int. J. Dev. Neurosci. 23, 125–141. doi:10.1016/j.ijdevneu.2004.12.012

Seeley, W.W., Menon, V., Schatzberg, A.F., Keller, J., Gary, H., Kenna, H., Reiss, A.L., Greicius, M.D., 2007. NIH Public Access. J. Neurosci. 27, 2349–2356. doi:10.1523/JNEUROSCI.5587-06.2007.Dissociable

Shannon, B.J., Buckner, R.L., 2004. Functional-Anatomic Correlates of Memory Retrieval That Suggest Nontraditional Processing Roles for Multiple Distinct Regions within Posterior Parietal Cortex. J. Neurosci. 24, 10084–10092. doi:10.1523/JNEUROSCI.2625-04.2004

Sharfitz, K.M., 2015. Neural system mediating decision-making and response inhibition for social and non social stimuli in autism. Prog Neuropsychopharmacol Biol Psychiatry 3, 112–120. doi:10.1016/j.pnpbp.2015.03.001.NEURAL

Shmuel, A., Leopold, D.A., 2008. Neuronal correlates of spontaneous fluctuations in fMRI signals in monkey visual cortex: Implications for functional connectivity at rest. Hum. Brain Mapp. 29, 751–761. doi:10.1002/hbm.20580

Shmuel, A., Yacoub, E., Pfeuffer, J., Van de Moortele, P.F., Adriany, G., Hu, X., Ugurbil, K., 2002. Sustained negative BOLD, blood flow and oxygen consumption response and its coupling to the positive response in the human brain. Neuron 36, 1195–1210. doi:10.1016/S0896-6273(02)01061-9

Shmueli, K., van Gelderen, P., de Zwart, J.A., Horovitz, S.G., Fukunaga, M., Jansma, J.M., Duyn, J.H., 2007. Low-frequency fluctuations in the cardiac rate as a source of variance in the resting-state fMRI BOLD signal. Neuroimage 38, 306–320. doi:10.1016/j.neuroimage.2007.07.037

Shumway, R.H., Stoffer, D.S., 2011. Time Series Analysis and Its Applications With R Examples, Book. doi:10.1007/978-1-4419-7865-3

Silvanto, J., Lavie, N., Walsh, V., 2006. Stimulation of the Human Frontal Eye Fields Modulates Sensitivity of Extrastriate Visual Cortex. J. Neurophysiol. 96,

941 LP-945.

Sled, J.G., Zijdenbos, A.P., Evans, A.C., 1998. A nonparametric method for automatic correction of intensity nonuniformity in MRI data. IEEE Trans. Med. Imaging. doi:10.1109/42.668698

Smith, S.M., Jenkinson, M., Woolrich, M.W., Beckmann, C.F., Behrens, T.E.J., Johansen-Berg, H., Bannister, P.R., De Luca, M., Drobnjak, I., Flitney, D.E., Niazy, R.K., Saunders, J., Vickers, J., Zhang, Y., De Stefano, N., Brady, J.M., Matthews, P.M., 2004. Advances in functional and structural MR image analysis and implementation as FSL. Neuroimage 23, 208–219. doi:10.1016/j.neuroimage.2004.07.051

Sparrow, S.S., Cicchetti, D. V, 1985. Diagnostic Uses of the Vineland Adaptive Behavior Scales. J. Pediatr. Psychol. 10, 215–225.

Spunt, R.P., Adolphs, R., 2017. The neuroscience of understanding the emotions of others. Neurosci. Lett. doi:10.1016/j.neulet.2017.06.018

Srivastava, A.K., Schwartz, C.E., 2014. Intellectual Disability and Autism Spectrum Disorders: Causal Genes and Molecular Mechanisms. Neurosci. Biobehav. Rev. 46 Pt 2, 161–174. doi:10.1016/j.neubiorev.2014.02.015

Strogatz, S.H., 2001. Exploring complex networks. Nature 410, 268–276. doi:10.1038/35065725

Subbaraju, V., Suresh, M.B., Sundaram, S., Narasimhan, S., 2017. Identifying differences in brain activities and an accurate detection of autism spectrum disorder using resting state functional-magnetic resonance imaging : A spatial filtering approach. Med. Image Anal. 35, 375–389.

doi:10.1016/j.media.2016.08.003

Svoboda, E., McKinnon, M.C., Levine, B., 2006. The functional neuroanatomy of autobiographical memory: A meta-analysis. Neuropsychologia 44, 2189–2208. doi:10.1016/j.neuropsychologia.2006.05.023

Talairach, J., Tournoux, P., 1988. Co-planar Stereotaxic Atlas of the Human Brain: 3-dimensional Proportional System : an Approach to Cerebral Imaging. G. Thieme.

Thomas Yeo, B.T., Krienen, F.M., Eickhoff, S.B., Yaakub, S.N., Fox, P.T., Buckner, R.L., Asplund, C.L., Chee, M.W.L., 2015. Functional specialization and flexibility in human association cortex. Cereb. Cortex 25, 3654–3672. doi:10.1093/cercor/bhu217

Turner, R., Jones, T., 2003. Techniques for imaging neuroscience. Br. Med. Bull. 65, 3–20. doi:10.1093/bmb/65.1.3

Uddin, L., Menon, V., 2010. The anterior insula in autism: Under-connected and under-examined. Neurosci. Biobehav. Rev. 33, 1198–1203. doi:10.1016/j.neubiorev.2009.06.002.The

Utevsky, A. V., Smith, D. V., Huettel, S.A., 2014. Precuneus Is a Functional Core of the Default-Mode Network. J. Neurosci. 34, 932–940. doi:10.1523/JNEUROSCI.4227-13.2014

Valenstein, E., Bowers, D., Verfaellie, M., Heilman, K.M., Day, A., Watson, R.T., 1987. Retrosplenial amnesia. Brain 110, 1631–1646. doi:10.1093/brain/110.6.1631

Van Buuren, M., Gladwin, T.E., Zandbelt, B.B., Van Den Heuvel, M., Ramsey, N.F., Kahn, R.S., Vink, M., 2009. Cardiorespiratory effects on default-mode network activity as measured with fMRI. Hum. Brain Mapp. 30, 3031–3042. doi:10.1002/hbm.20729

Vercelli, U., Diano, M., Costa, T., Duca, S., Geminiani, G., Nani, A., Vercelli, A., Cauda, F., 2014. Node Detection Using High- Dimensional Fuzzy Parcellation Applied To the Insular Cortex 2016, 1–15.

Vercelli, U., Nani, A., Moia, S., Manuello, J., Diano, M., Costa, T., Duca, S., Cauda, F., 2017. The spatial distribution and physiological significance of autocorrelation in resting state BOLD signal. Under Submiss.

Vincent, J.L., Snyder, A.Z., Fox, M.D., Shannon, B.J., Andrews, J.R., Raichle, M.E., Buckner, R.L., 2006. Coherent spontaneous activity identifies a hippocampal-parietal memory network. J. Neurophysiol. 96, 3517–31. doi:10.1152/jn.00048.2006

Vossel, S., Geng, J.J., Fink, G.R., 2014. Dorsal and Ventral Attention Systems. Neurosci. 20, 150–159. doi:10.1177/1073858413494269

Wandell, B.A., Dumoulin, S.O., Brewer, A.A., 2007. Review Visual Field Maps in Human Cortex 366–383. doi:10.1016/j.neuron.2007.10.012

Watanabe, S., 2005. Multi-Lorentzian Model and 1 / f noise spectra. J. Korean Phys. Soc. 46, 646–650. doi:10.1209/0295-5075/96/60007

Weng, S.-J., Wiggins, J.L., Peltier, S.J., Carrasco, M., Risi, S., Lord, C., Monk, C.S., 2010. Alterations of resting state functional connectivity in the default network in adolescents with autism spectrum disorders. Brain Res. 1313,

202–214. doi:http://dx.doi.org/10.1016/j.brainres.2009.11.057

Wheeler, M.E., Buckner, R.L., 2004. Functional-anatomic correlates of remembering and knowing. Neuroimage 21, 1337–1349. doi:10.1016/j.neuroimage.2003.11.001

Wicker, B., Michel, F., Henaff, M.A., Decety, J., 1998. Brain regions involved in the perception of gaze: a PET study. Neuroimage 8, 221–227. doi:10.1006/nimg.1998.0357

Wiener, N., 1930. Generalized harmonic analysis. Acta Math. 55, 117–258. doi:10.1007/BF02546511

Wink, A.M., Bernard, F., Salvador, R., Bullmore, E., Suckling, J., 2006. Age and cholinergic effects on hemodynamics and functional coherence of human hippocampus. Neurobiol. Aging 27, 1395–1404. doi:10.1016/j.neurobiolaging.2005.08.011

Wink, A.M., Bullmore, E., Barnes, A., Bernard, F., Suckling, J., 2008. Monofractal and multifractal dynamics of low frequency endogenous brain oscillations in functional MRI. Hum. Brain Mapp. 29, 791–801. doi:10.1002/hbm.20593

Winkler, A.M., Ridgway, G.R., Webster, M.A., Smith, S.M., Nichols, T.E., 2014. Permutation inference for the general linear model. Neuroimage 92, 381–397. doi:10.1016/j.neuroimage.2014.01.060

Wise, R.G., Ide, K., Poulin, M.J., Tracey, I., 2004. Resting fluctuations in arterial carbon dioxide induce significant low frequency variations in BOLD signal. Neuroimage 21, 1652–1664. doi:10.1016/j.neuroimage.2003.11.025

Woolrich, M.W., Jbabdi, S., Patenaude, B., Chappell, M., Makni, S., Behrens, T., Beckmann, C., Jenkinson, M., Smith, S.M., 2009. Bayesian analysis of neuroimaging data in FSL. Neuroimage 45, S173–S186. doi:10.1016/j.neuroimage.2008.10.055

Wylie, K.P., Tregellas, J.R., 2010. The Role of the Insula in Schizophrenia. Schizophr. Res. 123, 93–104. doi:10.1016/j.schres.2010.08.027

Yarkoni, T., Poldrack, R.A., Nichols, T.E., Van Essen, D.C., Wager, T.D., 2011. Large-scale automated synthesis of human functional neuroimaging data. Nat Meth 8, 665–670.

Yeo, B.T.T., Krienen, F.M., Sepulcre, J., Sabuncu, M.R., Lashkari, D., Hollinshead, M., Roffman, J.L., Smoller, J.W., Zöllei, L., Polimeni, J.R., Fischl, B., Liu, H., Buckner, R.L., 2011. The organization of the human cerebral cortex estimated by intrinsic functional connectivity. J. Neurophysiol. 106, 1125–65. doi:10.1152/jn.00338.2011

Zarahn, E., Aguirre, G.K., D'Esposito, M., 1997. Empirical Analyses of BOLD fMRI Statistics. Neuroimage 5, 179–197. doi:10.1006/nimg.1997.0263

Zuo, X., Martino, A. Di, Kelly, C., Shehzad, Z.E., Gee, D.G., Klein, D.F., Castellanos, F.X., Biswal, B.B., Michael, P., 2010. The Oscillating Brain: Complex and Reliable. Neuroimage 49, 1432–1445. doi:10.1016/j.neuroimage.2009.09.037.The